IDŐJÁRÁS

QUARTERLY JOURNAL
OF THE HUNGARIAN METEOROLOGICAL SERVICE

CONTENTS

VOL. 126 * NO. 3 * JULY – SEPTEMBER 2022

IDŐJÁRÁS

Quarterly Journal of the Hungarian Meteorological Service

Editorial Office: Kitaibel P.u. 1, H-1024 Budapest, Hungary
P.O. Box 38, H-1525 Budapest, Hungary
E-mail: journal.idojaras@met.hu

Indexed and abstracted in Science Citation Index Expanded™ and Journal Citation Reports/Science Edition
Covered in the abstract and citation database SCOPUS®
Included in EBSCO's database

Subscription by mail:
IDŐJÁRÁS, P.O. Box 38, H-1525 Budapest, Hungary
E-mail: journal.idojaras@met.hu

DOI:10.28974/idojaras.2022.3.1

IDŐJÁRÁS

Quarterly Journal of the Hungarian Meteorological Service
Vol. 126, No. 3, July – September, 2022, pp. 297–304

Heat capacity of the climate system derived from planetary radiation budget measurements

György Major

Hungarian Meteorological Service
Kitaibel Pál u. 1., 1024 Budapest, Hungary

Author E-mail: major.gy@met.hu

(Manuscript received in final form June 30, 2022)

Abstract—The new edition of the satellite measured radiation budget data have the smallest ever random and systematic error. From them, mean yearly cycle of the planetary heat capacity has been calculated for the period of 2000–2014. The radiation budget data measured before 2000 have serious systematic error. Using the new radiation budget data as well as the total solar irradiance data, the old yearly radiation budget values have been corrected. From the corrected data, the average heat capacity of the climate system has been calculated for the 1964–2014 half century.

Key–words: satellite measured radiation budget data, yeraly cycle of the planetary heat capacity, average planetary heat capacity of the period 1964–2014.

1. Introduction

Since the beginning of the satellite era, several efforts have been made to measure the state of the energy equilibrium between the Earth-atmosphere system and its outer environment. Even in the early years it was known, that these measured radiation budget data had significant random error (uncertainty). Later became obvious that their systematic error (bias) is large compared to the level that is necessary to the investigation of the energy processes of the climate system. The data from the recent experiment (CERES–Clouds and the Earth's Radiant Energy System) have small random error; however, their systematic error is in the same range as earlier. Therefore, the CERES Team transformed the CERES data into EBAF data; these could be regarded as nearly free from systematic error. The last edition of EBAF data was released in February 2017; this is the CERES EBAF Ed4.0 (*Loeb et al.,* 2009).

The most simple use of the measured planetary radiation budget data is to calculate the heat capacity of the climate system, since the energy exchange of the system with its environment is given by the *NET* radiation, the change of the temperature of the system can be calculated from the outgoing longwave radiation part of the radiation budget as radiation (brightness) temperature. This heat capacity is an effective one: it is the heat capacity of that portion of the climate system that is coupled to the processes determining the outgoing longwave radiation (see *Schwartz,* 2007; *Foster et al.,* 2008).

$$\frac{d(QT)}{dt} = NET\ , \tag{1}$$

where Q is the effective heat capacity, T is the radiation temperature of the outgoing longwave radiation, *NET* is the measured planetary net radiation.

Since the used unit of the planetary *NET* value is W m^{-2}, therefore the unit of Q is W year m^{-2} K^{-1} or W month m^{-2} K^{-1}, depending on the time-period of averaging the *NET* value.

In the first part of this work, the effective heat capacity of the yearly cycle of the climate system is calculated from the March 2000 – February 2015 monthly EBAF Ed.4 data. In the second part, the half-century (1964 – 2014) heat capacity is derived from corrected yearly planetary radiation budget measurements.

2. The heat capacity of the yearly cycle

The EBAF Ed.4 data series starts with March 2000. The data were obtained from the NASA Langley Center CERES ordering tool at http://ceres.larc.nasa.gov/. The heat capacity calculation is made from the average yearly cycle. The radiation temperature change in the yearly cycle is nearly 2 K, while the max - min in the 15 yearly values is 0.2 K only.

The average yearly course of the measured planetary *NET* radiation is not exactly sinusoid and has a 0.66 W m^{-2} imbalance. In *Fig. 1*, two-yearly curves are shown to see better the difference between the measurements and the sinusoid approximation that is used in the calculations. This latter is free from the imbalance, its equation is:

$$NET = 1.78\ \sin(2\pi/12*t) + 7.89\ \cos(2\pi/12*t), \tag{2}$$

where t is the number of the months of the year (more precisely 1/12 part of the year).

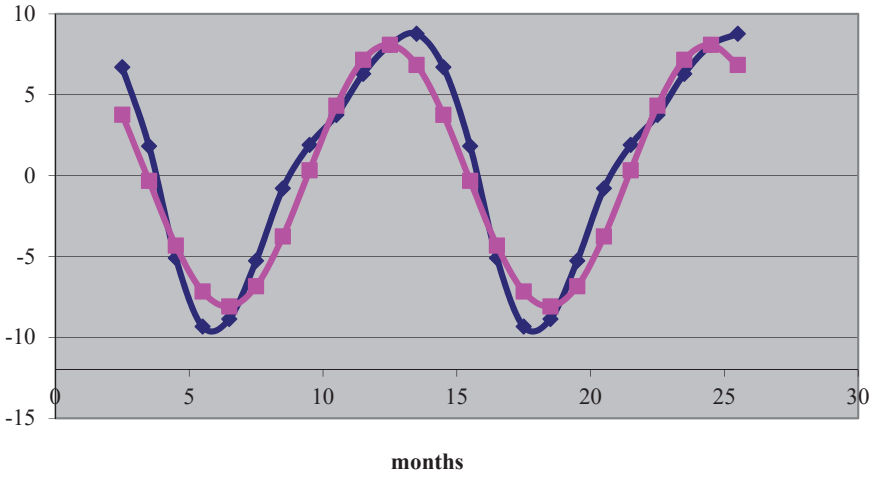

Fig. 1. Two-yearly cycle of the average planetary EBAF *NET* radiation, blue: measured, pink: sinusoid and balanced approximation.

The average yearly course of the brightness temperature and its approximation is shown in *Fig. 2.*

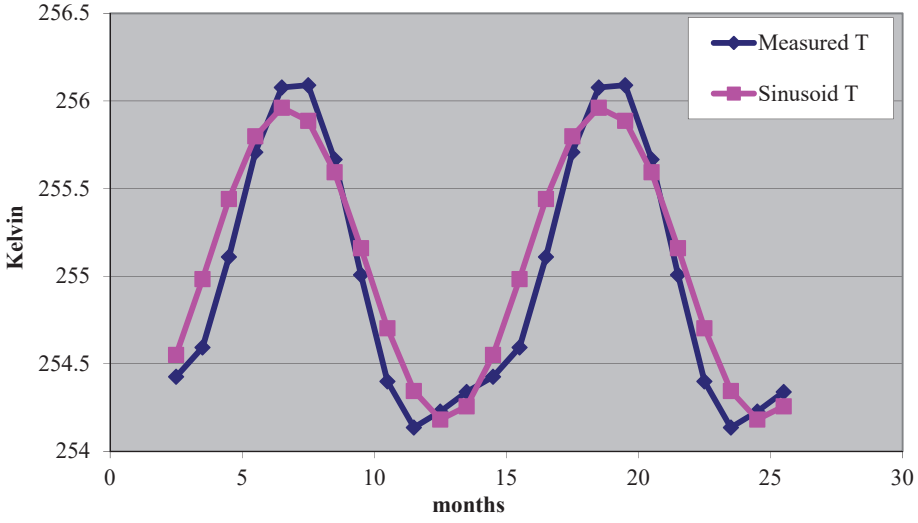

Fig. 2. Mean yearly cycle of the EBAF monthly radiation temperature and its approximation.

The equation used in the calculations is:

$$T = 255.07 - 0.316\ \sin(2\pi/12*t) - 0.837\ \cos(2\pi/12*t)\ . \qquad (3)$$

Having the formulae for the *NET* radiation and the *T* radiation temperature, the solution of the yearly heat capacity is looked for in the form:

$$Q = Q_0 + Q_1\ \sin(2\pi/12*t) + Q_2 \cos(2\pi/12*t), \qquad (4)$$

where Q_0, Q_1, and Q_2 are constants. The solution of Eq.(1) provides the following values: *1.04*, *0.061*, and *0.009 W month* m^{-2} K^{-1}, respectively. The numbers show, that the yearly course of the effective heat capacity is not really important. The relation between the *NET* and *Q* parameters is shown in *Fig. 3*.

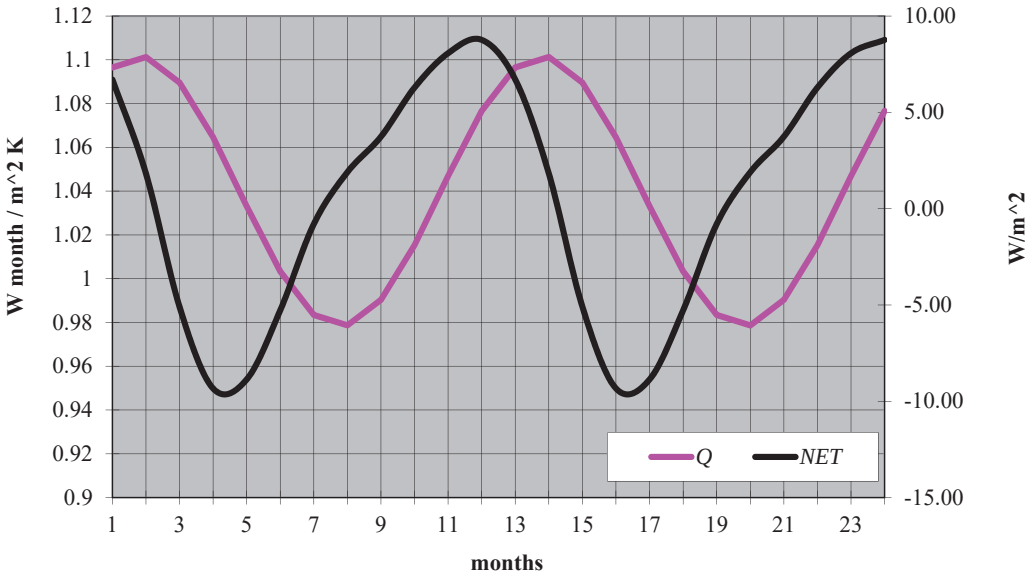

Fig. 3. Mean yearly course of the measured planetary *NET* radiation and of the calculated planetary effective heat capacity.

3. The heat capacity of the 1964 – 2014 half century

This period is not covered by continuous satellite radiation budget measurements. The used original data and their sources are listed in *Table 1*.

Table 1. The sources of original planetary radiation budget data

Time period	Data	Source
1962–1966	Five-yearly mean from 33 monthly measurements	*VonderHaar* and *Raschke*, 1972
1964 –1971	Eight-yearly mean from 29 monthly measurements	*Ellis* and *VonderHaar*, 1976
1964 –1977	Fourteen-yearly mean from 48 monthly measurements	*Stephens et al.*, 1981
1979 –1986	Calendar yearly mean ERB values	*Ardanuy et al.*, 1992
1985 –1989	Calendar yearly mean ERBE values	*Larc NASA S4G data CD*
1994. 03 - 1994.09 1994.11- 1995.02	Monthly ScaRaB values, the missing October have been interpolated	*ScaRaB CD-s* *Kandel et al.*, 1994
2000. 03 - 2015.02	Monthly CERES Ed.3A values	NASA Langley Center CERES ordering tool at http://ceres.larc.nasa.gov/

It is supposed that the several yearly effective heat capacity of the climate system is constant, this way the relation:

$$Q\frac{dT}{dt} = NET \tag{5}$$

shall be used for the calculation of Q. To obtain realistic value for the heat capacity, all measured components of the planetary net radiation have to be corrected to decrease their systematic error.

The satellites measure the total solar irradiance (*TSI*), the reflected solar radiation (*REF*) and the outgoing longwave radiation (*OUT*). The planetary radiation budget is:

$$NET=ICO - REF – OUT. \quad (6)$$

Taking into account the non-spherical shape of the Earth,

$$4.0032\ ICO = TSI \quad (7)$$

has been used. Continuous satellite measurements of *TSI* are made since November 1978. The previous *TSI* or solar constant values have to be corrected to the newest one (see, e.g., *Major,* 2016). For the period before 1990, the *ICO* values have been changed by those calculated from TSI values by *Coddington al.* (2016). The ScaRaB *ICO*-s have been changed for the whole March 1994 - February 1995 cycle by those derived from the SARR-DIARAD TSI measurements (*Dewitte et al.,* 2004) decreased by 5.512 Wm^{-2} to convert to the NIST pyrheliometric scale. For the CERES period, the EBAF Ed.4 *ICO* values are used for the March-February yearly cycles, started from the March of 2000.

The reflected solar radiation values and the outgoing longwave radiation values have been corrected to the EBAF scale by using the following correction factors:

– sum of monthly EBAF from March 2000 to February of 2015,

– sum of monthly CERES from March 2000 to February of 2015.

The numerical value of the correction of the reflected radiation is 1.01623, that of the outgoing longwave radiation is 1.00545. These corrections have been applied to all data provided by USA experiments including CERES. The ScaRaB measurements have not been changed.

In the calculation, those early measurements that cover more year have been regarded as one-yearly values of the central years of their periods (since they have been compiled from less monthly data, see *Table 1*). All the used yearly radition budget components are shown in *Fig. 4*. The radiation (brightness) temperature values have been calculated from each yearly outgoing radiation, their linear time regression coefficient is 0.285 K $year^{-1}$. The average *NET* radiation is 0.383 Wm^{-2}, this way the effective heat capacity *Q* of the 1964–2014 half century is 13.45 W year m^{-2} K^{-1}.

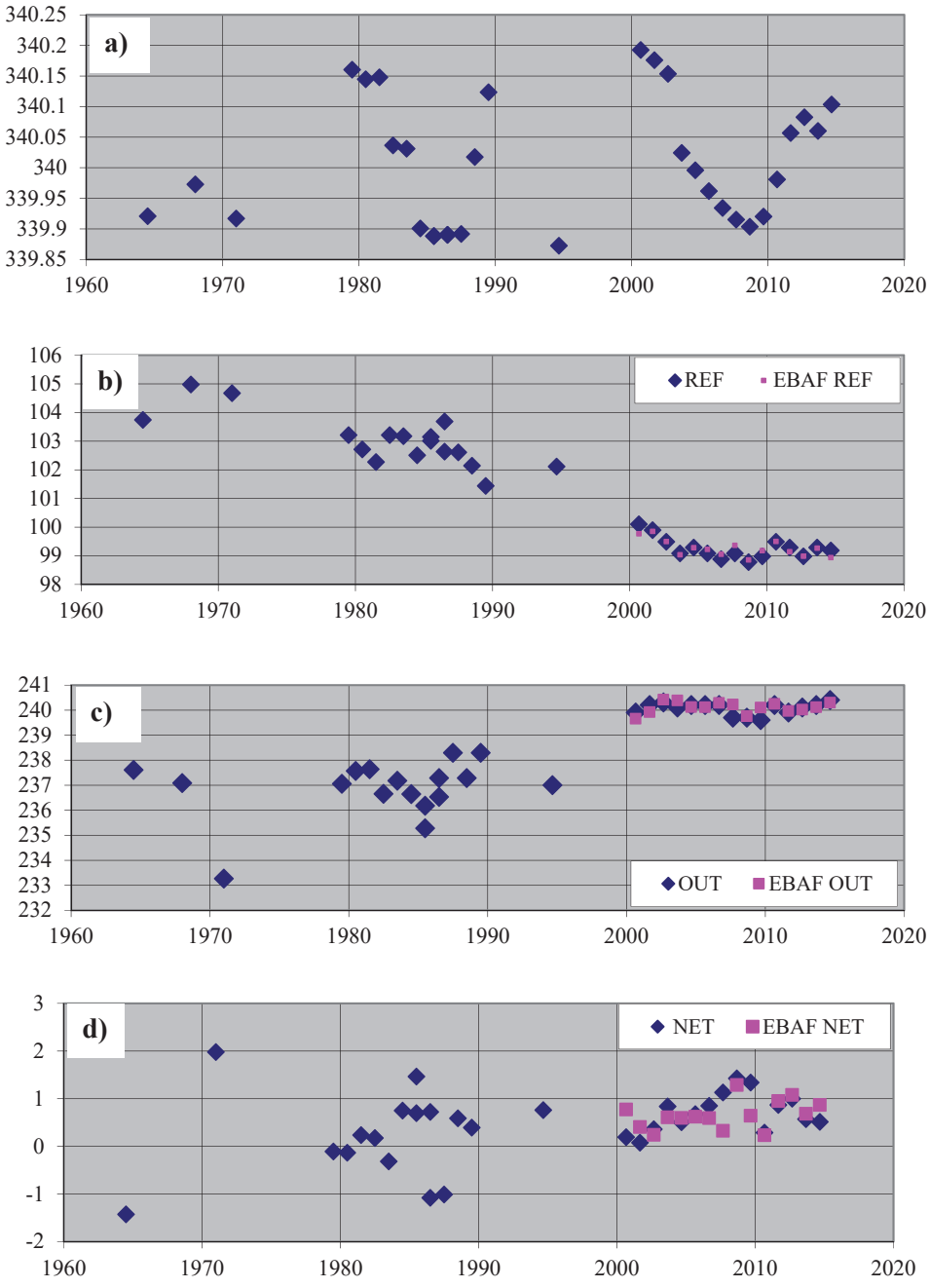

Fig. 4. The yearly corrected radiation budget values used in the calculation of the heat capacity. a) *ICO*, b) *REF*, c) *OUT*, d) NET. The corrected CERES and the EBAF values are not exactly the same.

4. Results

- The effective heat capacity coupled to the radiation temperature of the yearly cycle of the outgoing longwave EBAF radiation is 1.04 W month m^{-2} K^{-1}, the yearly amplitude is 0.06 W month m^{-2} K^{-1}.
- The effective heat capacity (Q) of the 1964–2014 period derived from measured and corrected planetary radiation budget measurements is 13.45 W year m^{-2} K^{-1}, a little larger than that of the yearly cycle.
- The corrected yearly *REF* radiation values show a consequent decrease in the full period, except the last 10 years.

References

Ardanuy P.E., Kyle H.L. and *Hoyt, D.,* 1992: Global Relationship among the Earth's Radiation Budget, Cloudiness, Volcanic Aerosols and Surface Temperature. *J. Climate 5*, 1120–1139. https://doi.org/10.1175/1520-0442(1992)005<1120:GRATER>2.0.CO;2

Coddington,O., Lean, J.L., Pilewskie, P., Snow, M. and *Lindholm*, *D.,* 2016: A Solar Irradiance Climate Data Record, *Bull. Amer. Meteorol. Soc. 97*, 1265–1282. https://doi.org/10.1175/BAMS-D-14-00265.1

Dewitte S., Crommelynck, *D.,* and *Joukof, A.,* 2004: Total Solar Irradiance Observations from DIARAD/VIRGO. *J. Geophys. Res.: Space Physics 109*, 2102. https://doi.org/10.1029/2002JA009694

Ellis, J.S. and *VonderHaar, T.H.,* 1976: Zonal Average Earth Radiation Budget Measurements from Satellites for Climate Studies. *Dept. Atm. Sci. CSU Paper* No 240.

Foster, G., Annan, J.D., Schmid, G.A., and *Mann, M.E.,* 2008: Comment on ''Heat capacity, time constant, and sensitivity of Earth's climate system'' by S. E. Schwartz. *J. Geophys. Res. 113*, https://doi.org/10.1029/2007JD009373

Kandel, R.S., Monge J.-L., Viollier M., Pakhomov L.A., Adasko V.I., Reitenbach R.G., Raschke E., and *Stuhlmann R.,* 1994: The SCARAB Project: Earth Radiation Budget Observations from METEOR Satellites. *Advances in Space Res. 14*, 147–154. https://doi.org/10.1016/0273-1177(94)90346-8

Loeb, N.G., Wielicki, B.A., Doelling, D.R., Smith, G.L., Keyes, D.F., Kato, S., Manalo-Smith, N., and *Wong, T.,* 2009: Toward optimal closure of the Earth's top-of-atmosphere radiation budget. *J. Climate, 22*, 748–766. https://doi.org/10.1175/2008JCLI2637.1

Major, Gy., 2016: An interpretation of the measured planetary radiation imbalance. *Időjárás 120*, 353–364.

Schwartz, S.E., 2007: Heat capacity, time constant, and sensitivity of Earth's climate system. *J. Geophys. Res. 112*, D24S05. https://doi.org/10.1029/2007JD008746

Stephens, G.L., Campbell, G.G., and *VonderHaar, T.H.*, 1981: Earth Radiation Budgets. *J. Geoph. Res. 86,* 9739–9760. https://doi.org/10.1029/JC086iC10p09739

VonderHaar, T.H. and *Raschke, E.,* 1972: Measurements of the Energy Exchange Between Earth and Space from Satellites During the 1960's. *Dept. Atm. Sci. CSU Paper No 184.*

DOI:10.28974/idojaras.2022.3.2

IDŐJÁRÁS

Quarterly Journal of the Hungarian Meteorological Service
Vol. 126, No. 3, July – September, 2022, pp. 305–318

Remote sensing study of cloud top absolute temperature with surface rainfall over Lahore (Pakistan) during monsoon

Jahanzeb Qureshi* and **Noor Fatima**

Department of Space Science
University of the Punjab
Quaid-e-Azam Campus, Lahore, Pakistan

**Corresponding author Email: jzebqureshipu@gmail.com*

(Manuscript received in final form April 19, 2021)

Abstract— The study attempts to build a relationship between clouds top absolute temperature and rainfall during monsoon period over Lahore during 2019. For this purpose, meteorological data was taken from Pakistan Meteorological Department (PMD) of few parameters (temperature and rainfall) for Lahore during monsoon period, i.e., from July to September, 2019. The study revealed interesting results for the observed three months. In July and August, the rainfall and temperature trend showed an inverse relation, whereas a decreased trend was observed for both temperature and rainfall during September, 2019. In Pakistan, most of the rainfall is a result of the depressions created over Bay of Bengal and Arabian Sea. High temperatures cause lower pressure that becomes a reason for originating of low pressures/depressions resulting in monsoon rainfall. During September, the average temperature of the study area was lower comparatively that ultimately resulted in low rainfall, and only 54 mm of total rainfall was recorded over Lahore during September, 2019 which was quite less than in July and August. Satellite cloud top temperatures were also taken from EUMETSAT to establish a relation between cloud top absolute temperature and surface rainfall over Lahore.

Key-words: clouds, absolute temperature, rainfall, monsoon, depressions, satellite

1. Introduction

Clouds enhance excitement to the atmosphere and are appealing aesthetically. One would not experience any snow, rain, lightning, thunder, halos, or rainbows without them. A cloud is considered as a visible accumulation of ice crystals or tiny water droplets that are suspended in the air. Cloud are found in a variety of forms at various altitudes (*Barry* and *Chorley*, 2003; *Richardson et al.,* 2017). One of the most observed features is the tropopause level clouds. Satellite based imageries have identified cirrus clouds in the tropics at the tropopause level (e.g., *Heymsfield,* 1986; *Nee et al.,* 1998; *Dessler et al.,* 2006; *Pan* and *Munchak*, 2011). The cloud pattern seems to correlate with the structure of fronts and tropopause in the sub-tropics (e.g., *Noël* and *Haeffelin*, 2007; *Posselt et al*., 2008; *Rani et al.,* 2015). This behavior is expected generally as following processes occur at such dynamical boundaries:

i. rapid variations in humidity and temperature,
ii. vertical development linked with frontal lifting.

Longwave (LW) cloud radiative forcing (CRF), and large shortwave (SW) are found in upper-tropospheric clouds linked with tropical convection. Clouds reflect SW radiation, that cools our earth, and its effect is mainly calculated by cloud optical depth. LW radiations are trapped by clouds, that in turn increases its temperature, warms the climate, and that primarily depends on cloud top temperature. (*Reed* and *Recker*, 1971; *Zeng*, 1999) investigated satellite imageries that observed a peak in stratiform anvil and thin cloud about 175 hPa, that corresponds to nearly 13 km. Upper level divergence measurements were also made, that proposed a peak at about the same level. Various researches have also recommended convective detrainment quite below the tropopause. (*Folkins et al*., 1999, 2000; *Sivakumar* and *Stefanski*, 2009) proposed that convective detrainment occurs below 14 km, based on the concentration of ozone, which is maximum at the stratospheric level (stratospheric ozone). Extreme weather events (floods, heat waves, heavy rainfall, and droughts) have a significant importance in regional and social situations. Changes in extreme precipitation events have significant impacts and pose serious challenges to societies, especially in arid and semi-arid environments (*Kubar et al*., 2007; *Zhisheng et al*., 2015; *Karimi at al.,* 2021).

Generally, most of the clouds are formed based on the following mechanisms:

i. convection and surface warming,
ii. surface topography, and
iii. widespread ascent due to surface air convergence (*Ahrens*, 2007).

1.1. Surface heating and convection

The global circulation pattern in terms of precipitation plays a vital role as far the functionality of the Earth's system is concerned. It transports heat from the tropics to the higher latitudes, and hence it helps to regulate the earth's temperature. The weather system is severely affected by the Southeast Asia monsoon season. Despite of the fact that lot of research has been conducted on the interactivity of the monsoon seasons, yet the influence of climate change in terms of rising temperatures on monsoon rainfall concentration has not gained much attention in Southeast Asia (*Kripalani* and *Kulkarni*, 1997; Loo et al., 2015; *Panda* and *Sahu*, 2019).

Some areas on the earth absorb the sunlight more than others. As a result, the air in contact with such areas becomes warmer than the surrounding air: a hot air bubble thermal results, it rises, and as it mixes with cooler drier air around, it starts losing its individuality. Now its upward motion slows down and before that it absolutely dilutes, another thermal comes and rises the air bit more (*Fig. 1a*). As the air cools, it becomes heavy and downward motion starts. Slowly and gradually the cool air descends and replaces the rising warm air. Now inside the cloud there is the rising air, and around it is the sinking air (*Barry* and *Chorley*, 2003).

1.2. Topography

Topography is the study of the shape and structures of the earth's surface, e.g., mountains, hills, basins, etc. Horizontally developed clouds can not pass through a big obstacle, e.g., mountain and air has to cross over it. Such forced lifting along an obstacle is known as orographic uplift. Usually large air masses rise, when they move across stretched mountainous belt (*Fig. 1b*). Due to this lifting, cooling takes place and here clouds will form in humid air. Clouds formed in this way are called orographic clouds. When the air sinks on the leeward (away from wind) of the mountain, it gets warm. While the air is moving downhill, it is drier as most of the moisture present occur as precipitation, and clouds was removed on the windward side. The region on the leeward side experiencing less precipitation is named rain shadow (*Kirshbaum et al*., 2018; *Stockham et al.,* 2018).

1.3. Widespread ascent and clouds

As the mountains force air to rise, the convergence (flowing together) of air in the lower troposphere will result in the lifting of air and formation of clouds. The main cause of this lifting of air is cyclonic storm system. Another cause of this air lifting are weather fronts (*Fig. 1c,d*).

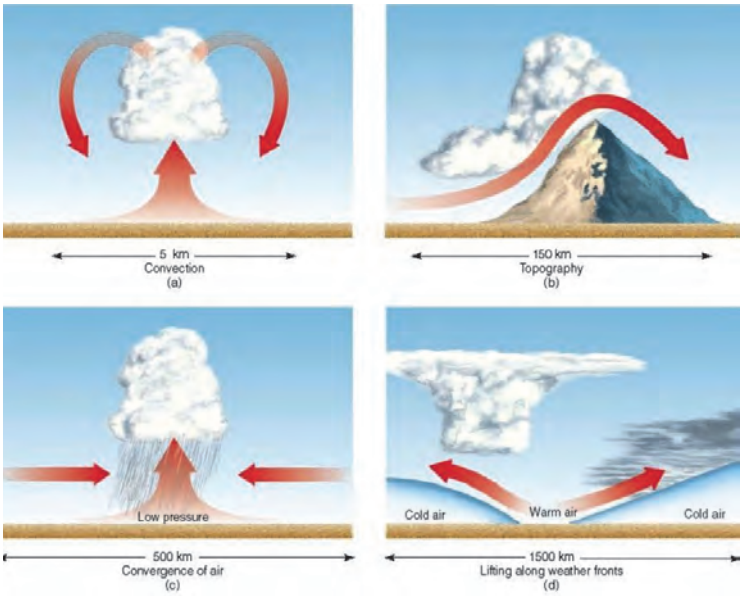

Fig. 1. (a-d): The primary ways clouds form: (a) surface heating and convection; (b) forced lifting along topographic barriers; (c) convergence of surface air; (d) forced lifting along weather fronts. (Source: *Ahrens* and *Henson*, 2021)

1.4. Occurrence of monsoon

The periods of pre-monsoon and post-monsoon are significant in a way that the changing wind pattern gives birth to cyclonic circulation over the Arabian Sea and Bay of Bengal. Almost 80 tropical storms (tropical cyclones with wind speeds greater than or equal to 17 m/s) generate in the world's water bodies annually (*Chang et al*., 2004). Among them, around 6.5% generate in the North Indian Ocean (Arabian Sea and Bay of Bengal) (*Knapp et al*., 2010; *Bewoor* and *Kulkarni*, 2009).

1.5. Monsoon rainfall and circulation

The major characteristic of monsoons is that they cause rainfall that might lead to coastal and urban flooding. As per study conducted by NASA, between 50–75% of the annual rainfall in Pakistan and India is due to monsoon (*Huang* and *Margulis*, 2011). Land and sea breezes occur as a result of the difference in heat capacity of land and sea surface (i.e., their temperature rises for a given heat input) (*Betts*, 2000). In summer, the solar radiation is strong, and during winter, the pressure is low, because land surface is cool and ocean is warmer as well (*Betts*,

2000). The winds gust gradually move from southwest (SW) during summer and from northeast (NE) during winter (*Fig. 2a,b*). Hence, the climatologists have defined monsoon as a large scale wind system that either prevails or powerfully affects the climate of a large regions, and also in which the direction of the wind flow reverses from winter to summer (*Margulis* and *Entekhabi*, 2001).

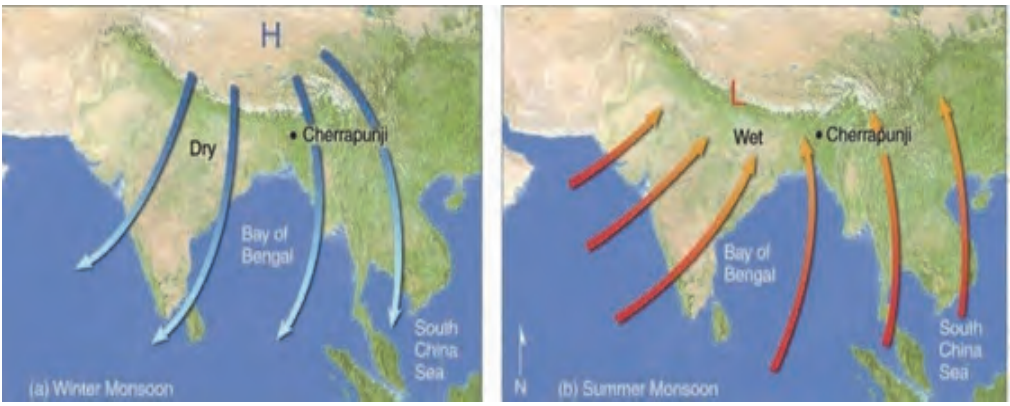

Fig. 2. Monsoon circulations. (source: *Ahrens* and *Henson*, 2021)

Plenty of valuable water is been provided to Asia by monsoon rainfall. The economy of most of the monsoon climatic region that includes South, East, and Southeast (SE) Asia depends mainly on agriculture, that is further dependent on monsoon rainfall. Hence, the fate of the region is dependent upon the direction and flow of the monsoon winds (*Barros* and *Hwu*, 2002). Any deviation of the monsoonal pattern can affect the agriculture operations over such regions threatening their economies.

2. Study area and methodology

Lahore is Pakistan's second largest metropolitan city and the provincial capital of Punjab Province. It stretches over a total land area of 404 square kilometers and is almost 24 kilometers away from the Indian border (*Daly et al*., 2004). Lahore is bounded by the Sheikhupura district on its north and west, on the south by Kasur district, while on the east by Wagha (*Fig. 3ab*). The geographical coordinates (latitude, longitude) of Lahore are 31°34' N, 74°18' E. The climate of Lahore is semi-arid, where in June (hottest month) the average temperature routinely exceeds 40 °C. The monsoon season extends from mid-July till mid-September

experiencing heavy rainfalls and thunderstorms with the possibility of cloudbursts resulting in coastal and urban flooding. January is the coolest month with dense fog (*Medeiros et al*., 2005). Lahore receives an average monsoon rainfall precipitation of 628.8 millimeters. In 2009, it received below normal monsoon rainfalls as a result of El-Nino over Pakistan (*Juang, et al*., 2007). In 2011, Lahore received the highest ever annual rainfall when 1,576.8 millimeter of rainfall was recorded. Normal rainfall was observed in Lahore in 2007 and 2010 (*Hunt et al.*, 2018; *Siddiqui* and *Siddiqui*, 2019). (*Fig. 4*) shows average maximum and minimum values of average monthly temperatures of Lahore, Pakistan.

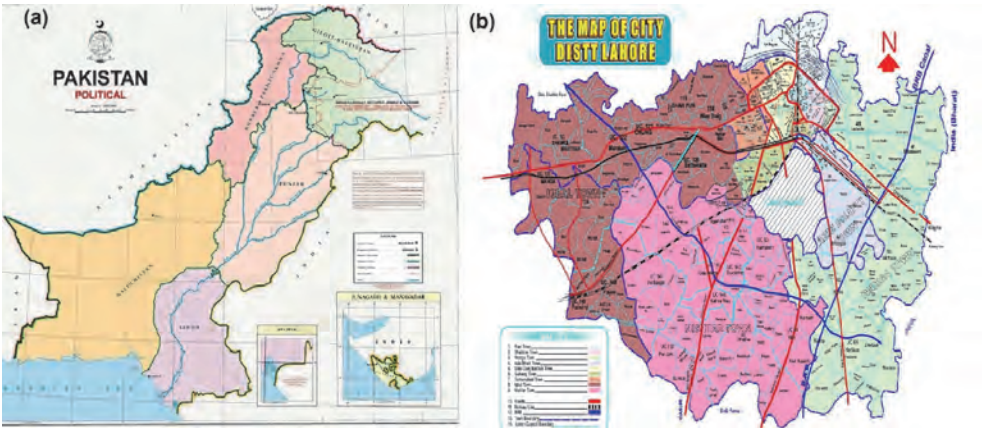

Fig. 3. Political map of Pakistan (source*: the news international*, 2020; *Ali et al.*, 2015).

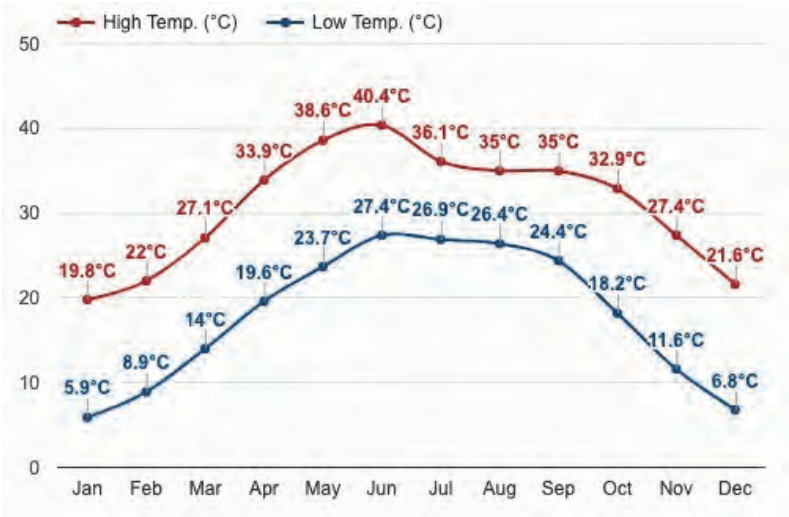

Fig. 4. Maximum and minimum values of average monthly temperatures of Lahore (Source: PMD, 07/12/2020).

Temperature and rainfall data was collected from Pakistan Meteorological Department, Lahore, for the months July-September, 2019. Graphs were plotted for daily maximum and minimum temperatures and rainfall of Lahore. Satellite images for the cloud top temperature were also taken from Pakistan Meteorological Department. For cloud top temperature, European Meteorological Satellite (EUMETSAT) was used.

3. Results and discussions

Rainfall is due to the result of two processes: condensation and evaporation. In summer, the process of evaporation increases because of heat from the sun which results in the gathering of more vapors in the atmosphere. These gathered vapors form tiny water droplets, and the process is called condensation. Ultimately, these droplets result in rain.

3.1. Temperature and rainfall analysis from July to September, 2019

A decreased trend was shown in the daily minimum and maximum temperatures of Lahore for July and September, while August exhibited an increased trend (*Figs. 5* and *6*). Two daily rainfall peaks were recorded for July (92 mm and 75.8 mm), August (57.8 mm and 63 mm), and September (22.2 mm and 14.4 mm), respectively (*Fig. 7*).

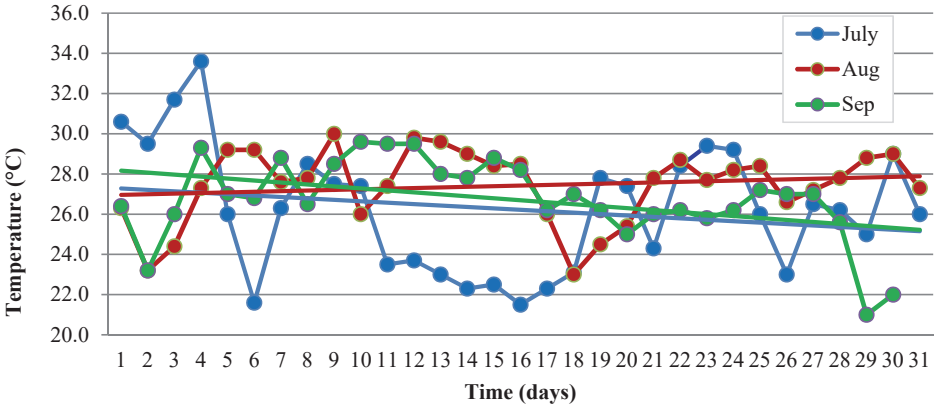

Fig. 5. Daily minimum temperature of Lahore from July to September, 2019.

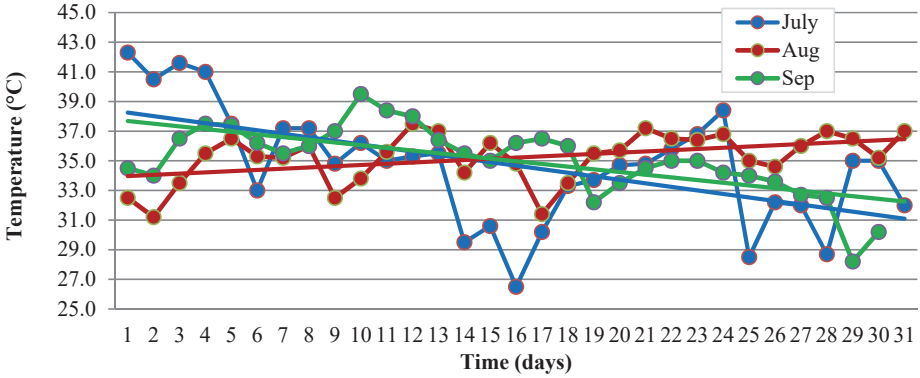

Fig.6. Daily maximum temperature of Lahore from July to September, 2019.

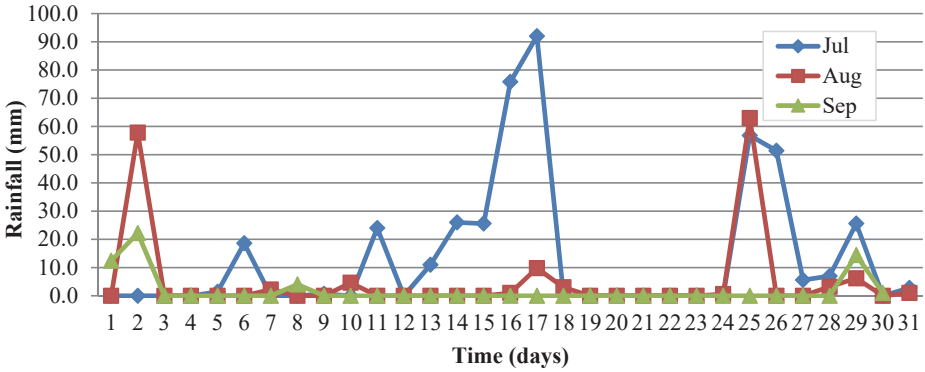

Fig. 7. Daily rainfall of Lahore from July to September, 2019.

3.2. Cloud top temperature

Satellite cloud top temperatures were also taken for moderate to heavy rainfall days of the monsoon months (July-September, 2019) to establish a relation between cloud top absolute temperature and surface rainfall over Lahore during the monsoon period, 2019. Selected days of July and August months were taken on the basis of their rainfall and corresponding cloud top temperatures (*Figs. 8a-f* and *9a-f*). Rainfall results after the process of evaporation and condensation. Vapors condense in the upper atmosphere shaping in water droplets and ice crystals to form clouds. The temperature of rainy clouds varies from 0 °C or below 0 °C. During the month of July, 424.3 mm rainfall was recorded, while a total of 152.4 mm rainfall was recorded in the month of August.

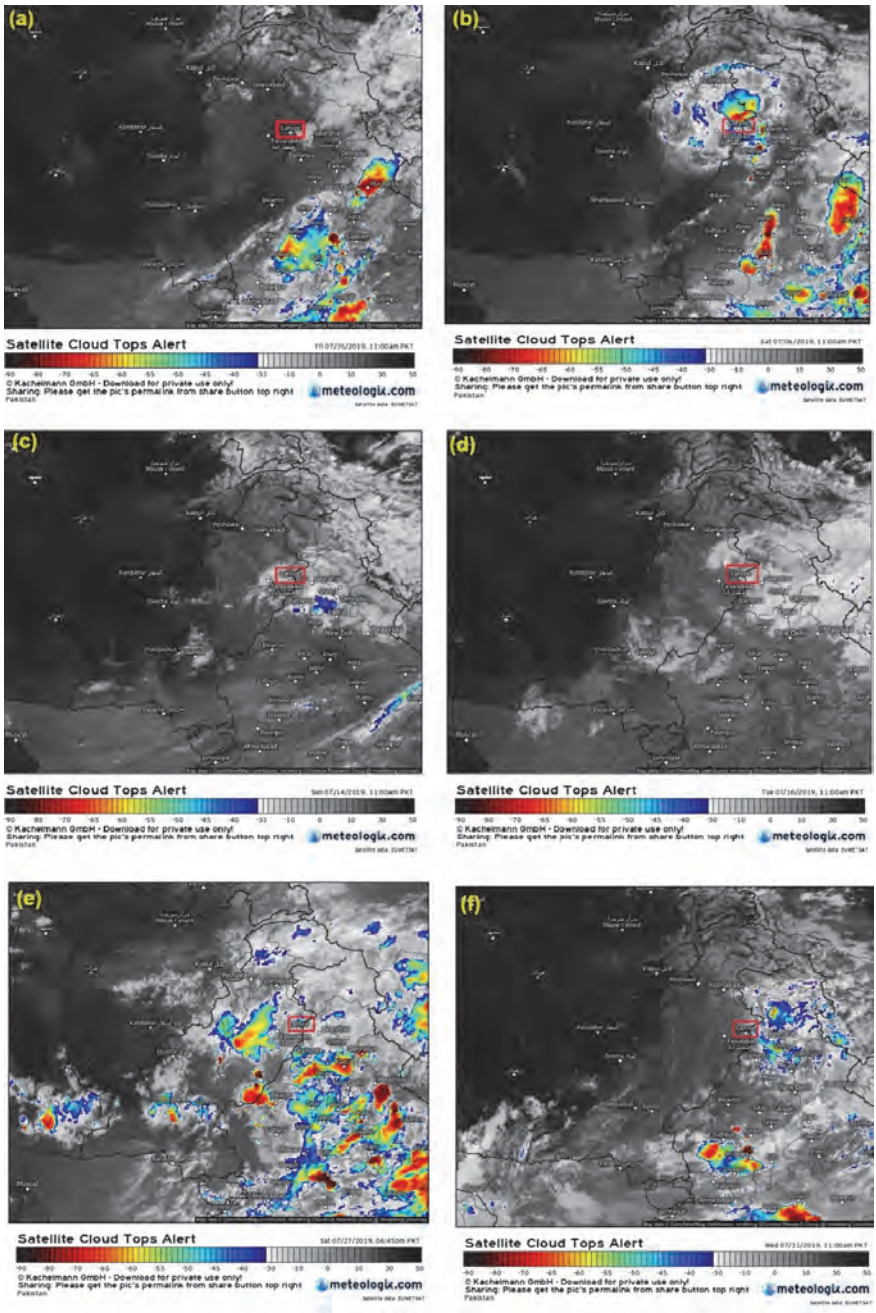

Fig. 8. Cloud top temperatures for the July monsoon spell: (a) July 5, 2019; (b) July 6, 2019; (c) July 14, 2019; (d) July 16, 2019; € July 27, 2019; (f) July 31, 2019.

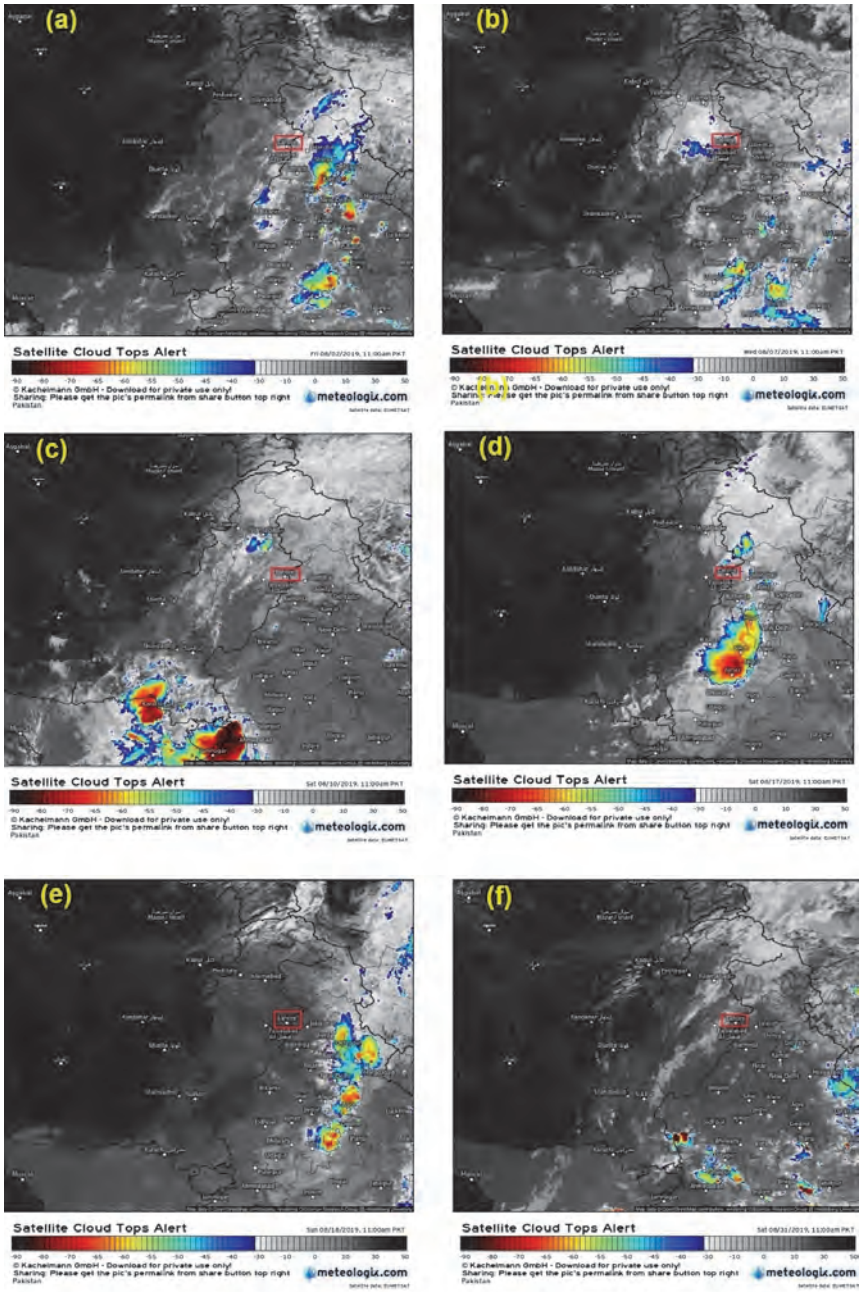

Fig. 9. Cloud top temperatures for the August monsoon spell: (a) August 02, 2019; (b) August 7, 2019; (c) August 10, 2019; (d) August 17, 2019; € August 18, 2019; (f) August 31, 2019.

3.3. *Cloud top temperature and rainfall relation*

Relations between the rainfall and cloud top temperature on the study area are shown in *Figs. 10* and *11*. The graphs clearly show as the cloud top temperature decreases and in accordance with the Bergeron Findeisen theory, where super cooled water droplets and ice crystals having high vapor pressure exist together, the rainfall becomes heavy and falls down as precipitation. The low cloud top temperatures in July and August have higher cloud tops resulting in more growth of cloud vertical column being the cause of rainfall. The saturation of water vapors is due to the influence of moist/humid air coming from Bay of Bengal and Arabian Sea resulting in precipitation.

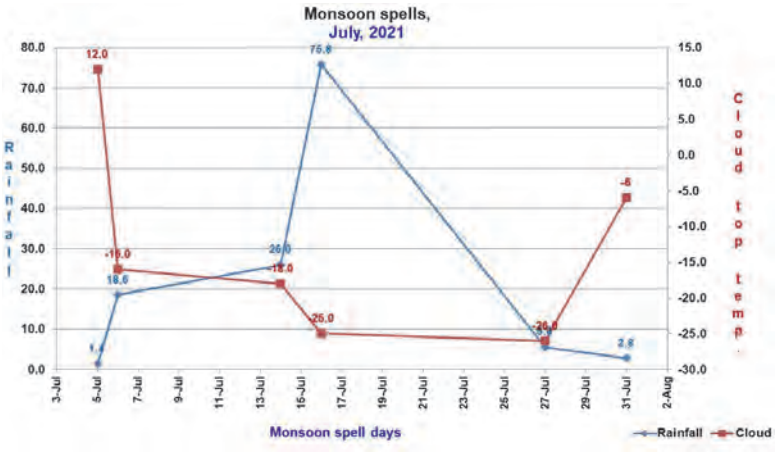

Fig. 10. Relation between cloud top temperature and rainfall (July, 2019).

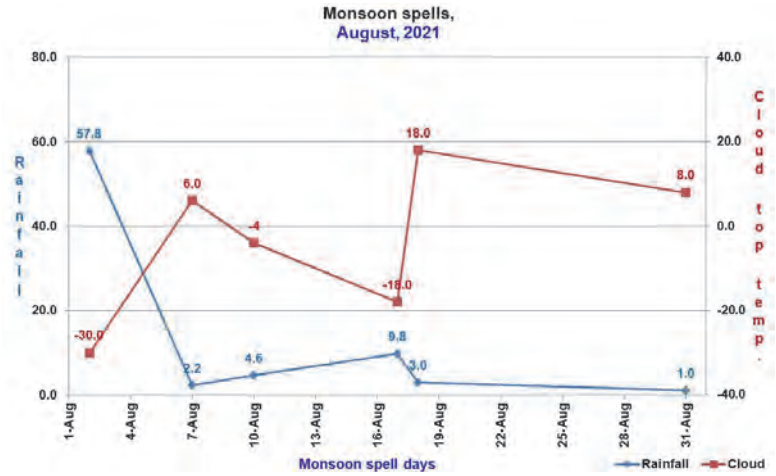

Fig. 11. Relation between cloud top temperature and rainfall (August, 2019).

4. Conclusions

In general, heavy rainfall occurs during the monsoon season over Pakistan, that normally lasts from mid-July till mid-September. This monsoon rainfall is a result of the depressions and low pressures originating over Bay of Bengal and Arabian Sea. July and August revealed a direct relation between temperature and rainfall, while a reverse trend was observed between these two parameters during September. Least rainfall was recorded during September, 2019 which means very few depressions originated over Bay of Bengal or Arabian Sea. In July, the moisture inflow was from moist sources, i.e., BoB and Arabian Sea resulting in precipitation, whereas in August, the saturation of water vapors is due to the condensation of the air lowering the cloud top temperature resulting in precipitation. It is recommended that a study may be made for the winter monsoon period (western disturbances) to observe the trend for that period. A detailed study can be made over the northern, central, and southern regions of Pakistan authenticated by satellite images (IR color code image, 6 GMT).

References

Ahrens, C.D. and *Henson, R.*, 2021: Meteorology today: an introduction to weather, climate, and the environment. Cengage Group learning.

Ahrens, C.D., 2007: Meteorology today: an introduction to weather, climate, and the environment. Thomson Brooks/Cole Belmont, CA.

Ali, Z., Zahra, G., Khan, B.N., Ali, H., Bibi, F., and *Khan, A.M.,* 2015: Prevalence of dengue fever during 2011-2012 in Punjab. *J. Animal Plant Sci. 25,* 348–354.

Barros, A.P. and *Hwu, W.,* 2002: A study of land-atmosphere interactions during summertime rainfall using a mesoscale model. *J. Geophys. Res.: Atmospheres, 107(D14)*, ACL-17. https://doi.org/10.1029/2000JD000254

Barry, R.G. and *Chorley, R.J.*, 2003: Atmosphere, weather, and climate. Psychology Press. https://doi.org/10.4324/9780203016206

Betts, A.K., 2000: Idealized model for equilibrium boundary layer over land. *J. Hydrometeorol. 1,* 507–523. https://doi.org/10.1175/1525-7541(2000)001<0507:IMFEBL>2.0.CO;2

Bewoor, A.K. and *Kulkarni, V.A.,* 2009: Metrology and measurement. McGraw-Hill Education.

Chang, C.P. Harr, P.A. McBride, J., and *Hsu, H.H.,* 2004: Maritime continent monsoon: annual cycle and boreal winter variability. In East Asian Monsoon. World Scientific,107–150. https://doi.org/10.1142/9789812701411_0003

Daly, E., Porporato, A., and *Rodriguez-Iturbe, I.,* 2004: Modeling photosynthesis, transpiration, and soil water balance: hourly dynamics during interstorm periods. *J. Hydrometeorol, 5*, 546–558. https://doi.org/10.1175/1525-7541(2004)005<0546:CDOPTA>2.0.CO;2

Dessler, A. E., Palm, S.P., Hart, W.D., and *J.D. Spinhirne.,* 2006: Tropo-pause-level thin cirrus coverage revealed by ICESat/Geoscience LaserAltimeter System. *J. Geophys. Res., 111*(D8). https://doi.org/10.1029/2005JD006586

Folkins, I., Loewenstein, M., Podolske, J., Oltmans, S.J., and *Proffitt, M.,* 1999: A barrier to vertical mixing at 14 km in the tropics: Evidence from ozonesondes and aircraft measurements. *J. Geophys. Res.: Atmospheres, 104(D18),* 22095–22102. https://doi.org/10.1029/1999JD900404

Folkins, I., Oltmans, S.J., and *Thompson, A.M.,* 2000: Tropical convective outflow and near surface equivalent potential temperatures. *Geophys. Res. Lett. 27(16),* 2549–2552. https://doi.org/10.1029/2000GL011524

Heymsfield, A.J., 1986: Ice particles observed in a cirriform cloud at−83 °C and implications for polar stratospheric clouds, *J. Atmos. Sci., 43*,851–855, https://doi.org/10.1175/1520-0469(1986)043<0851:IPOIAC>2.0.CO;2

Huang, H.Y. and *Margulis, S.A,*. 2011: Investigating the impact of soil moisture and atmospheric stability on cloud development and distribution using a coupled large-eddy simulation and land surface model. *J. Hydrometeorol. 12,* 787–804. https://doi.org/10.1175/2011JHM1315.1

Hunt, K.M., Turner, A.G., and *Shaffrey, L.C.*, 2018: Extreme daily rainfall in Pakistan and north India: Scale interactions, mechanisms, and precursors. *Month. Weather Rev. 146,* 1005–1022. https://doi.org/10.1175/MWR-D-17-0258.1

Juang, J.Y., Porporato, A., Stoy, P.C., Siqueira, M.S., Oishi, A.C., Detto, M., Kim, H.S., and *Katul, G.G.*, 2007: Hydrologic and atmospheric controls on initiation of convective precipitation events. *Water Resour. Res. 43(3)* 1-10. https://doi.org/10.1029/2006WR004954

Karimi, S., Nazaripour, H., and *Hamidianpour, M.,* 2021: Spatial and temporal variability of precipitation extreme indices in arid and semi-arid regions of Iran for the last half-century. *Időjárás 125,* 83–104. https://doi.org/10.28974/idojaras.2021.1.4

Kirshbaum, D.J., Adler, B., Kalthoff, N., Barthlott, C., and *Serafin, S.,* 2018: Moist orographic convection: Physical mechanisms and links to surface-exchange processes. *Atmosphere, 9(3),* 80. https://doi.org/10.3390/atmos9030080

Knapp, K.R., Kruk, M.C., Levinson, D.H., Diamond, H.J., and Neumann, C.J., 2010: The international best track archive for climate stewardship (IBTrACS) unifying tropical cyclone data. *Bull. Amer. Meteorol. Soc. 91,* 363–376. https://doi.org/10.1175/2009BAMS2755.1

Kripalani, R.H. and *Kulkarni, A.,* 1997: Rainfall variability over South–east Asia—connections with Indian monsoon and ENSO extremes: new perspectives. International *J. Climatol. 17,* 1155–1168. https://doi.org/10.1002/(SICI)1097-0088(199709)17:11<1155::AID-JOC188>3.0.CO;2-B

Kubar, T.L., Hartmann, D. L., and *Wood, R.,* 2007: Radiative and convective driving of tropical high clouds. *J. Climate, 20,* 5510–5526. https://doi.org/10.1175/2007JCLI1628.1

Loo, Y.Y., Billa, L., and *Singh, A.,* 2015: Effect of climate change on seasonal monsoon in Asia and its impact on the variability of monsoon rainfall in Southeast Asia. *Geosci. Frontiers 6,* 817–823. https://doi.org/10.1016/j.gsf.2014.02.009

Margulis, S.A. and *Entekhabi, D.,* 2001: Feedback between the land surface energy balance and atmospheric boundary layer diagnosed through a model and its adjoint. *J. Hydrometeorol 2,* 599–620. https://doi.org/10.1175/1525-7541(2001)002<0599:FBTLSE>2.0.CO;2

Medeiros, B., Hall, A., and *Stevens, B.,* 2005: What controls the mean depth of the PBL?. *J. Climate 18,* 3157–3172. https://doi.org/10.1175/JCLI3417.1

Nee, J.B., C.N. Len, W.N. Chen, and *C.I. Lin.,* 1998: Lidar observation ofthe cirrus cloud in the tropopause at Chung-Li (25°N, 121°E). *J. Atmosph. Sci. 55,* 2249– 2257. https://doi.org/10.1175/1520-0469(1998)055<2249:LOOTCC>2.0.CO;2

Noël, V. and *M. Haeffelin.*, 2007: Mid latitude cirrus clouds and multiple tropopauses from a 2002–2006 climatology over the SIRTA observatory. *J. Geophys. Res. 112(D13),* 1–11. https://doi.org/10.1029/2006JD007753

Pakistan Meteorological Department, 2020. Retrieved from: https://www.weather-atlas.com/en/pakistan/lahore-climate

Pan, L.L. and *Munchak, L.A.,* 2011: Relationship of cloud top to the tropopause and jet structure from CALIPSO data. *J. Geophys. Res.: Atmospheres 116(D12),* 1–17. https://doi.org/10.1029/2010JD015462

Panda, A. and *Sahu, N.,* 2019: Trend analysis of seasonal rainfall and temperature pattern in Kalahandi, Bolangir and Koraput districts of Odisha, India. *Atmosph. Sci. Lett. 20(10),* e932. https://doi.org/10.1002/asl.932

Posselt, D.J., G.L. Stephens, and *M. Miller.,* 2008: CloudSat: Adding a new dimension to a classical view of extra tropical cyclones, *Bull. Amer. Meteorol. Soc. 89,* 599–609. https://doi.org/10.1175/BAMS-89-5-599

Rani, B.K., Rani, B.P., and *Babu, A.* ., 2015: Cloud computing and inter-clouds–types, topologies and research issues. *Procedia Comput. Sci. 50*, 24–29. https://doi.org/10.1016/j.procs.2015.04.006

Reed, R.J. and *Recker, E.E.,* 1971: Structure and properties of synoptic-scale wave disturbances in the equatorial western Pacific. *J. Atmosph. Sci. 28,* 1117–1133. https://doi.org/10.1175/1520-0469(1971)028<1117:SAPOSS>2.0.CO;2

Richardson, W., Krishnaswami, H., Vega, R., and *Cervantes, M.,* 2017: A low cost, edge computing, all-sky imager for cloud tracking and intra-hour irradiance forecasting. *Sustainability, 9(4),* 482. https://doi.org/10.3390/su9040482

Siddiqui, R. and *Siddiqui, S.,* 2019: Assessing the rooftop rainwater harvesting potential in urban residential areas of Pakistan: a case study of model town, Lahore, Pakistan. *Int. J. Economic Environ. Geology 9(2),* 11–19.

Sivakumar, M.V. and *Stefanski, R.,* 2009: Climate change mitigation, adaptation, and sustainability in agriculture. *Időjárás 113,* 89–102.

Stockham, A.J., Schultz, D.M., Fairman Jr, J.G., and Draude, A.P. 2018: Quantifying the rain-shadow effect: results from the Peak District, British Isles. *Bull. Amer. Meteorol. Soc. 99,* 777–790. https://doi.org/10.1175/BAMS-D-17-0256.1

The news international, 2020. Retrieved from: https://www.thenews.com.pk/tns/detail/697368-a-map-for-a-map

Zeng, X., 1999: The relationship among precipitation, cloud-top temperature, and precipitable water over the tropics. *J. Climate 12,* 2503–2514. https://doi.org/10.1175/1520-0442(1999)012<2503:TRAPCT>2.0.CO;2

Zhisheng, A., Guoxiong, W., Jianping, L., Youbin, S., Yimin, L., Weijian, Z., Yanjun, C., Anmin, D., Li, L., Jiangyu, M., Hai, C., Zhengguo, Z., Liangcheng, T., Hong, Y., Hong, A., Hong, C., and *Juan, F.*, 2015: Global monsoon dynamics and climate change. *Ann.Rev. Earth Planet. Sci. 43,* 29–77. https://doi.org/10.1146/annurev-earth-060313-054623

DOI:10.28974/idojaras.2022.3.3

IDŐJÁRÁS

Quarterly Journal of the Hungarian Meteorological Service
Vol. 126, No. 3, July – September, 2022, pp. 319–334

Frequency and variability trends of extreme meteorological events in theMoson Plain, Hungary (1961–2018)

Tamás Füzi and **Márta Ladányi**

Hungarian University of Agriculture and Life Sciences
Department of Applied Statistics
Villányi út 29-43, 1118 Budapest, Hungary

**Corresponding author E-mail: fuzi.tamas@kertk.szie.hu*

(Manuscript received in final form June 11, 2021)

Abstract— Corresponding to the global trends, the territory of Hungary is endangered by extreme weather manifestations. The increased frequency of the unfavorable effects (inland water, flood, drought, heat stress) can be detected. These harmful manifestations result in a significant economic and environmental risk. To investigate adverse environmental effects and risks that have an impact on economic and productive activities is essential. The aim of our research is to present the transformation of the climatic system of the Moson Plain in the northwestern part of Hungary by analyzing special indicators based on daily temperature and precipitation data covering approximately two climatic cycles (1961–1990; 1991–2018). Based on our results, we can report the formation of a warming microclimate with whimsical precipitation rates, which is accompanied by a decrease in low temperature values. At the same time, we can observe more prominent manifestations of heat waves.

Key-words: climate change, Moson Plain, heat waves, drought, frost-free

1. Introduction

The global change of the climate system has different effects at the regional and local levels. The analysis and subsequent evaluation of past manifestations is the most important task, as regional measurements and modeling are the best ways to

reproduce the climatic characteristics of a large geographical area, such as the Carpathian Basin (*Illy et al.,* 2015).

Regional consequences of climate change manifestations are also of increased importance, because the climate sensitivity and vulnerability of the Carpathian Basin and Hungary are unique, and this region is extremely vulnerable to weather conditions.

Climate change is not just about rising temperatures. In the future, we need to anticipate and prepare for more and more frequent and intense manifestations of exaggerated and extreme weather events (*Ummenhofer* and *Meehl,* 2017). These are the changes to which our social and economic systems have to adapt to (*Buzási et al.,* 2018). The significance of this lies in their dependence on the weather. Such changes in the climate system affect the successful operation and fertility of many areas, from landscape, natural geography and hydrography to public welfare and provisioning opportunities.

These changes are mainly reflected in the alteration of temperature and precipitation data, which show the shift of vegetation zones (*Dunkel et al*., 2018; *Gáborjányi et al*., 2007), and the prolongation of vegetation periods (*Jolánkai et al.,* 2016). The transformation of cultivation conditions and the distortion of regional weather conditions are also faced.

We investigated the signs of climate system change and explored the consequences and effects of these changes, in order to precisely identifying the need of adaptation to adverse conditions. In the present study, we analyze the microclimate of the Moson Plain in the northwestern part of the country based on temperature and precipitation data of the past nearly 60 years, with a particular focus on changes in the frequency of extreme events. We do all this in order to supply producers, farmers, and other actors of the economy with information that helps them carry out successful and productive work for the national economy, in spite of adverse environmental factors.

2. Literature review

The rise in the concentration of atmospheric pollutants, which was considered drastic as early as the middle of the 20th century, was noted by *Landsberg* (1979) nearly half a century ago. It was mentioned in regard of global warming, which was confirmed by Flohn in his 1980 study (*Flohn*, 1980). Since then, climate change has been the subject of numerous international and Hungarian scientific publications, which have become more and more complex and severe over the years. *Faragó et al.* (1990) drew a clear parallel between human activity and climate change, global warming, and the emergence of extreme weather events and their signs in Hungary. According to a 2019 report by the World Meteorological Organization, 2019 was the second warmest year since the start of instrumental measurements, with global average temperatures 1.1 °C higher

than pre-industrial temperatures. Furthermore, the decade of 2010–2019 was found to be the hottest ten years since 1850 (*WMO*, 2019).

According to a report by the European Environment Agency, Europe is also experiencing continued warming (*EEA*, 2017) and the accompanying increase in the number of hot days (*EEA,* 2018). This phenomenon is particularly harmful to our daily lives, and it may lead to other extreme atmospheric conditions and adverse environmental changes. These may include, but are not limited to, rising land and ocean temperatures, changes in rainfall distribution, inland watering in some areas, or even droughts, all of which can adversely affect the environment throughout the year (*Mika,* 2018; *Nordhaus,* 2019). Droughts in Europe were most pronounced in the Mediterranean and the Carpathian Basin, with an increase in frequency, severity, and duration since the 1950s (*Spinoni et al.,* 2015a). According to *Gosic* and *Trajkovic* (2013), droughts occurring every 3–5 years are the greatest environmental threat in the Carpathians, and it is also becoming a global problem due to increasing global warming (*Maracchi*, 2000; *Spinoni et al.,* 2015b). According to *Bozó et al.* (2010), an additional risk is that the Carpathian Basin is one of the most climate-sensitive areas. Climate change is expressed in a unique way due to territorial heterogeneity, as different climatic zones exert their effects on radically different regions (*Gelybó et al*., 2018).

According to the report of the Hungarian Meteorological Service, the average temperature in Hungary has increased by more than 1.1 °C since 1901, but in recent decades (since 1981), the increase in average temperature has become even more intense (1.97 °C between 1981 and 2016), which varied between 1.2 and 1.8 °C in different parts of the country, and became particularly strong in the heat wave days typical during the summer months (*Bartholy et al*., 2011; *Lábó et al.,* 2018). According to *Pálvölgyi et al.* (2011), 52% of Hungary's territory is particularly vulnerable to heat waves, and this is in line with Hoyk's (2015) statement that the regional climate models (ALADIN-Climatemodel, REMO-model, PRECIS-model, RegCM-model) used in Hungary, forecast a significant increase in temperature by 2050. Thus, throughout the territory of Hungary, the unfavorable effects of climate change and the extreme manifestations of weather occurrences (heat waves, hot days) are becoming more and more typical. This means that the average temperature of the annual and summer days will increase significantly, while the number of frost winter days and the average rainfall during the summer will decrease greatly (*Uzzoli*, 2015).

As a result of climate change in Central Europe, and also in Hungary, we have to reckon with wetter and milder winters and drier summers with higher average temperatures (*Sassi et al*., 2019; *Feurdean et al.,* 2020).

Consequently, water shortage can be expected to become more severe as heat causes an increase in the water consumption, which is accentuated by declining rainfall and increasing evaporation at the surface of water and soil. During the drought period, the moisture of the soil decreases, with which the groundwater level drops (*Harnos* and *Csete*, 2008). Temporal and spatial fluctuations of

meteorological conditions can affect soil conditions, water supply, and agricultural yields (*Boubacar*, 2010; *Łabędzki* and *Bąk*, 2017). It can also accelerate the spread of new types of pests and pathogens (*Szabó* and *Fári*, 2017; *Bánáti*, 2019). In warmer climates, the activity and geographical spread of pests are also changing, which may lead to increased use of agrochemicals, accompanied by increasing health, ecological, and economic difficulties (*Rosenzweig et al*., 2001).

This process indicates that crop production must face the challenges posed by climate change and the cumulative negative effects as the transformation of the climate system is projected to be accompanied by rapidly rising temperatures, more frequent droughts, and other hydroclimatic extremes (*Pinke* and *Lövei*, 2017). As such, the crop production sector needs to be prepared for the more frequent water shortages, the drought stress caused by the intensifying heat waves, and the associated significant crop losses (*Challinor et al*., 2010; *Teixeira et al.,* 2013). All of these extremes, associated with climate change, affect continental climate berry fruits in highly unfavorable ways, as in the ripening phase – in the warmest and driest phase of the year –, the leaf and fruit scorching of plants can result in decreased photosynthesis, decline in plant development, and crop loss (*Keller et al.,* 2017).

However, the adverse effects of the consequences of climate change diverge considerably from region to region depending, among other things, on differences in biophysical resources, farming, adaptability, or even crop production. These experienced and observed adverse effects could lead to further territorial differentiation in a situation, where inequality already exists. As such, the less well-conditioned areas, which are still experiencing economic difficulties, may fall further behind due to a lack of resources (*Lobell et al.,* 2008; *Bognár* and *Erdélyi*, 2018).

Therefore, according to *Mcleman* and *Smit* (2006), we need to focus not only on understanding the climate system but also on the dangers of climate change manifestations, as these changes represent physical hazards that manifest in extreme forms.

3. Data and methods

In our study, we investigated the changes in weather conditions of the Moson Plain. Daily data (average, minimum, maximum temperature (°C) and precipitation (mm)) for this area were requested from the database of the local measuring station in Mosonmagyaróvár, maintained by the Hungarian Meteorological Service. Our research takes approximately two climatic cycles into consideration: the reference period 1961–1990 and the recent time zone 1991–2018.

Based on indicators formed from various temperature thresholds, we examined their frequencies of occurrences (days) in 30 and 28 years on a monthly basis.

The following temperature indicators were examined (days):

- Extremely hot days (T_{max}>35 °C): the maximum daily temperature was above 35 °C,
- Hot days (30°C<T_{max}<35 °C): maximum daily temperature was between 30 °C and 35 °C,
- Summer days (25 °C<T_{max} 30 °C): maximum daily temperature was between 25 °C and 30 °C,
- Mild days (0 °C<T_{max}<25 °C): maximum daily temperature was between 0 °C and 25 °C,
- Winter days (T_{max}<0 °C): maximum daily temperature was below 0 °C,
- Tropical nights (T_{min}>20 °C): the minimum night temperature was above 20 °C,
- Warm nights (18°C<T_{min}<20 °C): the minimum night temperature was between 18 °C and 20 °C,
- Frost days (-5 °C<T_{min}<0 °C): the daily minimum temperature was between -5 °C and 0 °C,
- Hard frost days (-15 °C<T_{min}<-5 °C): the daily minimum temperature was between -15 °C and -5 °C, and
- Extremely frosty days (T_{min}<-15 °C): the daily minimum temperature was below -15 °C.

In addition to the above, in the time interval between April and September, we examined the lengths (days) of the three longest continuously precipitation-free periods of the years. We also examined the lengths (days) of the precipitation periods immediately preceding and following the precipitation-free periods and the amount (mm) and average (mm) of precipitation during these time intervals as well.

We examined and illustrated the change in the length of the precipitation-free periods according to time categories (shorter than 7 days, 8–10 days, 11–14 days, and longer than 2 weeks). Our analyses were performed on a monthly basis, and the changes were summarized for the reference period 1961–1990 and the recent time period 1991–2018.

Two-sample ratio test (Z-test) was used to compare the differences of the occurrence frequencies (i.e., the temperature indicator values) between the reference period and the recent climate cycle. We also performed frequency analysis with cross-tabulation (Chi-square tests) to compare the time intervals 1961–1990 and 1991–2018, according to the distributions of the three longest precipitation-free periods between April and September, in Mosonmagyaróvár. In the case of precipitation indicators, linear trend analysis was also performed: using Student's t tests for the linear regression slopes, we tested whether they showed significant change. The distributions of lengths of the three longest precipitation-free periods are compared also by Chi-square test (cross-tabulation).

4. Results

Our results obtained by evaluating the temperature data are shown in *Tables 1–3*. These tables show the temperature indicators we have defined, the Z-values obtained by the statistical tests, the directions of changes, the levels of significances of the changes, the occurrences experienced in climate cycles by decades expressed in days, and the extents of changes between the two climate cycles.

Table 1 shows the indicators formed from the daily maximum temperature values.

The number of days with maximum temperatures (summer, heat, and hot between 25–30 °C, 30–35 °C, and above 35 °C, respectively) show an increasing trend. This change is typically significant in the spring-summer months ($p<0.05$). Among the examined indicators, the number of extremely hot days ($T_{max}>35$ °C) increased the most, the change was also significant in June-July and August ($p<0.001$).

Their number – by the end of summer, in August – in the recent climate cycle (1991–2016) – increased more than 20-fold compared to the reference period (1961–2016) (*Table 1*). This implies a notable risk of temperature rise and heat stress, which is also supported by Németh's (2019) study, according to which, an increase in the frequency of heat waves and average annual temperature in Vas and Győr-Moson-Sopron counties can be observed and experienced by producers.

Table 1. Frequencies of maximum temperature indicators for two climate cycles (1961–1990; 1991–2018): the significance level of the change (Z-value), direction and extent of change within the climate cycle (days) and in the comparison of the two climate cycles (Mosonmagyaróvár)

Indicators	Months	Z-value	Direction of change between the two climate cycles	Decade average incidence (days) (1961–1990)	Decade average incidence (days) (1991–2018)	The change between the two climate cycles
Extremely hot days T_{max}>35 °C	June-July	4.105***	increasing	1	9	6.7
	August	5.98***	increasing	<1	14	20.4
Hot days 30 °C<T_{max} <35 °C	April-May	3.30***	increasing	1	6	6.1
	June	6.16***	increasing	18	45	2.5
	July	6.71***	increasing	50	91	1.8
	August	4.88***	increasing	42	69	1.7
	September	0.83ns		6	6	
Summer days 25 °C<T_{max} <30 °C	April-May	4.28***	increasing	65	95	1.4
	June	2.44*	increasing	102	119	1.2
	July	0.12ns		128	127	
	August	2.04*	increasing	121	135	1.1
	September	1.86ns		56	66	
	October	0.56ns		4	5	
Mild days 0 °C<T_{max} <25 °C	January	2.96**	increasing	196	217	1.1
	February	1.68ns		235	244	
	March	1.06ns		300	303	
	April	1.74ns		290	285	
	May	4.63***	decreasing	254	225	0.9
	June	6.21***	decreasing	180	135	0.8
	July	6.66***	decreasing	130	84	0.6
	August	7.64***	decreasing	147	93	0.6
	September	1.81ns		238	228	
	October	0.56ns		47	39	
	November	0.67ns		291	289	
	December	2.23*	increasing	230	244	1.1
Winter days T_{max}<0 °C	January	2.96**	decreasing	114	93	0.8
	February	1.61ns		47	39	
	March	1.06ns		10	7	
	November	0.67ns		9	11	
	December	2.23*	decreasing	94	66	0.7

In contrast to the increase in the number of extremely hot, hot, and summer days, the number of mild days (T_{max} 0–25 °C) free from extreme heat, decreased significantly in the late spring-summer months ($p<0.001$). The reason for this change is that non-extreme and risk-free days have been replaced by high and extremely high temperature days associated with intense warming (*Table 1*).

Table 1 also shows a special category of frost days (referred to 'winter days'), when even the daily maximum temperature does not reach 0 °C. The number of such days in late autumn (November) and late winter - early spring (February and March) has not changed significantly during the past nearly 60 years ($p>0.05$). However, during the dormant period (December and January), their number decreased significantly ($p<0.05$) in Mosonmagyaróvár in the recent climate cycle (1991–2018) compared to the reference period (1961–1990).

The disappearance of frosts together with the less frequent appearance of snow-cover, are accompanied by a transformation of the ecosystem structure, the phenomenon of plant species shifting further north (*Bokhorst et al.,* 2008). The lack of winter days results in a warming and drying environment, intensified evapotranspiration processes during the dormant period, and, due to the insufficient development of frost tolerance, leads to increased frost sensitivity and early loss of resistance (*Lun et al*., 2020). This result was also reached by *Ferguson et al.* (2011). Using a thermal time model, he estimated the temperature thresholds required to achieve frost tolerance of three grapevine varieties are between 4.25 °C and 5.75 °C, i.e., the thresholds below which the chilling effect can prevail.

According to *Horváth* and *Komarek* (2016), in the temperate zone, some perennial cultivars may require a minimum temperature sum during the dormant period below -6 °C, which, if not obtained, may cause similar degree of damage as too high temperatures.

In parallel with the increasing frequency of high-temperature days, during the past nearly six decades, the time interval of potential high temperature occurrences also widened from the late spring months to the early autumn months. In contrast, the occurrence of lower temperature (winter) values within a year has become rarer, and the appearance of such values narrowed down to an ever-shorter period. The occurrences of indicators determined by daily minimum temperature values are shown in *Table 2*.

Table 2. Frequencies of minimum temperature indicators for two climate cycles (1961–1990; 1991–2018): the significance level of the change (Z-value), direction and extent of change within the climate cycle (days) and in the comparison of the two climate cycles (Mosonmagyaróvár)

Indicators	Months	Z value	Direction of change between the two climate cycles	Decade average incidence (days) (1961–1990)	Decade average incidence (days) (1991–2018)	The change between the two climate cycles
Tropical nights T_{min}>20 °C	July	4.70***	increasing	2	12	6.1
	August	3.23**	increasing	2	8	3.9
Warm nights 18 °C<T_{min} <20 °C	May	1.42ns		0	1	
	June	3.19**	increasing	9	17	1.8
	Jule	4.93***	increasing	16	35	2.3
	August	4.68***	increasing	16	35	2.2
	September	2.23*	increasing	1	3	4.8
Frost days -5 °C<T_{min} <0 °C	January	0.42ns		127	130	
	February	1.50ns		114	125	
	March	0.61ns		92	96	
	April	0.06ns		23	24	
	May	1.05ns		2	1	
	October	1.48ns		30	24	
	November	0.52ns		83	81	
	December	1.48ns		140	129	
Hard frost days -15 °C<T_{min} <-5 °C	January	3.42***	decreasing	107	84	0.8
	February	0.31ns		60	58	
	March	1.64ns		21	15	
	October	0.71ns		3	2	
	November	2.20*	decreasing	17	10	0.6
	December	0.99ns		64	58	
Extremely frost days T_{min}<-15 °C	January	3.09**	decreasing	12	5	0.4
	February	1.95ns		6	3	
	December	1.30ns		2	4	

In general, the number of days with different strengths of frost (frost days, hard and extremely frost days T_{min}<0 °C) decreased, although in terms of their frequency, in most cases, the change between the two climate cycles (1961–1990; 1991–2016) was not significant (p>0.05). There was no significant change in the number of frost days (-5 °C<T_{min}<0 °C) during any month (p>0.05). However, the number of hard frost days (-15 °C<T_{min}<-5 °C) decreased significantly in January and November

($p<0.001$; $p<0.05$). The frequency of extremely frost days (T_{min}<-15 °C) fell to less than its half in January for the recent climate cycle (1991–2018, $p<0.01$).

Among the daily minimum temperatures, special attention should be paid to the increase in the number of hot events (T_{min}>20 °C), that is also referred to in the literature as a tropical night (*Cantos et al*., 2019). Changing its frequency is one of the greatest risk factors in agriculture, because tropical nights are more injurious to crop quality, plant growth, and development than daytime heat (*Ryu et al*., 2017). In our analytical work, we found that, compared to the reference period (1961–1990), the number of tropical nights in the recent climate cycle increased more than sixfold in July and approximately fourfold in August (*Table 2*). The change was significant in both cases ($p<0.001$).

Of the nights without adequate cooling, the number of warm nights (18 °C<T_{min}<20 °C) increased significantly in all the three summer months ($p<0.01$): 1.8 times in June and more than twice in July and August. The incidence of nights with heat stress was no longer limited to the summer months (*Table 2*), but also extended to the first autumn month: in September, in the recent climate cycle (1991–2018), their number increased approximately five-fold ($p<0.05$).

Table 3. Minimum, maximum, mean, variance and range of the annual frequencies of the examined indicators for 28 and 30 years in the reference and recent periods (1961–1990; 1991–2018) in Mosonmagyaróvár

Indicators	1961–1990					1991–2018				
	min	max	mean	variance	range	min	max	mean	variance	range
Extremely hot days Tmax>35 °C	0	2	0.20	0.55	2	0	14	2.25	3.44	14
Hot days 30 °C<Tmax<35 °C	2	20	11.70	5.22	18	3	40	21.79	9.65	37
Summer days 25 °C<Tmax 30 °C	28	69	47.60	9.97	41	33	85	54.79	11.78	52
Mild days 0 °C<Tmax<25 °C	234	311	279.73	18.50	77	236	285	265.00	12.99	49
Winter days Tmax<0 °C	7	63	26	11.88	56	4	50	21.68	9.68	46
Tropical nights Tmin>20 °C	0	3	0.40	0.72	3	0	9	2.64	2.45	9
Warm nights 18 °C<Tmin<20 °C	0	10	4.07	2.82	10	1	20	9.18	5.26	19
Frost days -5 °C<Tmin<0 °C	39	96	61.23	12.49	57	39	82	60.79	12.33	43
Hard frost days -15 °C<Tmin<-5 °C	0	58	27.13	11.34	58	7	40	22.75	9.96	33
Extremely frost days Tmin<-15 °C	0	13	2.23	3.39	13	0	10	1.18	2.04	10

The average, the variance, and the range of the occurrences of high temperature days (extremely hot days, hot days, summer days, tropical nights, and warm nights) also increased in the recent climate cycle (1991–2018, *Table 3*). This means that the events defined by the examined indicators have become more frequent. Furthermore, the exaggerated manifestations of extreme high temperature events and their increasingly unpredictable recurrence have become commonplace. In many cases, the maximum annual frequencies of the examined indicators doubled (T_{max} 30–35 °C; T_{min} 18–20 °C), tripled (T_{min}>20 °C), or even increased sevenfold (T_{max}>35 °C) for the 1991–2018 climate cycle. As a result, the appearance of some extreme high temperature events become more and more uncertain year by year. Therefore, preparing for and defending against the adverse effects of extreme weather events form a great and unavoidable challenge.

In contrast, the average, the variance, and the range of the extreme-free mild days (T_{max} 0–25 °C) and low-temperature days (frost, hard frost, and extremely frost days) have decreased over the past three decades (1991–2018, *Table 3*). This means that low temperature values have become decreasingly frequent and more predictable in the time periods studied.

Xie et al. (2015) also confirmed that the frequency and the probability distribution of extreme weather events associated with warming are also changing across the globe, which may even manifest itself in an unfavorable form (flooding rain, prolonged drought).

To analyze the occurrence of long precipitation-free periods (daily precipitation<1 mm), we first calculated the lengths (days) of the three longest and uninterrupted precipitation-free periods in both cycles (1961–1990; 1991–2016) between April and September. We also examined the characteristics of precipitation periods directly before and after these periods, such as their lengths (days) and the amount (mm) and average (mm) of precipitation during these time intervals. The lengths of the long precipitation-free period were split into four categories: shorter than 7 days, 8–10 days long, 11–14 days long, and longer than 2 weeks.

Using linear trend analysis, we have found that in the period 1961–2018, considering the time intervals before and after the three longest precipitation-free periods between April and September, the change in the lengths of precipitation periods (before: slope<0.000 p=0.967; after: slope=-0.003; p=0.551), the amount of precipitation (before: slope=0.097 p=0.107; after: slope=-0.004 p=0.944), and the average of precipitation (before: slope=0.039 p=0.053; after: slope=-0.008 p=0.708) were not significant. The same insignificant result was found when we considered the change in the number of days during the three longest continuous rainless periods in the last nearly 60 years (first: slope=0.043 p=0.371; second: slope=0.017 p=0.434; third: slope=0.036 p=0.066).

The distribution of lengths of the three longest precipitation-free periods is expressed in percentages in *Fig. 1*. The distributions of the three longest precipitation-free periods in the two cycles differ significantly ($Khi^2(3)=12.58$;

p<0.01). The first three longest precipitation-free periods lasting less than seven days occurred most frequently (33%) in the reference period (1961–1990) and the most rarely (13%) in the recent climate cycle (1991–2018). This change was significant (Z=3.32, p<0.001).

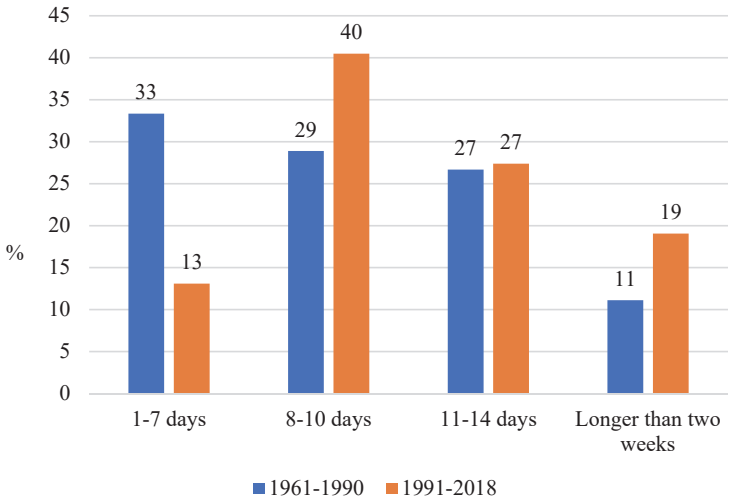

Fig. 1. Distribution of the length of the three longest precipitation-free periods between April and September, expressed in percentages (1961–1990 and 1991–2018 Mosonmagyaróvár).

In recent decades (1991–2018), the length of the three longest uninterrupted precipitation-free periods typically lasted 8–10 days (40%), but in more than a quarter of cases (27%), these periods lasted for up to two weeks, and in nearly a fifth of them (19%) for more than 2 weeks. These values are higher in all three cases than in the reference period (1961–1990), although the difference is not significant in either case (p>0.05).

Our comparative work indicates that the danger of droughts followed by heavy rainfall can reduce the water uptake of soil and increase the potential for runoff and leaching, thereby creating unfavorable conditions for fungal infection of the leaf and root (*Rosenzweig et al*., 2001). The proportion of loss resulting from rainfall-abundance damage (flood, inland water) has increased since the 1970s, which, within Europe, affected Central European countries the most (*EEA*, 2016).

5. Conclusions

In addition to the average values of climatic parameters, the probability, frequency, and severity of their effects on the environment must be taken into consideration when examining changes in the climate system. In the form of statistical evaluation, this knowledge provides more extensive and usable quantified information about the current state of atmospheric conditions affecting our immediate environment.

The results of our studies show an unequivocal warming in the two examined climate cycles (1961–1990; 1991–2018). This is also accompanied not only by the increasing frequency of high or extremely high temperatures, but also by the drastic decrease in the number of low temperatures.

Our results show a change in the length of the three longest uninterrupted precipitation-free periods (days) in the time interval between April and September. We also examined the lengths (days) of the rainy periods immediately preceding and following these precipitation-free periods, the amount (mm) and the average (mm) of precipitation during these time intervals. Although the difference between the two climate cycles was not significant, the combined assessment of quantity and occurrence (i.e., the distribution of precipitation-free days) shows less frequent but more intense precipitation. In addition, the lengths of the longest precipitation-free periods in the April–September interval has been extended significantly, which contributes to severe drought and water scarcity. Based on our results and the work of *Szász* (2002), the long-term lack of precipitation accompanied by extremely high temperatures further amplifies its adverse effect. In addition to rising temperatures, water-stress and unpredictable heavy rainfall events, the disappearance of winter frosts also result in a rearrangement of the ecosystem. The changing environmental conditions affects the plant-production-based economic system seriously, which forces the agro-economic actors find their adaptation strategies.

Our task in the future is to mitigate the anthropogenic impacts that amplify climate change and to prevent the damage to natural resources. While this process is tried to be got under control, we must be prepared to deal with damages that affect our living conditions, health, food production, economy and also to avoid possible disasters. The greatest problem is the simultaneous occurrence of heat and the drought which greatly affects the livelihood of farmers and the success of their production activities. Therefore, water-saving and water-retaining tillage can help against the adverse effects of climate change.

In addition, there is a need to disseminate and develop tools and methods that can counter extreme effects – such as flooding rains, long precipitation-free periods, heat waves, or even the complete absence of frost – and mitigate their consequences.

Such solutions could be the extension of irrigation systems or the breeding of new stress-tolerant plant varieties, which are costly but can effectively result in a reduction of negative impacts (*Lobell et al*., 2008).

References

Bánáti, D., 2019: Az élelmiszerek jövője. Műszaki, technológiai és gazdasági kihívások a 21. században című konferencia: nemzetközi magyar nyelvű tudományos konferencia: előadások és poszterek összefoglalói. (Eds*: Bíró, I., et al*.) Szegedi Tudományegyetem 16. (In Hungarian)

Bartholy, J., Bozó, L., and *Haszpra, L.*, 2011: Klímaváltozás – 2011. Klímaszcenáriók a Kárpát–medence térségére. Magyar Tudományos Akadémia és az Eötvös Loránd Tudományegyetem Meteorológiai Tanszéke, Budapest. (In Hungarian)

Bognár, R. and *Erdélyi, D.*, 2018: Az éghajlatváltozás kihívásai a GDP alapú gazdasági teljesítmény-értékelés számára Magyarország példáján bemutatva. *Studia Mundi–Economica 5*(4), 3–13. (In Hungarian) https://doi.org/10.18531/Studia.Mundi.2018.05.04.3-13

Bokhorst, S., Bjerke, J.W., Bowles, F.W., Melillo, J., Callaghan, T.V., and *Phoenix, G.K.*, 2008: Impacts of extreme winter warming in the sub-Arctic: growing season responses of dwarf shrub heathland. *Glob. Change Biology 14*, 2603–2612. https://doi.org/10.1111/j.1365-2486.2008.01689.x

Boubacar, I., 2010: The effects of drought on crop yields and yield variability in Sahel. Selected Paper prepared for presentation at the Southern Agricultural Economics Association Annual Meeting, Orlando, FL, February 6-9, 2010 (No. 1370-2016-108718).

Bozó, L., Horváth, L., Láng, I., and *Vári, A.*, 2010: Környezeti jövőkép Környezet- és klímabiztonság. Magyar Tudományos Akadémia, Budapest. (In Hungarian)

Buzási, A., Pálvölgyi, T. and *Szalmáné Csete M.*, 2018: K-faktor: Klíma, gazdaság, társadalom. BME Gazdaság-és Társadalomtudományi Kar Környezetgazdaságtan Tanszék, Budapest. (In Hungarian)

Cantos, J.O., Serrano-Notivoli R., Miró J., and *Meseguer-Ruiz, O*., 2019: Tropical nights on the Spanish Mediterranean coast, 1950-2014. *Climate Res. 78*, 225–236. https://doi.org/10.3354/cr01569

Challinor, A.J., Simelton, E.S., Fraser, E.D., Hemming, D., and *Collins, M.*, 2010: Increased crop failure due to climate change: assessing adaptation options using models and socio-economic data for wheat in China. *Environ. Res. Lett. 5*(3), 034012. https://doi.org/10.1088/1748-9326/5/3/034012

Dunkel, Z., Bozó, L. and *Geresdi, I*., 2018: Az éghajlatváltozás hatására fellépő környezeti változások és természeti veszélyek. *Földrajzi Közlemények 142*, 261–271. (In Hungarian) https://doi.org/10.32643/fk.142.4.1

Dunkerley, D., 2015: Intra-event intermittency of rainfall: an analysis of the metrics of rain and no-rain periods. *Hydrol. Proces. 29*, 3294–3305. https://doi.org/10.1002/hyp.10454

EEA, 2016: Floodplain management: reducing flood risks and restoring healthy ecosystems. https://www.eea.europa.eu/highlights/floodplain-management-reducing-flood-risks.

EEA, 2017: Climate change, impacts and vulnerability in Europe 2016. An indicator-based report. European Environment Agency, 71.; 76..

EEA. 2018: Global and European temperature, https://www.eea.european.eu/data-and-maps/indicators/global-and-european-temperature-9/assessment

Faragó, T., Führer, E., Iványi, Z., Járó, Z., Jászay, T., and *Práger, T.*, 1990: Az éghajlat változékonysága és változása: okok, folyamatok, regionális hatásaik különös tekintettel a lehetséges társadalmi-gazdasági következményekre. Környezetvédelmi és Területfejlesztési Minisztérium, Országos Meteorológiai Szolgálat. Budapest. (In Hungarian)

Feurdean, A., Vannière, B., Finsinger, W., Warren, D., Connor, S. C., Forrest, M., Liakka, J., Panait, A., Werner, C., Andricˇ, M., Bobek, P., Carter, A. V., Davis, B., Diaconu A-C., Dietzel, E., Feeser, I., Florescu, G., Gałka, M., Giesecke, T., Jahns, S., Jamrichová, E., Kajukało, K., Kaplan, J., Karpinska-Kołaczek, M., Kołaczek, P., Kuneš, P., Kupriyanov, D., Lamentowicz, M., Lemmen, C., Magyari, E. K., Marcisz, K., Marinova, E., Niamir, A., Novenko, E., Obremska, E., P˛edziszewska, A., Pfeiffer, M., Poska, A., Rösch, M., Słowinski , M., Stan ˙cikait ˇe˙, M., Szal, M., Swi˛eta-Musznicka ´, J., Tan˛tauˇ I., Theuerkauf, M., Tonkov, S., Valkó, O., Vassiljev, J., Veski, S., Vincze, I., Wacnik, A., Wiethold, J., and *Hickler T.*, 2020: Fire hazard modulation by long-term dynamics in land cover and dominant forest type in eastern and central Europe. *Biogeosci. 17*, 1213–1230. https://doi.org/10.5194/bg-17-1213-2020

Flohn, H., 1980: Possible climatic consequences of a man-made global warming. IIASA, RR80-30.

Gáborjányi, R., Barna, B., Basky, Z., Benedek, P., Holb, I., Kazinczi, G., and *Kövics, G.*, 2007: A globális éghajlatváltozás várható hatásai a növényvédelemben. Szaktudás Ház Kiadó, 204–206. (In Hungarian)

Gelybó, G., Tóth, E., Farkas, C., Horel, Á., Kása, I., and *Bakacsi, Z.*, 2018: Potential impacts of climate change on soil properties. Agrokémia és Talajtan 67, 121–141. https://doi.org/10.1556/0088.2018.67.1.9

Gosic, M., and *Trajkovic, S.*, 2013: Analysis of precipitation and drought data in Serbia over the period 1980–2010. *J. Hydrology 494*, 32–42. https://doi.org/10.1016/j.jhydrol.2013.04.044

Harnos, Zs. and *Csete, L.* (szerk.) 2008: Klímaváltozás: környezet - kockázat – társadalom, Szaktudás Kiadó Ház, Budapest. (In Hungarian)

Horváth, J. and *Komarek, L.*, 2016: A világ mezőgazdaságának fejlődési tendenciái. Hódmezővásárhely, Innovariant Nyomdaipari Kft, NKA. 19. (In Hungarian)

Illy, T., Sábitz, J., and *Szépszó, G.*, 2015: Az ALADIN-Climate modellkísérletek eredményeinek validációja. RCMTéR (EEA-C13-10) projekt beszámoló, Országos Meteorológiai Szolgálat, Budapest, 19. (In Hungarian)

Ferguson, J.C., Tarara J.M., Mills, L.J., Grove, G.G., and *Keller, M.*, 2011: Dynamic thermal time model of cold hardiness for dormant grapevine buds. *Ann. Botany 107*, 389–396. https://doi.org/10.1093/aob/mcq263

Jolánkai, M., Tarnawa, A., Horvath, C., Nyárai, F.H., and *Kassai, K.*, 2016: Impact of climaticfactors on yield quantity and quality of grain crops. *Időjárás120*, 73–84.

Keller, B., Jung, A., Nagy, G.M., Dénes, F., Péterfalvi, N., Szalay, K.D., 2017: Hiperspektrális távérzékelés alkalmazási lehetőségeinek bemutatása egy málna ültetvény példáján keresztül. A Kutatói utánpótlást elősegítő program a Nemzeti Agrárkutatási és Innovációs Központban a Földművelésügyi Minisztérium támogatásával valósul meg. fiatalkutato. naik. hu, 63.

Łabędzki, L.Ł. and *Bąk, B.*, 2017: Impact of meteorological drought on crop water deficit and crop yield reduction in Polish agriculture. *J. Water Land Develop. 34*, 181–190. https://doi.org/10.1515/jwld-2017-0052

Lábó, E., Zsebeházi, G., and *Lakatos, M.*, 2018: Az IPCC 1,5 fokos globális hőmérséklet-emelkedést értékelő Tematikus Jelentésének margójára. OMSZ. https://www.met.hu/ismeret-tar/erdekessegek_tanulmanyok/index.php?id=2334&hir=Az_IPCC_1,5_fokos_globalis_homerseklet-emelkedest_ertekelo_Tematikus_Jelentesenek_margojara (Donwloaded: 2020. 08. 25.) (In Hungarian)

Landsberg, H.E., 1979: Climatic fluctuations. In "Yearbook. Science and Technology", McGraw Hill.

Lobell, D.B., Burke, M.B., Tebaldi, C., Mastrandrea, M.D., Falcon, W.P., Naylor, R.L., 2008: Prioritizing climate change adaptation needs for food security in 2030. *Science 319*(5863), 607–610. https://doi.org/10.1126/science.1152339

Lun, D., Fischer, S., Viglione, A., and *Blöschl, G*. 2020: Detecting flood-rich and flood-poor periods in annual peak discharges across Europe. *Water Resour. Res. 56*(7), e2019WR026575. https://doi.org/10.1029/2019WR026575

Maracchi, G., 2000: Agricultural drought—A practical approach to definition, assessment and mitigation strategies. In (Eds. *J.V. Vogt*, and *F. Somma*) Drought and drought mitigation in Europe. Advances in natural and technological hazards research14, 63–78. https://doi.org/10.1007/978-94-015-9472-1_5

Mcleman, R. and *Smit, B.* 2006: Vulnerability to climate change hazards and risks: crop and flood insurance. *Canadian Geographer/Le Géographe canadien*, *50*, 217–226. https://doi.org/10.1111/j.0008-3658.2006.00136.x

Mika, J., 2018: A klímaváltozás világléptékű, európai és hazai újdonságai. Természet-, műszaki-és gazdaságtudományok alkalmazása nemzetközi konferencia, 8–18. (In Hungarian)

Németh, N., 2019: A magyar mezőgazdálkodók éghajlatváltozáshoz való alkalmazkodóképességének vizsgálata Győr-Moson-Sopron és Vas megyékben (Doctoral dissertation, nyme). (In Hungarian)

Nordhaus, W., 2019: Climate change: The ultimate challenge for Economics. *Amer. Economic Rev. 109*, 1991–2014. https://doi.org/10.1257/aer.109.6.1991

Pálvölgyi, T., Czira, T., Bartholy, J., and *Pongrácz, R.* 2011: Éghajlati sérülékenység a hazai kistérségek szintjén. In: (Eds.: *Bartholy J., Bozó L., Haszpra L.*) : Klímaváltozás – 2011. Klímaszcenáriók a Kárpát-medence térségére. MTA, ELTE, Budapest, 236–256. (In Hungarian)

Pinke, Z. and *Lövei, G.L.*, 2017: Increasing temperature cuts back crop yields in Hungary over the last 90 years. *Glob. Change Biol. 23*, 5426–5435. https://doi.org/10.1111/gcb.13808

Rosenzweig, C., Iglesias, A., Yang, X.B., Epstein, P.R., and *Chivian, E.* 2001: Climate change and extreme weather events; implications for food production, plant diseases, and pests. *Glob. Change Human Health 2*(2), 90–104. https://doi.org/10.1023/A:1015086831467

Ryu, S., Han, H.H., Jeong, J.H., Kwon, Y., Han, J.H., Do, G. R., ChoiI, M. and *Lee, H.J.*, 2017: Night temperatures affect fruit coloration and expressions of anthocyanin biosynthetic genes in 'Hongro'apple fruit skins. *Eur. J. Hortic. Sci. 82*, 232–238. https://doi.org/10.17660/eJHS.2017/82.5.2

Sassi, M., Nicotina, L., Pall, P., Stone, D., Hilberts, A., Wehner, M., and *Jewson S.*, 2019: Impact of climate change on European winter and summer flood losses. *Adv. Water Resour. 129*, 165–177. https://doi.org/10.1016/j.advwatres.2019.05.014

Spinoni, J., Naumann, G., Vogt, J., and *Barbosa, P.*, 2015a: European drought climatologies and trends based on a multi-indicator approach. *Glob. Planet. Change 127*, 50–57. https://doi.org/10.1016/j.gloplacha.2015.01.012

Spinoni, J., Szalai, S., Szentimrey, T., Lakatos, M., Bihari, Z., Nagy, A., Németh, A., Kovács, T., Mihic, D,. Dacic, M., Petrovic, P., Krži˘c, A., Hiebl, J., Auer, I., Milkovic, J., Štepánek, P., Zahradnícek, P., Kilar, P., Limanowka, D., Pyrc, R., Cheval, S., Birsan, M. V., Dumitrescu, A., Deak, G., Matei, M., Antolovic, I., Nejedlík, P., Štastný, P., Kajaba, P., Bochnícek, O., Galo, D., Mikulová, K., Nabyvanets, Y., Skrynyk, O., Krakovska, S., Gnatiuk, N., Tolasz, R., Antofie T., and *Jürgen V.*, 2015b: Climate of the Carpathian Region in the period 1961–2010: climatologies and trends of 10 variables. *Int. J. Climatol. 35*, 1322–1341. https://doi.org/10.1002/joc.4059

Szabó, M. and *Fári, M.G.*, 2017: Új egynyári dísznövény nemesítési alapanyag létrehozása mutáns-indukcióval és a vegetatív szaporítás lehetőségei, XXIII. Növénynemesítési Tudományos Nap, Szerk.: Veisz Ottó, MTA Agrártudományok Osztálya 71. (In Hungarian)

Szász, G., 2002: Utilization of Climatic Natural Resources in Domestic Crop Production. *Acta Agraria Debreceniensis 9*, 101–106. https://doi.org/10.34101/actaagrar/9/3567

Teixeira, E.I., Fischer, G., Van Velthuizen, H., Walter, C., and *Ewert, F.* 2013: Global hot-spots of heat stress on agricultural crops due to climate change. *Agricult. Forest Meteorol. 170*, 206–215. https://doi.org/10.1016/j.agrformet.2011.09.002

Ummenhofer, C.C. and *Meehl, G.A.*, 2017: Extreme weather and climate events with ecological relevance: a review. *Philosop. Trans.Roy. Soc. B: Biological Sciences*, 372(1723), 20160135. https://doi.org/10.1098/rstb.2016.0135

Uzzoli, A., 2015: Klímamodellek a társadalmi alkalmazkodásban–A sérülékenységvizsgálatok hazai eredményei és tapasztalatai. 109–126.

WMO, 2019: World Meteorological Organization Statement on the State of the Global Climate in 2019, WMO, ISBN 978-92-62-11248-5

Xie, S. P., Deser, C., Vecchi, G. A., Collins, M., Delworth, T. L., Hall, A., and *Watanabe, M.* 2015: Towards predictive understanding of regional climate change. Nat. Climate Change 5(10), 921-930. https://doi.org/10.1038/nclimate2689

DOI:10.28974/idojaras.2022.3.4

IDŐJÁRÁS

Quarterly Journal of the Hungarian Meteorological Service
Vol. 126, No. 3, July – September, 2022, pp. 335–353

Precipitation trends in Turkey (1969–2018): A spatiotemporal analysis

Saffet Erdoğan*, **Mustafa Ulukavak**, and **Mehmet Yılmaz**

Harran University, Engineering Faculty
Department of Geomatics,
Osmanbey Campus Haliliye Şanlıurfa,63100 Turkey

**Corresponding Author e-mail: serdogan@harran.edu.tr*

(Manuscript received in final form April 3 2021)

Abstract— Global climate change can have significant impacts on different geographical regions. It is very important to analyze the changes in temporal and spatial precipitation patterns. In this study, the monthly and yearly precipitation values in Turkey were examined by combining the nonparametric Mann-Kendall rank correlation test and Getis-Ord G spatial clustering test. The study was carried out by integrating and compiling the data in different formats related to the years 1969–2018 for 233 stations in Turkey. It was observed that the annual total precipitation amounts had decreased significantly in many stations during the studied period. Though most of the stations show a decreasing trend in annual precipitation, only the inner and southern part of the country has significant decreasing trends. The trend analysis on monthly precipitation data reveals that there are significant (confidence level ≥ 95%) decreasing trends in most of the regions of Turkey.

Key-words: spatiotemporal analysis, Mann-Kendall test, Turkey, precipitation hotspot analysis

1. Introduction

Water is vital for both humans and as well as all living beings. It is the main source of life and the sustainable supply of food resources for the continuation of life. The use and management of water have been important since the world existed. Today, due to the increasing environmental pollution, water resources pollution, global warming, and climate change, it becomes more important to learn about the amount of precipitation to protect, use, and manage effectively the existing water resources.

All of the water needed for the life cycle is supplied by precipitation in the world. Changes in the amount of precipitation on earth directly affect agriculture, hydrology, ecosystems, and the management of water resources (*Aslan*, 2017; *Bostan* and *Akyürek*, 2007). Hence, it is very essential to have knowledge about the dynamic balance of water in regard to the efficient management of water resources. Besides, it is essential to understand the spatial and temporal patterns of precipitation and their changes over time to devise strategies for solving problems such as increasing the accuracy of predictions of natural disasters arising from precipitation (*Cannarozzo et al*., 2006; *Diodato et al*., 2010; *Shoji* and *Kitaura*, 2006). Determining the spatial distribution and diversity of precipitation at different time periods in various regions contributes to researches on the identification and management of usable water resources, and planning for the sustainable management of natural resources (*Aslan*, 2017). Examining the changes in the spatial and temporal patterns of precipitation regimes plays a very important role to solve the problems of the population growth, economic developments, climate change, food, and agricultural products (*Basistha et al*., 2008; *Shoji* and *Kitaura*, 2006; *Yilmaz* and *Harmancioglu*, 2010).

The use of geographic information systems (GIS) as a supportive tool for decision-making is gaining popularity. With the emergence of the GIS technology, a large amount of spatial data can be easily analyzed. These data can be analyzed with several spatial statistical techniques (*Erdoğan*, 2010). The main objectives of spatial analysis in the GIS technology are to be able to identify and visualize the geographic phenomenon, and to perform spatial analysis of the pattern of events, and spatial modeling (*Haining*, 2003). As stated by many researchers, studies on meteorology and climatology aim to examine the spatial and temporal distributions and variations of these parameters through various climate parameters (*Goovaerts*, 2000; *Li et al*., 2010; *Naoum* and *Tsanis*, 2004; *Şen* and *Habib*, 2001).

In meteorological studies, it is common practice to use interpolation methods to determine the spatial changes of different parameters. Different methods have been proposed for the interpolation of the meteorological parameter measurements, obtained from irregularly distributed stations (*Kebaili Bargaoui* and *Chebbi*, 2009; *Sen* and *Habib*, 2000). These methods often provide an approach to determining the spatial distribution or temporal changes of the meteorological parameters or parameters studied in a given area (*Basistha et al*., 2008; *Mardikis et al*., 2005). However, the spatiotemporal analysis of these parameters is rarely performed *(De Luís et al., 2000; Suppiah* and *Hennessy*, 1998). With the development of spatial statistical methods, studies on spatial clustering of temporal trends have recently become prominent. Spatiotemporal analysis takes care of the change in the examined parameter in terms of both time and space simultaneously, while interpolation methods only consider the distribution of the parameters in space. With the inclusion of these issues in GIS software, there is an increase in spatiotemporal studies.

When the studies on precipitation studies in the world and Turkey were examined, numerous papers and studies have investigated on drought and desertification (*Türkeş*, 2012). These studies suggest that different meteorological parameters (*Goovaerts*, 2000; *Li et al*., 2010; *Naoum* and *Tsanis*, 2004; *Şen* and *Habib,* 2001; *Shantz et al*., 2012), especially precipitation values on the scale of a basin (*Karpouzos et al*., 2010; *Tosunoğlu*, 2017) or the scale of a river/lake (*Asfaw et al*., 2018; *Edossa et al*., 2010; *Suryabhagavan*, 2017; *Taxak et al.,* 2014), on the scale of a city (*Bigi et al*., 2018; *Mendoza* and *Mas*, 2018), are fully country based (*Jain et al*., 2013; *Markets* and *Prohibited*, 2012). In some studies, while only the temporal trend of precipitation has been examined (*Adarsh* and *Janga Reddy*, 2015; *Feng et al*., 2016; *Gluhovsky* and *Agee*, 2007; *Jones et al*., 2016) in some spatial distribution of precipitation (*Arora et al*., 2006; *Ayugi et al*., 2016; *Koumare*, 2014; *Millán et al*., 2005) has also been examined.

Various studies of climate variables in Turkey have concentrated on temperature changes (*Kadioğlu,* 1997; *Türkes*, 1996), spatial changes of precipitation (*Sariş et al*., 2010; *Türkeş et al*., 2009; *Ustaoğlu,* 2012), and temporal changes (*Demircan Mesut et al*., 2017; *Hadi* and *Tombul*, 2018; *Yurtseven* and *Serengil*, 2016). Studies on trend analysis have examined changes in narrow areas of the basins. For example, *Altın* and *Barak* (2014) have examined the long-term trends and changes in annual precipitation in the Antalya Peninsula located on the western Mediterranean coast of Turkey (*Altın* and *Barak*, 2014). *Taylan* and *Aydın*, (2018) studied the trends in the Göller Region, *Gümüş et al*. (2017) examined the hydrological meteorological data (minimum temperature, maximum temperature, average temperature, average humidity, average wind speed, and total precipitation) between 1975 and 2015 in Şanlıurfa. *Asikoglu* and *Ciftlik* (2015) examined the precipitation in the Aegean region using the trend analysis method. In this study, long-term trend changes were investigated using Mann-Kendall rank correlation coefficients between 1970 and 2011.

By a review of the literature indicates that very few studies have carried out analyses covering the whole country (*Partal* and *Küçük*, 2006; *Tayanç et al*., 2009; *Türkes*, 1996; *Türkeş et al*., 2009; *Yavuz* and *Erdoğan*, 2012). The studies related to Turkey have generally focused on the spatial data representation of the temporal evolution of precipitation, especially regarding the main climatic parameters using meteorological data. In other words, most of the studies are regional. Although the number of stations has increased in recent years, a very limited number of station data are being used in studies involving Turkey. It has been observed that the number of stations in the long-term analyses is very low, and there are very few studies relating to the recent era. However, no study in the literature has examined the spatiotemporal analysis of precipitation data in Turkey. Hence, the goal of this study is a spatiotemporal analysis of the monthly and annual average and total precipitation values of 233 meteorological stations for the 1969–2018 period to examine the precipitation values at different scales in Turkey.

2. Material and methods

2.1. Study area and data

Turkey is located in the world's northern subtropical climate. While the coastal areas of Turkey are affected by the mild Mediterranean climate occurring in the sea air, the inner areas show continental climate (*Şen* and *Habib*, 2001). Due to the landforms and peninsula shape of Turkey, the areas of the basins are generally show different climate forms. According to the Köppen-Geiger climate classification, temperate climate (C) has the widest area, while arid climate (B) has the narrowest area. While common B type climate is observed in Central Anatolia, C type climate is dominant in the coastal regions. Terrestrial climate (D) is observed in the plateaus of the Central Taurus and almost all the Eastern Anatolian regions (*Oztürk et al*., 2017). In this study, the monthly and yearly average precipitation data of 233 meteorological measurement stations were used to examine the spatiotemporal precipitation trends in both station and basin based belong to the 1969–2018 period. The monthly and annual precipitation values (mm) were obtained from the General Directorate of Meteorology of the Turkish Ministry of Agriculture and Forestry. The location of the stations and basins in the country are shown in *Fig. 1*. These stations consist of both manual and automatic monitoring stations. At the stations, there is an instrument that directly measures the precipitation falling from the atmosphere to the ground surface (Pluviometer) and one instrument (Pluviograph) that records the precipitation falling from the atmosphere to the ground surface on the diagram. The amount of precipitation collected in the pluviometer is measured in millimeters (mm) with a graduated precipitation scale. Some stations in the study area have been established as automatic meteorological stations. These stations consist of sensors sensitive to changes in meteorological parameters, measuring the amount of these changes. The unit of measurement in these sensors is expressed as the amount of water (kilogram) at 1 mm^2. This is equal to 1mm of water height in a rain gauge (MGM, 2020). These sensors also have devices that heat the precipitation collector in order to measure the amount of rainfall in snowy weather conditions (*Gultepe*, 2015; *Gultepe et al*., 2017).

For the study, stations which have the criteria of continuous measurements throughout the 50 years were selected from the meteorological data registers. Despite these criteria, the data suggested that there was missing information in various stations in some months. When missing data were analyzed, a deficiency in 5% of the total data was discovered, and the missing data has been completed using the average values of the nearest 5 neighbors.

Fig. 1. Distribution of the meteorological stations and basins.

2.2. Methods

Although there are different techniques for detecting space-time patterns, we used local indicators of spatial dependence and the Mann-Kendall test to describe the spatiotemporal precipitation trends.

The trends in the precipitation data were determined using the Mann-Kendall nonparametric test. The Mann and the conventional Mann-Kendall test by Kendall were widely used to assess the importance of the monotonic trends in the hydrometeorological time series, such as precipitation, temperature, and flow rate (*Burn* and *Hag Elnur*, 2002; *Gan*, 1998; *Xu et al.,* 2003; *Yang et al.,* 2004; *Zhang et al*., 2001). The World Meteorological Organization (WMO) has proposed using the Mann-Kendall method for assessing the trends in meteorological data *(World Meteorological Organization*, 1988). This test is also known as Kendall's Tau statistics that are not given any priority in the distribution of data and gives a trend of precipitation data to be observed for a long time. The Mann-Kendall rank correlation statistics τ are derived from the following equation:

$$\tau = \frac{4\sum_{i=1}^{N-1} n_i}{N(N-1)} - 1\,. \tag{1}$$

The Mann-Kendall test has two parameters that are particularly important for the trend. These parameters indicate the significance of the test as well as the magnitude of the direction. In the test results, the positive values indicate the existence of an upward trend, whereas the negative values indicate a declining trend.

For testing the existence of spatial dependence and also clustering in the trends of precipitation values, the Getis-Ord Gi*, known also as hotspot analysis was used. The Getis-Ord Gi* calculates the degree of clustering of the precipitation values' trends belong to the stations and basins. The statistic measures the intensity of the clustering of precipitation trend values in a station/basin relative to its neighboring stations/basins in the whole country. It is computed as the sum of precipitation values within a predefined radius distance from a station/basin as a proportion of the sum of values for all the stations/basins within the entire country. The Getis-Ord Gi* statistic also produces standard deviations and statistical probabilities for each station and basin.

The formula for $G_i^*(d)$ is as follows

$$G_i^*(d) = \frac{\sum_{j=1}^{N} w_{ij}(d)x_j - \bar{x}\sum_{j=1}^{N} w_{ij}(d)x_j}{S\sqrt{[N\sum_{j=1}^{N} w_{ij}^2(d) - (\sum_{j=1}^{N} w_{ij}(d))^2]/(N-1)}}, \tag{2}$$

where $w_{ij}(d)$ is the weight between stations i and j with a specified threshold distance d, which is used to specify the neighborhood size around the station/basin of interest to examine if the station/basin is a high/low spot; and S is the standard deviation of all observations. The G_i^* statistic is a z-score, meaning that G_i^* values greater than 1.96 or less than -1.96 are considered statistically significant (p=0.05). A statistically significant positive G_i^* value (G_i^*>1.96) represents a 'hot spot', indicating that there is a clustering of high values around station/basin i. A statistically significant negative G_i^* value (G_i^*<-1.96) is a 'cold spot', indicating that the clustering of low values is present around that station/basin.

2.3. Methodology

In order to examine the spatiotemporal analysis of precipitation trends in Turkey, Getis-Ord Gi* and Mann-Kendall tests were performed jointly. The precipitation values were analyzed by using Space Time Pattern Mining module of the ArcGIS

software (ESRI). In this procedure, spatiotemporal analysis is performed in two stages. In the first stage, a space-time cube is produced by summarizing the meteorological stations into space-time bins that are saved in a network common data form. This form is a file format used to store array-oriented data in the software. This process will result in a cube. While producing the space-time cube, we set a one-year time step interval, which defines the bin dimensions for the meteorological stations. The time step interval defines the time span for each bin. We produced time cubes for both the stations and basins separately. To compare and understand the regional differences between station and basin borders, station and basin trends were examined separately. The stations and basins were used as input features and were structured into space-time bins. The data structure can be thought of as a three-dimensional cube, made up of space-time bins with the *x* and *y* dimensions representing space and the z dimension representing time. For every meteorological station, a precipitation value was assigned for that date and location. For every basin, the sum of precipitation values of meteorological stations in that basin was also assigned for that date and basin's location. Based on the input parameters, the space-time cube took these attribute values and aggregated all the stations inside the basin border and a time-step interval of one year to create a bin (ESRI).

In the second stage, the *Gi** statistics values, z-score values, and p values of each station/bin were computed for each year. The neighborhood distance and neighborhood time step parameters in the software defined how many surrounding bins in both space and time would be considered when calculating the statistic for a specific bin. It then compared the precipitation value of a bin and its neighbors with the mean attribute value of all bins. Calculated z-score values of *Gi** statistics were compared to the expected z-score values to determine the statistically significant hot and cold spots. After the statistically significant hot and cold spots had been computed, the hot spot/cold spot values were analyzed using the Mann-Kendall trend test to detect the temporal trends at each meteorological station and basin. In this stage, the Getis-Ord G^*_i took the space-time cube as an input, and time series of Getis-Ord G^*_i values and z scores of these values were assessed using the Mann-Kendall test for each individual bin. By using the resultant trend z-score and the hot spot z-score values of each station and basin, software categorizes the characteristic of trends as shown in *Table 1*. The clusters and trends resulting from the combination of spatial and temporal statistics were then used to categorize each station and basin's situation in the analysis period.

Table 1. Spatiotemporal cluster characteristics tipes

Type of Characteristic	Description
New hot spot	Precipitation trend of station/basin is increasing for the first time in the final time interval of the period 1969–2018.
New cold spot	Precipitation trend of station/basin is decreasing for the first time in the final time interval of the period1969–2018.
Consecutive hot spot	Precipitation trend of station/basin never shows an increase prior to the final run, and less than 90% of all years have statistically significant increase. This location has a single uninterrupted run of a significant increase in the final time-step intervals.
Consecutive cold spot	Precipitation trend of station/basin never shows a decrease prior to the final run, and less than 90% of all years have statistically significant decrease. This location has a single uninterrupted run of a significant decrease in the final time-step intervals.
Intensifying hot spot	At least 90% of the period 1969–2018 have an increasing trend including the final time step, the intensity of clustering of high trends in each time step is increasing overall.
Intensifying cold spot	At least 90% of the period 1969–2018 have a decreasing trend including the final time step, the intensity of clustering of low trends in each time step is increasing overall.
Persistent hot spot	A station/basin that has an increase for 90% of the time-step intervals with no discernible trend indicating an increase or decrease in the intensity of clustering over the period 1969–2018.
Persistent cold spot	A station/basin that has a decrease for 90% of the time-step intervals with no discernible trend indicating an increase or decrease in the intensity of clustering over the period 1969–2018.
Diminishing hot spot	A station/basin that has an increase for 90% of the time-step intervals, including the final time step. In addition, the intensity of an increase in each time step is decreasing overall.
Diminishing cold spot	A station/basin that has a decrease for 90% of the time-step intervals, including the final time step. In addition, the intensity of decrease in each time step is decreasing overall.
Sporadic hot spot	A station/basin that has an on-again then off-again increase. Less than 90% of the time step intervals show an increase, and none of the time-step intervals shows statistically significant decrease.
Sporadic cold spot	A station/basin that has an on-again then off-again decrease. Less than 90% of the time step intervals show a decrease, and none of the time step intervals shows statistically significant increase.
Oscillating hot spot	A station/basin that shows mixed characteristic: some time intervals have an increase, some time intervals have a decrease. For the final time step the interval has an increase.
Oscillating /cold spot	A station/basin that shows mixed characteristic: some time intervals have an increase, some time intervals have a decrease. For the final time step the interval has a decrease.
Historical hot spot	Except the most recent period, at least 90% of the period have an increase.
Historical cold spot	Except the most recent period, at least 90% of the period have a decrease.

3. Results

Maximum values of monthly and annual average precipitation data for the entire country are taken into account in this study. When examining the exploratory statistics of the precipitation values, we noticed that the highest annual precipitation value for Turkey was 796.95 mm in 2009, while the lowest value was 502.11 mm in 2008. The lowest total annual average precipitation value was 113.80 mm in Mardin station in 2010 and the highest was 3380.40 mm in Hopa station in 2016. Precipitation values throughout Turkey between 1969 and 2018 were examined according to maximum, average, and minimum amounts of precipitation value (*Fig. 2*).

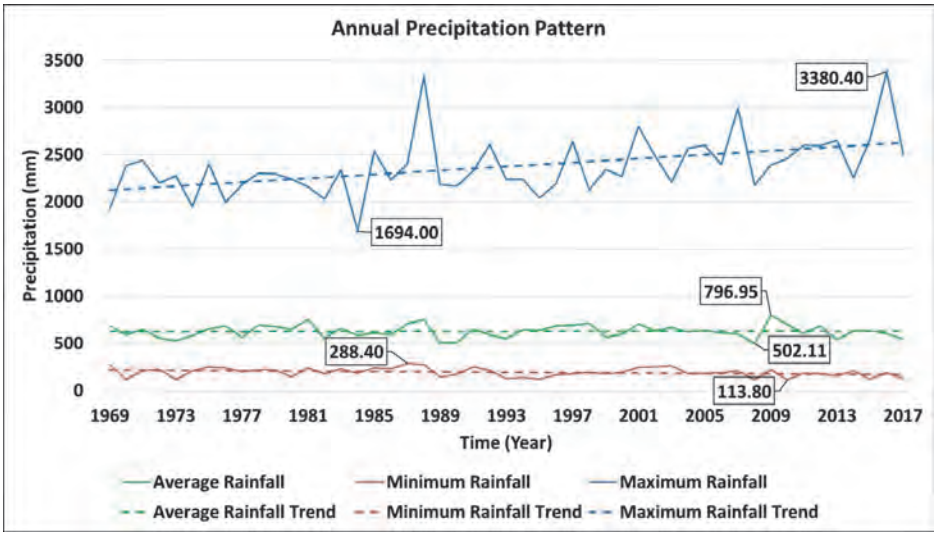

Fig. 2. Precipitation statistics of Turkey.

The plotted graph with the linear trend analysis in *Fig. 2* illustrates the general annual maximum amount of change in precipitation value in Turkey. *Fig. 2* suggests an increasing trend in the maximum precipitation data from 1969 to 2018. The examination of the annual average precipitation value in the same data illustrates a slight, albeit positive change. The minimum precipitation data also suggest a decreasing trend from 1969 to 2018. This situation shows the negative change in both maximum and minimum precipitation values in terms of arising in the extreme precipitation gauges in this period. The monthly average precipitation amounts per decade and their descriptive statistics are shown in *Fig. 3*.

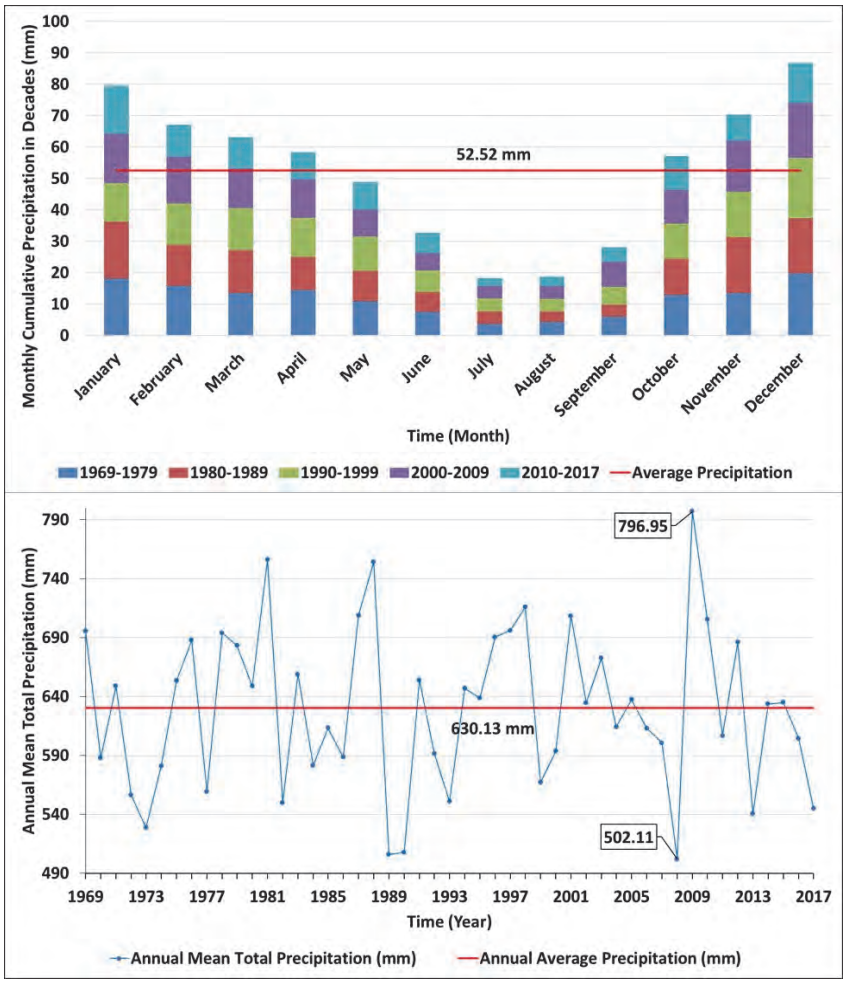

Fig. 3. Percentage of precipitation and total annual precipitation per decade across Turkey.

Monthly precipitation data suggest that the amount of the highest precipitation was 86.79 mm in December, 79.63 mm in January, 70.34 mm in November, and 67.10 mm in February. On the other hand, the amount of the least precipitation value was 18.32 mm in July, 18.78 mm in August, 28.18 mm in September, and 32.72 mm in June. Between 1969 and 2018, the first three stations with the highest precipitation value were Hopa (2264.03 mm), Rize (2228.91 mm), and Rize/Pazar (2033.75 mm). Conversely, Iğdır (260.74 mm), Akçakale (278.02 mm), and

Karapınar (295.73 mm) were the first three stations with the least precipitation value areas between 1969 and 2018. When we examine the extreme precipitations, *Table 2* shows the precipitation dates and amounts of the stations that received the highest amount of precipitation on a monthly basis between 1969 and 2018.

Table 2. The extreme precipitation values

Month	Station	Year	Maximum precipitation (mm)	Monthly mean precipitation (mm)
January	Antalya Havalimani	1969	798	80
February	Antalya Havalimani	1974	625	67
March	Antalya Havalimani	2003	399	63
April	Kilis	2015	592	58
May	Hakkari	2015	789	49
June	Hopa	2007	373	33
July	Giresun	2009	522	18
August	Hopa	1988	589	19
September	Hopa	2016	779	28
October	Hopa	2015	626	57
November	Antalya Havalimani	2001	907	70
December	Alanya	1997	705	87

According to *Table 2*, the station that had the most precipitation in Turkey in this period is Antalya Havalimani in November 2001. While in summer and autumn, the northeast region of Turkey has higher extreme values, the Antalya region in winter has extremely high values. Interestingly, the Antalya region has extreme values for five months of the year, and for the other five months of the year, the northeast region shows extreme values.

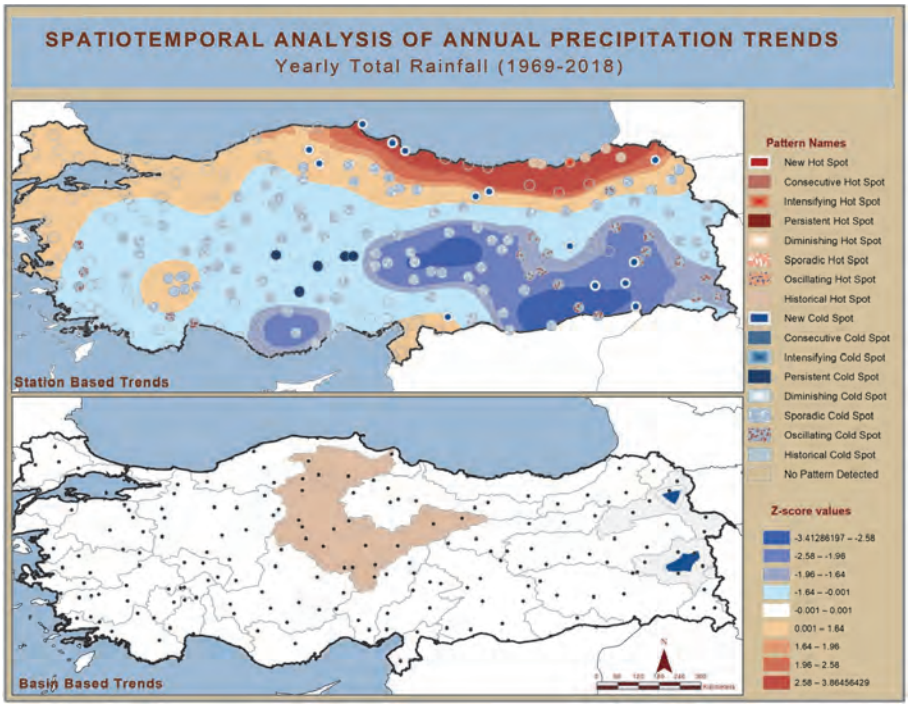

Fig. 4. Spatiotemporal trends of station- and basin-based average annual precipitation values.

When we examine the results of the spatiotemporal analysis, station-based annual average precipitation space-time trends are shown in *Fig. 4*. An outline of the information about the stations was also presented in *Table 2*. It was observed from the data, that the average annual precipitation did not show any significant change for 93 out of 223 stations. Moreover, sporicidal cold spot, oscillating cold spot, persistent cold spot, and new cold spot were observed for 93, 22, 5, and 14 stations, respectively. Considering the increasing trends, while the persistent hot spot has been identified in only five stations, the new hot spot in one station only. The location of the stations with decreasing precipitation trends indicates that the sporicidal cold spots are clustered in Central Anatolia (Karapınar, Aksaray, Ürgüp, Nevşehir, Cihanbeyli, and around the Tuz Gölü stations); the southeastern Anatolia region (Batman, Bingöl, Bitlis, Siirt, and Cizre station), the Western Black Sea (Sinop, Tosya, Samsun, Bafra, and Kastamonu stations), and the Middle Black Sea Region (Susehri and Şebinkarahisar stations). It has been determined that the precipitation with oscillating cold spot has been decreasing recently in 22 stations located in Elazığ, Van, Hakkari, and Erzincan provinces.

According to *Table 3* and *Fig. 5*, the stations with a decreasing trend are around twice as many as those with an increasing trend. The station-based

precipitation trends illustrate that the decreases in the trends are dominant in months of January, February, April, October, November, and December. The number of stations showing a dominant increase in precipitation is higher in May and June than those showing a decrease. It is evident that most of the fluctuations in the stations are determined as oscillating and sporadic cold spots. The stations exhibiting cold spot patterns in terms of a decrease in the precipitation are usually located in the central and eastern parts of the country for the months of January, February, April, November, and December. On the other hand, the stations exhibiting hot spot patterns are usually located in the north and northeast regions of the country for the months of May, June, July, August, and September.

Table 3. Summary of spatiotemporal trend statistics of station-based average yearly precipitation values

Trend type	No pattern detected	New cold spot	Persistent cold spot	Persistent hot spot	Sporadic cold spot	Sporadic hot spot	Oscillating hot spot	Oscillating cold spot	Intensify hot spot	Intensify cold spot	Historical hot spot	Total hot spot	Total cold spot
January	171				13	8		41				8	54
February	85	8	1		78			61				0	148
March	208				11		12	2				12	13
April	113	6			17	1		96				1	119
May	116				1	45	61	10				106	11
June	134		2	7	20	30	39	1				76	23
July	216			4		10			3			17	0
August	208			2		19			4			25	0
September	208					19			6			25	0
October	119			3	45	3		61	2			8	106
November	148				45	4	9	27				13	72
December	146			4	42	5	16	18		2		25	62
Annual	93	14	5		93			22	1		5		

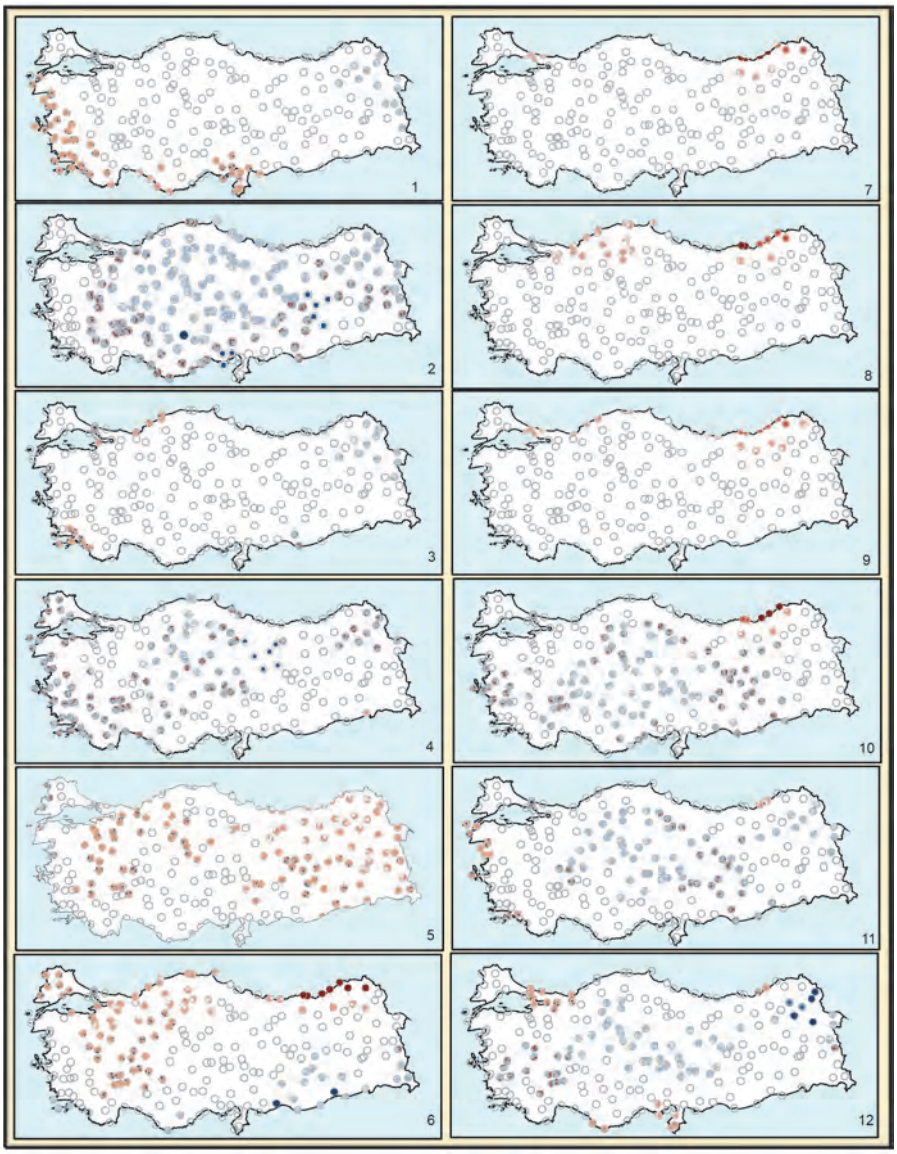

Fig. 5. Spatiotemporal trends of station-based average monthly precipitation values.

Basin-based monthly average precipitation spatiotemporal analysis results are shown in *Fig. 6*. The trends demonstrate a significant decrease in the total amount of precipitation in the basins in February and April. It is noticeable that an increase in precipitation trends are dominant in March, June, and September. Compared with station-based trends, both similarities and differences can be seen.

In many months, the station-based precipitation values were summed and balanced with neighboring stations in the same basin. Therefore, the basin-based maps show smoother surfaces while the station-based values illustrate the minor regional differences. While Konya, East Akdeniz, and Aras basins show a significant decrease in precipitation in February, Büyük and Küçük Menderes, Gediz, West Mediterranean, Meriç Ergene, Marmara Suları Basins show a significant decrease in precipitation in April.

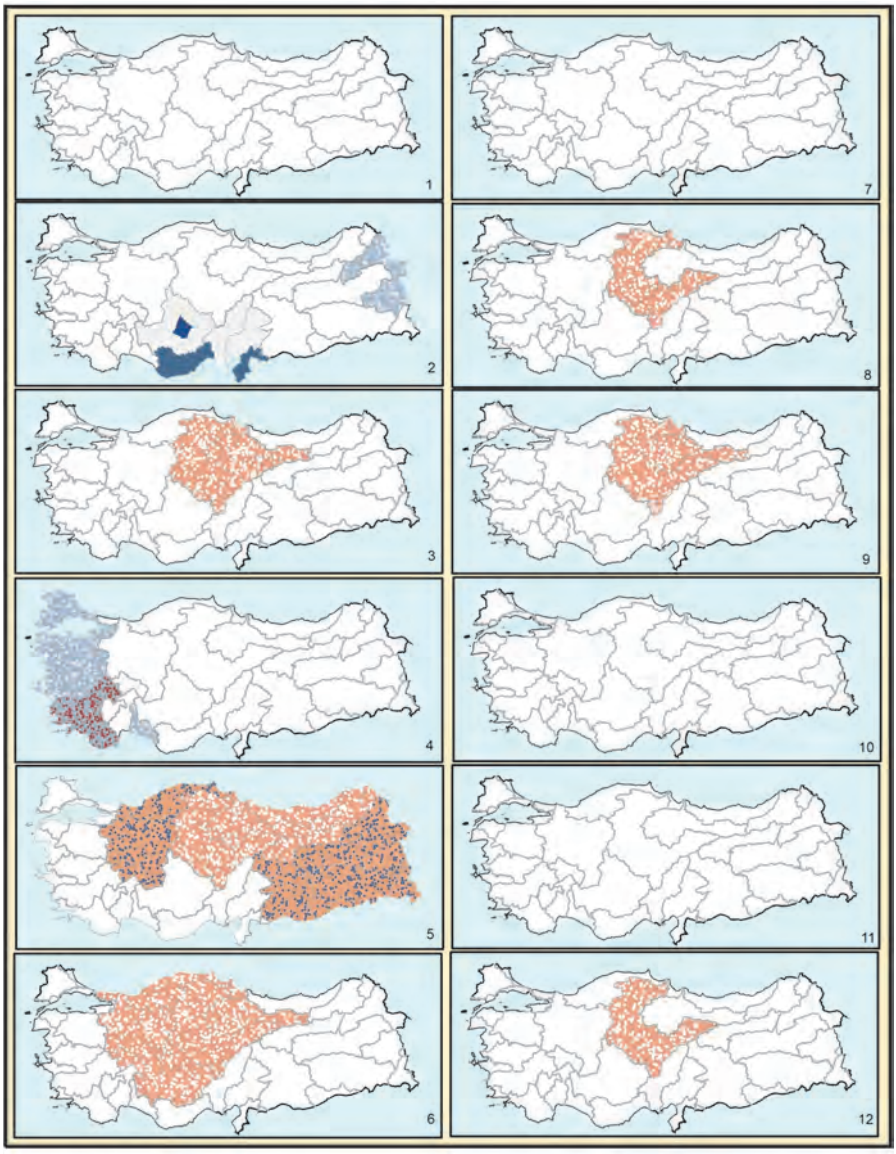

Fig. 6. Spatiotemporal trends of basin-based average monthly precipitation values.

4. Discussion and conclusions

The main objective of this study was to examine in detail the precipitation trends in Turkey from 1969 to 2018. The annual and monthly trends were analyzed using spatiotemporal analysis, which integrates Getis Ord G* hot-spot analysis and Mann Kendall trend analysis.

- Our data demonstrated that the northern part of the country, especially the eastern part of the Black Sea region, had an increasing trend in its annual precipitation, while the middle and south parts of the country, especially the southeastern Anatolian and Central Anatolia regions, had decreasing trends.
- The analyses indicated that the biggest regional changes in the trends of precipitation of stations occurred during February, April, May, and October.
- The monthly precipitation trends generally exhibited a decreasing trend, with the greatest magnitude in February, April, and October. In May, in particular, the trends totally changed in such a way that the upward, dominant trends shifted to June.
- Many of the decreasing trends were recorded for the annual mean precipitation values, predominantly in the center and southern parts of Turkey; however, only six decrease trends were found in the southeast part of the country.

It is estimated that the change in the water cycle will adversely affect agriculture and food security, public health, land and sea ecosystems, coastal regions, and especially, water resources in the world. In this context, it is important to work on precipitation related research in order to minimize the effects of precipitation on our water resources, to understand the expected effects, to complete sectoral and regional fragility studies, and to plan adaptation studies to these. Therefore, we analyzed the monthly and annual average and total precipitation values of 233 meteorological stations for the 1969–2018 period in Turkey. In this concept, we used a combination of spatiotemporal analysis and Mann-Kendall trend analysis. Our study is the first one in Turkey on the subject of the spatiotemporal analysis that analyzing the precipitation and trend of precipitation in both spatially and temporally. Our visualization method improved the understanding of trends by showing decreases, increases, and fluctuations in 17 different symbologies. In the study, we also elaborated on both the small-scale regional precipitation changes, using station-based data and the large-scale regional precipitation changes, using basin-based data. This way, we tried to understand Turkey's small-scale differences and basin-based large-scale trends separately. Given some different results (e.g., *Partal* and *Kahya*, 2006; *Türkeş et al*., 2009), our results largely covers the findings of many of the previous studies (e.g., *Hadi* and *Tombul*, 2018; *Toros*, 2012; *Yavuz* and *Erdoğan*, 2012). In the study, by using a huge number of stations and an efficient classification and visualization technique, we managed to obtain accurate, elaborate, and useful results. In short, the paper presents a detailed and updated summary of the actual precipitation trends in Turkey.

References

Adarsh, S. and *Janga Reddy, M*., 2015:Trend analysis of rainfall in four meteorological subdivisions of southern India using nonparametric methods and discrete wavelet transforms. *Int. J. Climatol. 35*, 1107–1124. https://doi.org/10.1002/joc.4042

Altın, T.B. and *Barak, B*., 2014: Changes and Trends in Total Yearly Precipitation of the Antalya District, Turkey. *Procedia - Soc. Behav. Sci. 120*, 586–599. https://doi.org/10.1016/j.sbspro.2014.02.139

Arora, M., Singh, P., Goel, N.K., and *Singh, R.D.,* 2006: Spatial distribution and seasonal variability of rainfall in a mountainous basin in the Himalayan region. *Water Resour. Manage. 20*, 489–508. https://doi.org/10.1007/s11269-006-8773-4

Asfaw, A., Simane, B., Hassen, A., and *Bantider, A*., 2018: Variability and time series trend analysis of rainfall and temperature in northcentral Ethiopia: A case study in Woleka sub-basin. *Weather Clim. Extrem. 19*, 20–28. https://doi.org/10.1016/j.wace.2017.12.002

Asikoglu, O.L. and *Ciftlik, D.,* 2015: Recent Rainfall Trends in the Aegean Region of Turkey. *J. Hydrometeorol. 16*, 1873–1885. https://doi.org/10.1175/JHM-D-15-0001.1

Aslan, R., 2017: Sürdürülebilir Çevre ve Kalkınma İçin Lokal Bir Belirteç: Eber Gölü. *Ayrıntı Derg* 5, 35–39. (In Turkish)

Ayugi, B.O., Wang, W., and *Chepkemoi, D*., 2016: Analysis of Spatial and Temporal Patterns of Rainfall Variations over Kenya. *J. Environ. Earth Sci. 6*, 69–83. https://doi.org/10.4271/840300

Basistha, A., Arya, D.S., and *Goel, N.K.,* 2008: Spatial distribution of rainfall in Indian Himalayas - A case study of Uttarakhand Region. *Water Resour. Manage. 22*, 1325–1346. https://doi.org/10.1007/s11269-007-9228-2

Bigi, V., Pezzoli, A., and *Rosso, M*., 2018: Past and Future Precipitation Trend Analysis for the City of Niamey (Niger): An Overview. *Climate 6*, 73. https://doi.org/10.3390/cli6030073

Bostan, P.A. and *Akyürek, S.Z*., 2007: Exploring the mean annual precipitation and temperature values over Turkey by using environmental variables, in: ISPRS: Visualization and Exploration of Geospatial Data. ISPRS, Stuttgart.

Burn, D.H. and *Hag Elnur, M.A*., 2002: Detection of hydrologic trends and variability. *J. Hydrol. 255*, 107–122. https://doi.org/10.1016/S0022-1694(01)00514-5

Cannarozzo, M., Noto, L. V., and *Viola, F*., 2006: Spatial distribution of rainfall trends in Sicily (1921-2000). *Phys. Chem. Earth 31*, 1201–1211. https://doi.org/10.1016/j.pce.2006.03.022

De Luís, M., Raventós, J., González-Hidalgo, J.C., Sánchez, J.R., and *Cortina, J*., 2000: Spatial analysis of rainfall trends in the region of valencia (East Spain). *Int. J. Climatol. 20*, 1451–1469. https://doi.org/10.1002/1097-0088(200010)20:12<1451::AID-JOC547>3.0.CO;2-0

Demircan, M., Gürkan, H., Eskioğlu, O., Arabaci H., and *Coşkun, M.,* 2017: Climate Change Projections for Turkey: Three Models and Two Scenarios. *Turkish J. Water Sci. Manage. 1*, 22–43. https://doi.org/10.31807/tjwsm.297183

Diodato, N., Tartari, G., and *Bellocchi, G.*, 2010: Geospatial Rainfall Modelling at Eastern Nepalese Highland from Ground Environmental Data. *Water Resour. Manage. 24*, 2703–2720. https://doi.org/10.1007/s11269-009-9575-2

Edossa, D.C., Babel, M.S., and *Gupta, A. Das,* 2010: Drought analysis in the Awash River Basin, Ethiopia. *Water Resour. Manage. 24*, 1441–1460. https://doi.org/10.1007/s11269-009-9508-0

Erdoğan, S., 2010: Modelling the spatial distribution of DEM error with geographically weighted regression: An experimental study. *Comput. Geosci. 36*, 34–43. https://doi.org/10.1016/j.cageo.2009.06.005

Feng, G., Cobb, S., Abdo, Z., Fisher, D.K., Ouyang, Y., Adeli, A., and *Jenkins, J.N.*, 2016: Trend analysis and forecast of precipitation, reference evapotranspiration, and rainfall deficit in the blackland prairie of eastern Mississippi. *J. Appl. Meteorol. Climatol. 55*, 1425–1439. https://doi.org/10.1175/JAMC-D-15-0265.1

Gan, T.Y., 1998: Hydroclimatic trends and possible climatic warming in the Canadian Prairies. *Water Resour Res.* https://doi.org/10.1029/98WR01265

Gluhovsky, A. and *Agee, E.,* 2007: On the analysis of atmospheric and climatic time series. *J. App.l Meteorol. Climatol. 46*, 1125–1129. https://doi.org/10.1175/JAM2512.1

Goovaerts, P., 2000: Geostatistical approaches for incorporating elevation into the spatial interpolation of rainfall. *J. Hydrol. 228*, 113–129. https://doi.org/10.1016/S0022-1694(00)00144-X

Gultepe, I. 2015: Mountain weather: Observation and modeling. In (Eds. *R. B. T.-A. G. Dmowska*), Advances in Geophysics Vol. 56, pp. 229–312. Elsevier. https://doi.org/10.1016/bs.agph.2015.01.001

Gultepe, I., Heymsfield, A. J., Gallagher, M., Ickes, L., and *Baumgardner, D.*, 2017: Ice Fog: The Current State of Knowledge and Future Challenges. Meteorological Monographs, 58, 4.1–4.24. https://doi.org/10.1175/AMSMONOGRAPHS-D-17-0002.1

Gümüş, V., Soydan, N., Şimşek, O., Algin, H., Aköz, M., and *Yenigun, K.*, 2017: Seasonal and annual trend analysis of meteorological data in Sanliurfa, Turkey. *Eur. Water 59*, 131–136.

Hadi, S.J. and *Tombul, M.*, 2018. Long-term spatiotemporal trend analysis of precipitation and temperature over Turkey. *Meteorol. Appl. 25*, 445–455. https://doi.org/10.1002/met.1712

Haining, R., 2003: Spatial Data Analysis: Theory and Practice. Cambridge University Press, Cambridge. https://doi.org/10.1017/CBO9780511754944

Jain, S.K., Kumar, V., and *Saharia, M.*, 2013: Analysis of rainfall and temperature trends in northeast India. *Int. J. Climatol. 33*, 968–978. https://doi.org/10.1002/joc.3483

Jones, P.D., Harpham, C., Harris, I., Goodess, C.M., Burton, A., Centella-Artola, A., Taylor, M.A., Bezanilla-Morlot, A., Campbell, J.D., Stephenson, T.S., Joslyn, O., Nicholls, K., and *Baur, T.*, 2016: Long-term trends in precipitation and temperature across the Caribbean. I*nt. J. Climatol. 36*, 3314–3333. https://doi.org/10.1002/joc.4557

Kadioğlu, M., 1997: Trends in surface air temperature data over Turkey. *Int. J. Climatol. 17*, 511–520. https://doi.org/10.1002/(SICI)1097-0088(199704)17:5<511::AID-JOC130>3.0.CO;2-0

Karpouzos, D.K., Kavalieratou, S., and *Babajimopoulos, C.*, 2010: Trend Analysis of Precipitation Data in Pieria Region (Greece). *Eur. Water 30*, 31–40.

Kebaili Bargaoui, Z., and *Chebbi, A.*, 2009: Comparison of two kriging interpolation methods applied to spatiotemporal rainfall. *J. Hydrol. 365*, 56–73. https://doi.org/10.1016/j.jhydrol.2008.11.025

Koumare, I., 2014: Temporal/Spatial Distribution of Rainfall and the Associated Circulation Anomalies over West Africa. *Pakistan J. Meteorol. 10*, 1–11.

Li, M., Shao, Q., and *Renzullo, L.*, 2010: Estimation and spatial interpolation of rainfall intensity distribution from the effective rate of precipitation. *Stoch. Environ. Res. Risk. Assess. 24*, 117–130. https://doi.org/10.1007/s00477-009-0305-3

Mann, H.B., 1945: Nonparametric Tests Against Trend. *Econometrica 13*, 245–259. https://doi.org/10.2307/1907187

Mardikis, M.G., Kalivas, D.P., and *Kollias, V.J.*, 2005: Comparison of interpolation methods for the prediction of reference evapotranspiration - An application in Greece. *Water Resour. Manage. 19*, 251–278. https://doi.org/10.1007/s11269-005-3179-2

Markets, I.S.I.E. and *Prohibited, U.D.*, 2012: Rainfall Variability and Trend Analysis of Annual Rainfall in North Africa. *Int. J. Atmos. Sci.* 2016, 12. https://doi.org/10.1002/9781119971641.ch8

Mendoza, R.R. and *Mas, M.*, 2018. Analysis of precipitation in Belém-PA city. (period 1967-2016). *Int J Hydro*. 2018;2:312-317. https://doi.org/10.15406/ijh.2018.02.00088

MGM, 2020: Automated Weather Station. https://www.mgm.gov.tr/genel/meteorolojikaletler.aspx?s=9. Accessed 28 September 2020

Millán, M.M., Estrela, M.J., and *Miró, J.*, 2005. Rainfall components: Variability and spatial distribution in a Mediterranean area (Valencia region). *J. Clim. 18*, 2682–2705. https://doi.org/10.1175/JCLI3426.1

Naoum, S. and *Tsanis, I.K.*, 2004. Ranking spatial interpolation techniques using a GIS-based DSS. *Glob. Nest J.26*, 168-175. https://doi.org/10.1111/nmo.12246

Ozturk, M.Z., Çetinkaya, G., and *Aydın, S.*, 2017: Climate Types of Turkey According to Köppen-Geiger Climate Classification. *J. Geography 35*. 17-27. https://doi.org/10.26650/JGEOG295515

Partal, T. and *Kahya, E.*, 2006: Trend analysis in Turkish precipitation data. *Hydrol Process 20*, 2011–2026. https://doi.org/10.1002/hyp.5993

Partal, T. and *Küçük, M.*, 2006: Long-term trend analysis using discrete wavelet components of annual precipitations measurements in Marmara region (Turkey). *Phys. Chem. Earth. 31,* 1189–1200. https://doi.org/10.1016/j.pce.2006.04.043

Sariş, F., Hannah, D.M., and *Eastwood, W.J.,* 2010: Spatial variability of precipitation regimes over Turkey. *Hydrol. Sci. J. 55*, 234–249. https://doi.org/10.1080/02626660903546142

Sen, Z. and *Habib, Z.*, 2000: Spatial analysis of monthly precipitation in Turkey. *Theor. Appl. Climatol.67,* 81–96. https://doi.org/10.1007/s007040070017

Sen, Z. and *Habib, Z.*, 2001: Monthly spatial rainfall correlation functions and interpretations for Turkey Monthly spatial rainfall correlation functions and. *Hydrol. Sci. J. 46,* 525–535. https://doi.org/10.1080/02626660109492848

Shantz, N.C., Gultepe, I., Liu, P.S.K., Earle, M.E. and *Zelenyuk, A.* 2012: Spatial and temporal variability of aerosol particles in Arctic spring. *Quart. J. Roy. Meteorol. Soc. 138*, 2229–2240. https://doi.org/10.1002/qj.1940

Shoji, T. and *Kitaura, H.*, 2006: Statistical and geostatistical analysis of rainfall in central Japan. *Comput Geosci* 32, 1007–1024. https://doi.org/10.1016/j.cageo.2004.12.012

S*uppiah, R.* and *Hennessy, K.J.,* 1998: Trends in total rainfall, heavy rain events and number of dry days in Australia, 1910–1990. *Int. J. Climatol. 18,* 1141–1164. https://doi.org/10.1002/(SICI)1097-0088(199808)18:10<1141::AID-JOC286>3.0.CO;2-P

Suryabhagavan, K.V., 2017: GIS-based climate variability and drought characterization in Ethiopia over three decades. *Weather Clim. Extrem 15*, 11–23. https://doi.org/10.1016/j.wace.2016.11.005

Taxak, A.K., Murumkar, A.R., and *Arya, D.S.*, 2014: Long term spatial and temporal rainfall trends and homogeneity analysis in Wainganga basin, Central India. *Weather Clim. Extrem 4*, 50–61. https://doi.org/10.1016/j.wace.2014.04.005

Tayanç, M., Im, U., Doğruel, M., and *Karaca, M.*, 2009: Climate change in Turkey for the last half century. *Clim. Change 94,* 483–502. https://doi.org/10.1007/s10584-008-9511-0

Taylan, D. and *Aydın, T.*, 2018: The Trend Analysis of Lakes Region Precipitation Data in Turkey. *Cumhur Sci. J. 39*, 258–273. https://doi.org/10.17776/csj.406271

Toros, H., 2012: Spatio-temporal variation of daily extreme temperatures over Turkey. *Int J Climatol* 32, 1047–1055. https://doi.org/10.1002/joc.2325

Tosunoğlu, F., 2017: Trend Analysis of Daily Maximum Rainfall Series in Çoruh Basin , Çoruh Havza ' sındaki Günlük Maksimum Yağış Serilerinin Trend Analizi. *Iğdır Üni Fen Bilim Enst Der 7*, 195–205. (In Turkish) https://doi.org/10.21597/jist.2017127432

Türkes, M., 1996: Spatial and Temporal Analysis of Annual Rainfall Variations I. I*nt. J. Climatol. 16*, 1057–1076. https://doi.org/10.1002/(SICI)1097-0088(199609)16:9<1057::AID-JOC75>3.0.CO;2-D

Türkeş, M., 2012: Observed and Projected Climate Change, Drought and Desertification in Turkey. *Ankara Univ J. Environ. Sci. 4*, 1–32.

Türkeş, M., Koç, T., and *Sariş, F.*, 2009. Spatiotemporal variability of precipitation total series over Turkey. *Int J Climatol*. *30*, 1056–1074. https://doi.org/10.1002/joc.1768

Ustaoğlu, B., 2012: Comparisons of Annual Meanprecipitation Gridded and Station Data: An Example from İstanbul, Turkey. *Marmara Coğrafya Derg 26*, 71–81.

World Meteorological Organization, 1988: Analyzing long time series of hidrological data with respect to climate variability. World Clim Program - Appl. https://doi.org/10.1016/j.strusafe.2008.11.002

Xu, Z.X., Takeuchi, K., and *Ishidaira, H.*, 2003: Monotonic trend and step changes in Japanese precipitation. J *Hydrol. 279*, 144–150. https://doi.org/10.1016/S0022-1694(03)00178-1

Yang, D., Li, C., Hu, H., Lei, Z., Yang, S., Kusuda, T., Koike, T., and *Musiake, K.*, 2004: Analysis of water resources variability in the Yellow River of China during the last half century using historical data. *Water Resour. Res. 40*, W06502. https://doi.org/10.1029/2003WR002763

Yavuz, H. and *Erdoğan, S.*, 2012: Spatial Analysis of Monthly and Annual Precipitation Trends in Turkey. *Water Resour Manag 26*, 609–621. https://doi.org/10.1007/s11269-011-9935-6

Yilmaz, B. and *Harmancioglu, N.B.,* 2010: An Indicator Based Assessment for Water Resources Management in Gediz River Basin, Turkey. *Water Resour. Manage. 24,* 4359–4379. https://doi.org/10.1007/s11269-010-9663-3

Yurtseven, İ. and *Serengil, Y.*, 2016: Changes and trends of seasonal total rainfall in the province of Istanbul, Turkey. *İstanbul Üniversitesi Orman Fakültesi Derg 67*, 1–12. https://doi.org/10.17099/jffiu.30673

Zhang, X., Harvey, K.D., Hogg, W.D., and *Yuzyk, T.R.*, 2001: Trends in Canadian Streamflow. *Water Resour. Res. 37*, 987–998. https://doi.org/10.1029/2000WR900357

DOI:10.28974/idojaras.2022.3.5

IDŐJÁRÁS

Quarterly Journal of the Hungarian Meteorological Service
Vol. 126, No. 3, July – September, 2022, pp. 355–374

The analysis of annual and seasonal surface air temperature trends of southern and southeastern Bosnia and Herzegovina from 1961 to 2017

Nikola R. Bačević[1], **Nikola Milentijević**[1], **Aleksandar Valjarević**[2], **Milena Nikolić**[1], **Vladica Stevanović**[1], **Dušan Kićović**[3], **Milica G. Radaković**[4], **Dragan Papić**[5], and **Slobodan B. Marković**[4]

[1]*University of Priština, Faculty of Sciences and Mathematics*
Department of Geography
38220 Kosovska Mitrovica, Serbia

[2] *University of Belgrade, Faculty of Geography*
Studentski Trg 3/III, Belgrade, Serbia

[3]*Academy for Applied studies Belgrade*
The College of Tourism, 11000 Belgrade, Serbia

[4]*University of Novi Sad, Faculty of Sciences Departmant of Geography*
Tourism and Hotel Management, 21000 Novi Sad, Serbia

[5] *University of Banja Luka, Faculty of Natural Sciences and Mathematics*
Department of Geography
78000 Banja Luka, Republic of Srpska, Bosnia and Herzegovina

**Corresponding Author e-mail: nikola.bacevic@pr.ac.rs*
(Manuscript received in final form April 1, 2021)

Abstract— In some areas of the world, regional climate change is in good agreement with global climate change. This study brings new information about what defines climate change in the contact area of Adriatic Sea and Southeastern Europe, and conclusions are based on trend analysis of annual and seasonal temperatures in the southern and southeastern parts of Bosnia and Herzegovina. Trend analysis was applied on mean annual surface air temperatures, mean maximum temperatures, and mean minimum temperatures of all four seasons. This study used 4 meteorological stations: Livno, Bileća, Mostar, and Ivan Sedlo for 56 years. The main statistical method is the Mann-Kendall test. The total number of analysis is 48. A statistically significant positive trend was determined in 36 analysis, while in the rest of the tests this was not the case. The highest amount of temperature increase is present in the mean maximum summer air temperatures in Livno and Ivan Sedlo. Mean minimum autumn air temperatures had the smallest increase. Negative trend is present in the mean autumn surface air temperatures and mean maximum autumn temperatures. Using a geographical information system resulted in visualizing regional differences in the spatial distribution of isotherms. The study area has combined the influence of orography and maritime effects of the Adriatic Sea. Having in mind these results, the growing temperature has been recognized

as a problem which needs more attention in Bosnia and Herzegovina. Unfortunately, official documents which propose economic adaptation on climate change in this country are not at a satisfactory level.

Key-words: climate change, temperature trends, Mann-Kendall test, GIS, Bosnia and Herzegovina

1. Introduction

Numerous papers have been published about climate variations, and their impact on the environment. It has been proven that the increase of global air temperature from 1906 to 2005 is 0.74 ℃ now. The study from *Trenberth et al.* (2007) shows how the growing air temperature on the Earth has been doubled up in the last fifty years, rising 0.13 ℃ per decade. Regional changes in temperature can be even greater than those on global level, from 0.65 ℃ to 1.06 ℃ (*Blunden* and *Arndt*, 2015). The Intergovernmental Panel for Climate Change proved existence of the warmest ever thirty year cycle on the Northern Hemisphere during the last 800 years (1983–2012). In Europe, a mean annual air temperature of this decade has been warmer than the last one (2008–2017) by 1.6–1.7 ℃ . This makes it the warmest decade ever recorded (*EEA*, 2018). In the Norhern Hemisphere, summer and autumn months were warmer during the last decades of 20th century than in the first half of the same century. The decade with the warmest spring and autumn months was 80s in the last century (*Jones* and *Briffa*, 1991). *Trenberth et al*. (2007) confirm this statement and add that the average global surface air temperature is now higher by 0.27 ℃ in comparison with the year 1979. The most intensified warming has been recorder during the winter and spring months in the Northern Hemisphere. *Luterbacher et al.* (2004) reconstructed monthly and seasonal temepratures in Europe during the last 1500 years. The reconstruction shows that the climate over the last decades of the 20th century and the beginning of the 21st century is most probably warmer than the climate in the last 500 years ($p<0.05$). The Medditerranean region is very vurnerable to climate change. Some studies show how temperature increases more in summer than in winter (*Alcamo et al.*, 2007). By doing analysis of data from 49 meteorological stations in Italy from 1961 to 2006, there are great differences between the seasons: a) during the winter months there is no trend, except for North Italy, where the temperature increase was present in the 60s.; b) during the summer months there was a negative trend until 1981, when the trend changed into positive; c) autumn months have temperature increasmnent which started in the 70s (*Toreti et al.*, 2010). *Espírito Santo et al.* (2014) analyzed 23 meteorological stations in Portugal. The study focused on extreme values of air temperature. The results show increasing mean air temeperature during the spring and summer months, from 1941 to 2006. *Bilbao et al.* (2019) confirm this, and conclude that the autumn months have the

lowest increase in temperature in Spain from 1950 to 2011. Over the past few decades, trends of aridity and the posibility for extreme climate events are present (*Mishra* and *Singh*, 2010; *Trenberth et al.*, 2015). Future predictions of climate in Medditerranean region are characterized by higher annual and seasonal surface air temepratures, where the summer months will be particulary affected (*Giorgi* and *Lionello*, 2008; *Spinoni et al.,* 2017).

In Southeastern Europe, there are a lot of papers which deal with analysis of mean temperatures on annual and seasonal levels, as well as aridity change as one the best indicators for climate change (*Jovanović et al.,* 2002; *Ducić* and *Radovanović,* 2005; *Milošević et al.,* 2013; *Unkašević* and *Tošić,* 2013; *Bajat et al.,* 2015; *Gavrilov et al*., 2015, 2016, 2018; *Tošić et al.,* 2016; *Trbić et al.,* 2017; *Bačević et al*., 2017, 2018, 2020; *Milošević et al*., 2017; *Radaković et al.,* 2017; *Vukoičić et al.,* 2018, *Milentijević et al.*, 2018, 2022).

In this paper, southern and southeastern Bosnia and Herzegovina (B&H) are being investigated in terms of annual and seasonal trends of surface air temperatures. Similar studies have been published (*Trbić et al.,* 2017; *Popov et al.,* 2017, 2018a, 2018b, 2019a, 2019b; *Papić et al*., 2020), but the aim of this study is to show the seasonal trends in temperature, because there is lack of such information in this country. This study can help in creating a more comprehensive picture of climate change in the Medditerranean.

2. Study area

Southern and southeastern Bosnia and Herzegovina are placed in the historical region called Herzegovina, which is bordered with Croatia and Montenegro on southwest and south, while at the north it is surrounded by municipalities of Livno, Tomislavgrad, Prozor, Konjic, Kalinovik, Foča, and Čajniče (*Fig. 1*). The study area is located between the 44°23’ and 42°55’N, and 16°52’ and 19°25’E. Meteorological stations, their geographic coordinates, and elevation are marked in *Fig. 1* and *Table 1*.

Table 1. Meteorological stations and their geographical coordinates and elevations in southern and southeastern Bosnia and Herzegovina.

Station No.	Station location	Altitude	Latitude	Longitude
1	Livno	739 m	43° 49′ 22″ N	17° 00′ 04″ E
2	Bileca	480 m	42° 52′ 04″ N	18° 25′ 29″ E
3	Mostar	48 m	43° 20′ 53″ N	17° 47′ 38″ E
4	Ivan Sedlo	955 m	43° 45′ 04″ N	18° 02′ 10″ E

Fig. 1. The location of southern and southeastern Bosnia and Herzegovina with used meteorological stations.

3. Material and methods

3.1. Material

The analyzed period in this study is from 1961 to 2017. The raw data is measured by the Federal Hydrometeorological Institute of Bosnia and Herzegovina (https://www.fhmzbih.gov.ba/) and Republic Hydrometeorological Service of Republika Srpska (https://rhmzrs.com/?script=lat). Because of the civil war during 1991–1995, the Service was not working, and thus, data for these years do not excist. The only exception is the meteorological station in the city of Mostar, which has continuous data. The method of interpolation was used to fill the missing data (*Kasam et al.,* 2014; *Kilibarda et al*., 2015). Different elevations of meteorological stations cause different climate types. For example, the relative elevation between the highest (Ivan Sedlo 955 m.a.s.l.) and the lowest meteorological stations (Mostar 48 m.a.s.l.) is 907 m. Obvious differences in elevation cause the presence of vertical thermic gradient. That means that the temperature decreases on every 100 m by 0.65 °C (*Oliver*, 2005). The specific

relief conditions combined with the influence of Adriatic Sea make need for analysis of climatological data for each station separately.

The average annual surface air temperatures (YT), mean maximal surface air temperatures (YT_x), and mean minimal surface air temperatures (YT_n) were analysed in this study. These three parameters were used for calculation of seasonal values: winter, spring, summer and autumn (*W, Sp, Su* and *A*). A total of 48 time series were analyzed. Each of these series is marked with different acronyms, which indicate meteorological station, season, and temperature type. They can be found in *Table 2*.

Table 2. The list of 48 time series with unique acronyms obtained in this study, separated by used meteorological stations.

Station	Time series	Station	Time series
Livno (L)	*L-W-YT*	**Mostar (M)**	*M-W-YT*
	L-W-Ytx		*M-W-Ytx*
	L-W-Ytn		*M-W-Ytn*
	L-Sp-YT		*M-Sp-YT*
	L-Sp-Ytx		*M-Sp-Ytx*
	L-Sp-Ytn		*M-Sp-Ytn*
	L-Su-YT		*M-Su-YT*
	L-Su-Ytx		*M-Su-Ytx*
	L-Su-Ytn		*M-Su-Ytn*
	L-A-YT		*M-A-YT*
	L-A-Ytx		*M-A-Ytx*
	L-A-Ytn		*M-A-Ytn*
Bileća (B)	*B-W-YT*	**Ivan Sedlo (IS)**	*IS-W-YT*
	B-W-Ytx		*IS-W-Ytx*
	B-W-Ytn		*IS-W-Ytn*
	B-Sp-YT		*IS-Sp-YT*
	B-Sp-Ytx		*IS-Sp-Ytx*
	B-Sp-Ytn		*IS-Sp-Ytn*
	B-Su-YT		*IS-Su-YT*
	B-Su-Ytx		*IS-Su-Ytx*
	B-Su-Ytn		*IS-Su-Ytn*
	B-A-YT		*IS-A-YT*
	B-A-Ytx		*IS-A-Ytx*
	B-A-YT		*IS-A-Ytn*

3.2. Methods

Three statistical approaches were used. The first one is a linear trend for each time series (*Draper* and *Smith*, 1966), the second one includes the Mann-Kendall test (*Mann,* 1945*; Kendall,* 1938; *Gilbert,* 1987), and the last is called the magnitude of trend (*Gavrilov et al.,* 2016). For data analysis, the software Microsoft Office Excel 2007 (12.0.6611.1000 SP3 MSO 12.0.6607.1000) and its extension XLSTAT (https://www.xlstat.com/en) were used.

3.2.1. Linear trend equation

The method of linear trend is commonly used for analysis, evaluation, and distribution of temperature changes in time (*Heim*, 2015; *Ghebrezgabher et al*., 2016). The trend line is the unique line that minimizes the sum of squared deviations from the data, measured in the vertical direction. It is expressed by the equation:

$$y = ax + b, \tag{1}$$

where*y* presents the temperature in °C, *a* is the slope, or in other words the increase per period, *x* represents year, while *b* is the value where the trend line intersects the ordinate in the beginning of the period. The trend will follow the value of the slope, where there are three possible options: a) the slope is higher than zero- the trend is positive; b) the slope is equal to zero- there is no trend; c) the slope is lower than zero- the trend is negative.

3.2.2. The magnitude of a trend

The linear trend equasion can be used for calculation of the magnitude of a trend (*Gavrilov et al.*, 2015, 2016). In this case it can be expressed as:

$$\Delta y = y(1961) - y(2017), \tag{2}$$

where Δy presents the magnitude of a trend in °C, $y(1961)$ is the temperature from the beginning of the period, and $y(2017)$ is the temperature of the last year in the used period. There are three cases for the trend: a) when Δy is greater then zero - the trend is negative; b) when Δy is lower than zero - the trend is positive; c) when Δy is zero - there is no trend magnitude.

3.2.3. Mann-Kendall trend tests

This is a famous nonparametric method for the validation of trend in geosciences (*Mohorji et al.* 2017), because of its robustness, as well as fast and simple use (*Mann,* 1945; *Kendall,* 1938; *Gilbert*, 1987). The purpose of this test is to show

which of the two possible hypotheses are true: the null hypothesis (H_o) – there is no trend in the time series; and the alternative hypothesis (H_a) – there is a statistically significant trend for the chosen α value. The main role in this test has a p value, or probability value (*Karmeshu,* 2012; *Razavi et al.*, 2016), which confirms the confidence of the hypothesis. If the p value is below than or equal to the alpha ($p< 0.05$), then the null hypothesis must be rejected, and the result is statistically significant. Contrary to this, if the p value is greater than alpha, the H_o is accepted (*Mudelsee,* 2014).

3.2.4. GIS numerical analysis

GIS (Geographical Information System) of data presents a very powerful tool for calculating and estimating the climate data. This meteorological data may be used in calculating the climate properties in the area. With the help of two open-source GIS softwares, QGIS 3.4.12 and SAGA, we calculated and elaborated climate data in the study area. Climate characteristics of a two-dimensional profile were analyzed in this paper (*Valjarević et al.,* 2018a). There are plenty of scientists which had used some advanced GIS algorithms and methods (*Valjarević et al.,* 2018b; *Zabel et al.*, 2014). The special algorithms used in this research are semi-kriging, spatial interpolation, interpolation, and grid analysis. Analyzed meteorological data were transformed with the usage of GIS tools and presented via maps. These maps present annual and seasonal climate properties and interpolated data.

4. Results

4.1. Trend parameters

Four meteorological stations (Livno, Bileća, Mostar, and Ivan Sedlo) have the four season time series for average annual surface air temperatures (YT), mean maximal surface air temperatures (YTx), and mean minimal surface air temperatures (YTn) which makes a total of 48 different time series. *Fig. 2* presents these parameters with their trend equations in the analysed area from 1961 to 2017. The trend magnitude (Δyt) and the probability (p), for each time series and each meteorological station, are presented in *Tables 3* and *4*.

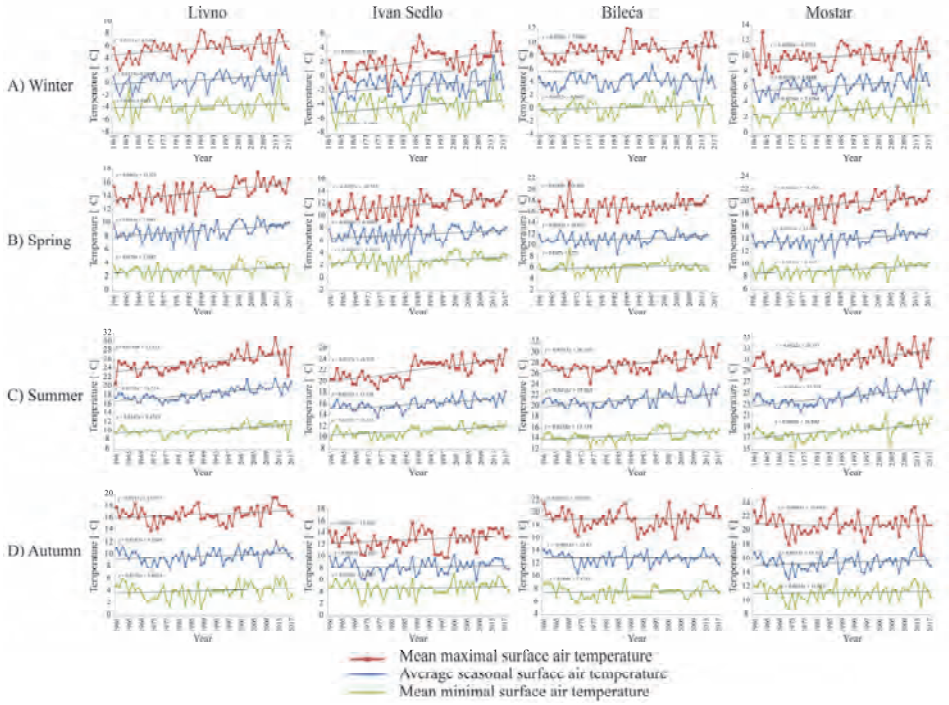

Fig. 2. A) Winter, B) spring, C) summer, and D) autumn; mean maximal surface air temperatures, average seasonal surface air temperatures, and mean minimal surface air temperatures, with linear trend equations from 1961 to 2017, for the four used meteorological stations.

Table 3. Trend equation y, trend magnitude Δy, and probability p of the confidences for 48 time series.

Time series	Trend equation	Δy(°C)	p(%)
L-W-YT	$y = 0.02x - 0.15$	1.5	0.009
L-W-YTx	$y = 0.03x + 4.54$	2.2	< 0.001
L-W-YTn	$y = 0.01x - 3.93$	0.6	0.380
B-W-YT	$y = 0.01x + 3.71$	0.4	0.815
B-W-YTx	$y = 0.02x + 7.98$	1.3	0.581
B-W-YTn	$y = 0.01x - 0.38$	0.6	0.336
M-W-YT	$y = 0.02x + 5.48$	1.3	0.002
M-W-YTx	$y = 0.02x + 9.37$	1.2	0.015
M-W-YTn	$y = 0.02x + 2.37$	1.2	0.013
IS-W-YT	$y = 0.03x - 2.20$	1.8	0.011

Table 3. Continued

Time series	Trend equation	*Δy(°C)*	*p(%)*
IS-W-YTx	$y = 0.05x + 0.48$	3.0	0.001
IS-W-YTn	$y = 0.03x - 5.10$	1.8	0.008
L-Sp-YT	$y = 0.03x + 7.98$	1.8	< 0.001
L-Sp-YTx	$y = 0.04x + 13.32$	2.6	< 0.001
L-Sp-YTn	$y = 0.01x + 2.58$	0.9	0.009
B-Sp-YT	$y = 0.01x + 10.83$	0.9	0.017
B-Sp-YTx	$y = 0.01x + 16.40$	1.1	0.007
B-Sp-YTn	$y = 0.01x + 5.77$	0.6	0.027
M-Sp-YT	$y = 0.03x + 13.20$	1.7	< 0.001
M-Sp-YTx	$y = 0.03x + 18.76$	1.9	0.001
M-Sp-YTn	$y = 0.02x + 8.46$	1.3	0.001
IS-Sp-YT	$y = 0.02x + 6.50$	1.1	0.0156
IS-Sp-YTx	$y = 0.03x + 10.75$	2.2	0.001
IS-Sp-YTn	$y = 0.02x + 2.26$	1.1	0.004
L-Su-YT	$y = 0.05x + 16.73$	3.2	< 0.001
L-Su-YTx	$y = 0.07x + 23.22$	4.2	< 0.001
L-Su-YTn	$y = 0.03x + 9.45$	1.9	< 0.001
B-Su-YT	$y = 0.04x + 19.96$	2.3	< 0.001
B-Su-YTx	$y = 0.05x + 26.35$	2.9	0.001
B-Su-YTn	$y = 0.02x + 13.73$	1.4	0.001
M-Su-YT	$y = 0.05x + 22.77$	3.0	< 0.001
M-Su-YTx	$y = 0.06x + 29.18$	3.5	< 0.001
M-Su-YTn	$y = 0.04x + 16.89$	2.6	< 0.001
IS-Su-YT	$y = 0.03x + 15.15$	1.8	< 0.001
IS-Su-YTx	$y = 0.07x + 19.97$	4.1	< 0.001
IS-Su-YTn	$y = 0.03x + 10.32$	1.8	< 0.001
L-A-YT	$y = 0.01x + 9.25$	1.0	0.008
L-A-YTx	$y = 0.02x + 16.07$	1.2	0.014
L-A-YTn	$y = 0.01x + 3.66$	0.8	0.135
B-A-YT	$y = -0.01x + 12.87$	-0.1	0.815
B-A-YTx	$y = 0.01x + 18.93$	0.1	0.581
B-A-YTn	$y = 0.01x + 7.47$	0.2	0.336
M-A-YT	$y = 0.02x + 15.12$	0.6	0.092
M-A-YTx	$y = -0.01x + 21.05$	-0.3	0.591
M-A-YTn	$y = 0.01x + 11.02$	0.3	0.292
IS-A-YT	$y = 0.01x + 8.20$	0.3	0.243
IS-A-YTx	$y = 0.02x + 12.30$	1.1	0.030
IS-A-YTn	$y = 0.01x + 4.42$	0.6	0.292

Table 4. The main results of the analysis of temperature trends for 48 time series.

Time series	Trend equation	The classical MK test
L-W-YT	positive trend	significant positive trend
L-W-YTx	positive trend	significant positive trend
L-W-YTn	positive trend	no trend
B-W-YT	positive trend	no trend
B-W-YTx	positive trend	significant positive trend
B-W-YTn	positive trend	no trend
M-W-YT	positive trend	significant positive trend
M-W-YTx	positive trend	significant positive trend
M-W-YTn	positive trend	significant positive trend
IS-W-YT	positive trend	significant positive trend
IS-W-YTx	positive trend	significant positive trend
IS-W-YTn	positive trend	significant positive trend
L-Sp-YT	positive trend	significant positive trend
L-Sp-YTx	positive trend	significant positive trend
L-Sp-YTn	positive trend	significant positive trend
B-Sp-YT	positive trend	significant positive trend
B-Sp-YTx	positive trend	significant positive trend
B-Sp-YTn	positive trend	significant positive trend
M-Sp-YT	positive trend	significant positive trend
M-Sp-YTx	positive trend	significant positive trend
M-Sp-YTn	positive trend	significant positive trend
IS-Sp-YT	positive trend	significant positive trend
IS-Sp-YTx	positive trend	significant positive trend
IS-Sp-YTn	positive trend	significant positive trend
L-Su-YT	positive trend	significant positive trend
L-Su-YTx	positive trend	significant positive trend
L-Su-YTn	positive trend	significant positive trend
B-Su-YT	positive trend	significant positive trend
B-Su-YTx	positive trend	significant positive trend
B-Su-YTn	positive trend	significant positive trend
M-Su-YT	positive trend	significant positive trend
M-Su-YTx	positive trend	significant positive trend
M-Su-YTn	positive trend	significant positive trend
IS-Su-YT	positive trend	significant positive trend
IS-Su-YTx	positive trend	significant positive trend
IS-Su-YTn	positive trend	significant positive trend
L-A-YT	positive trend	significant positive trend
L-A-YTx	positive trend	significant positive trend
L-A-YTn	positive trend	no trend
B-A-YT	negative trend	no trend
B-A-YTx	no trend	no trend
B-A-YTn	no trend	no trend
M-A-YT	Positive trend	no trend
M-A-YTx	negative trend	no trend
M-A-YTn	no trend	no trend
IS-A-YT	positive trend	no trend
IS-A-YTx	positive trend	significant positive trend
IS-A-YTn	positive trend	no trend

4.2. The Mann-Kendall test

The results of the Mann-Kendall trend test for seasonal temperatures from 1961 to 2017 in the territory of southern and southeastern Bosnia and Herzegovina are presented in *Table 4*. In most of the analyzed cases, the trend is statistically significant and positive. For the final evaluation of the surface air temperature trend, all the numerical parameters and graphical interpretations included in Mann-Kendall tests were considered. The hypothesis H_a was accepted for 36 time series. The Mann-Kendall test proved wrong - eight time series which had a positive linear trend. The similar situation occurred when the linear trend in two cases was negative, but the Mann-Kendall test accepted the H_0 hypothesis.

If the probability p in the time series YT, YTx, and YTn was lower than α, the hypothesis H_0 (there is no trend) was rejected and the hypothesis H_a (there is trend) was accepted.

In the next paragraph, the results will be presented by seasonal criterium. During the spring and summer months, all of the 24 cases had significant positive trend in mean maximal surface air temperatures, mean minimal surface air temperatures, and average summer and average spring surface air temperatures. This brings to conclusion that the rising temperature trend is present for at least half of the year in the entire analyzed territory. In all of the mentioned situations during the spring and summer, the H_a hypothesis is accepted. During the autumn, from the 12 analyzed cases (three for each station), only 25% had a positive significant trend. These are the mean maximal surface air temperatures of Livno and Ivan Sedlo. Livno is the only station, where the average autumn surface air temperature has a significant positive trend proven by the Mann-Kendall test. The other 9 cases had no trend: *L-A-YTn, B-A-YT, B-A-YTx, B-A-YTn, M-A-YT, M-A-YTx, M-A-YTn, IS-A-YT,* and *IS-A-YTn*; where their *p* values were 0.1357, 0.0273, 0.5813, 0.3362, 0.0923, 0.5911, 0.2921, 0.2434, and 0.2921; while the risk to reject the H_0 while it is true was 13.58%, 2.74%, 58.13%, 33.63%, 9.24%, 59.11%, 29.21%, 24.35%, and 29.22%, respectively. The winter period has a different situation from the other seasons. It is shown that only 25% of the cases had no trend detected by the Mann-Kendall test. These include mean minimal winter surface air temperature of Livno and Bileća. Even though they are not on the highest elevation on the study area, their winter conditions are being conserved, especially in Bileća, where even the average winter temperatures were found to have no trend. For the time series *L-W-YTn, p* value is 0.3860. The risk to reject the H_0 while it is true, is lower than 38.07%. The *p* value for meteorological station Bileća in the time series *B-W-YTn* is 0.0740. The risk to reject the H*0* while it is true, is lower than 7.37%. For the time series *B-W-YT, p* values is 0.8155. The risk to reject the H_0 while it is true, is lower than 81.55%.

4.3. GIS numerical analysis

Average annual surface air temperatures (YT), mean maximal (YTx) and mean minimal (YTn) surface air temperatures per seasons for the period from 1961 to 2017 are shown in *Figs. 3, 4, 5,* and *6*. Isotherms follow the temperatures and indicate the effect of the Adriatic Sea and higher terrain. Meteorological station Ivan Sedlo is a mountainous station, while meteorological station Livno is situated in the karst polje. This is the reason they have lower temperatures, while meteorological stations Mostar and Bileća are in the lower terrain, and thus have the Adriatic influence.

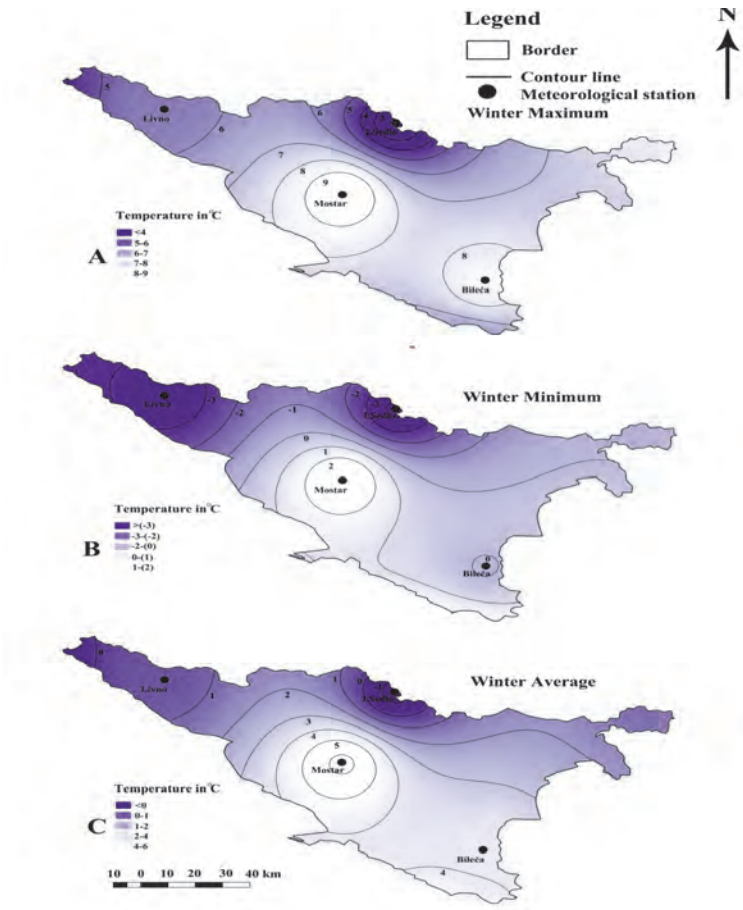

Fig. 3. Average winter, mean maximal, and mean minimal surface air temperatures during the winter from 1961 to 2017 in southern and southeastern Bosnia and Herzegovina.

Fig. 3 shows the analyzed temperatures during the winter. The average annual surface air temperatures go from -1 °C to 5 °C. The mean minimal temperatures go from 0 °C to -3 °C, while the mean maximal temperatures go from 3 °C to 9 °C.

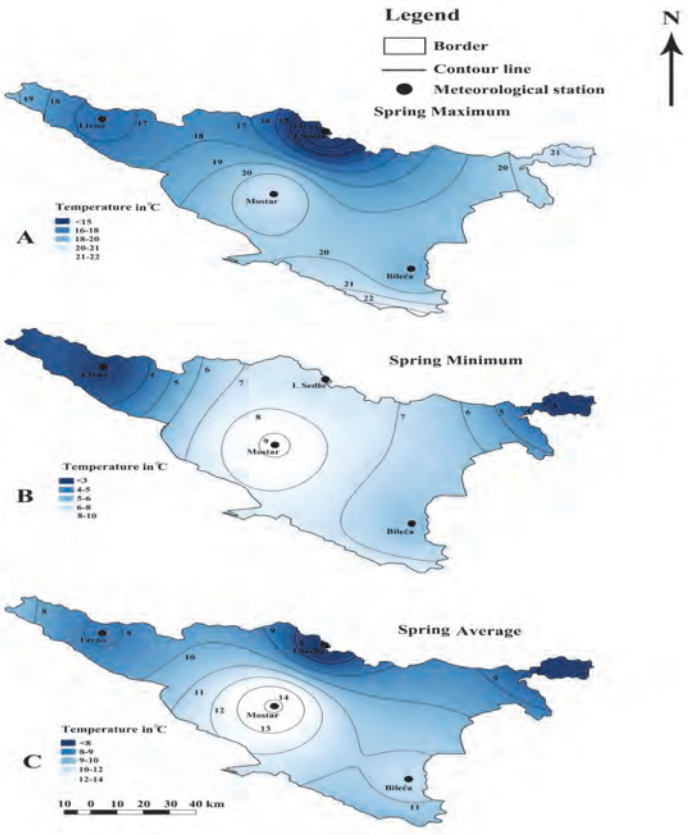

Fig. 4. Average spring, mean maximal, and mean minimal surface air temperatures during the spring from 1961 to 2017 in southern and southeastern Bosnia and Herzegovina.

Fig. 4 shows the analyzed temperatures during the spring. The average annual surface air temperatures go from 8 °C to 14 °C. The mean minimal temperatures go from 3 °C to 9 °C, while the mean maximal temperatures go from 13 °C to 22 °C.

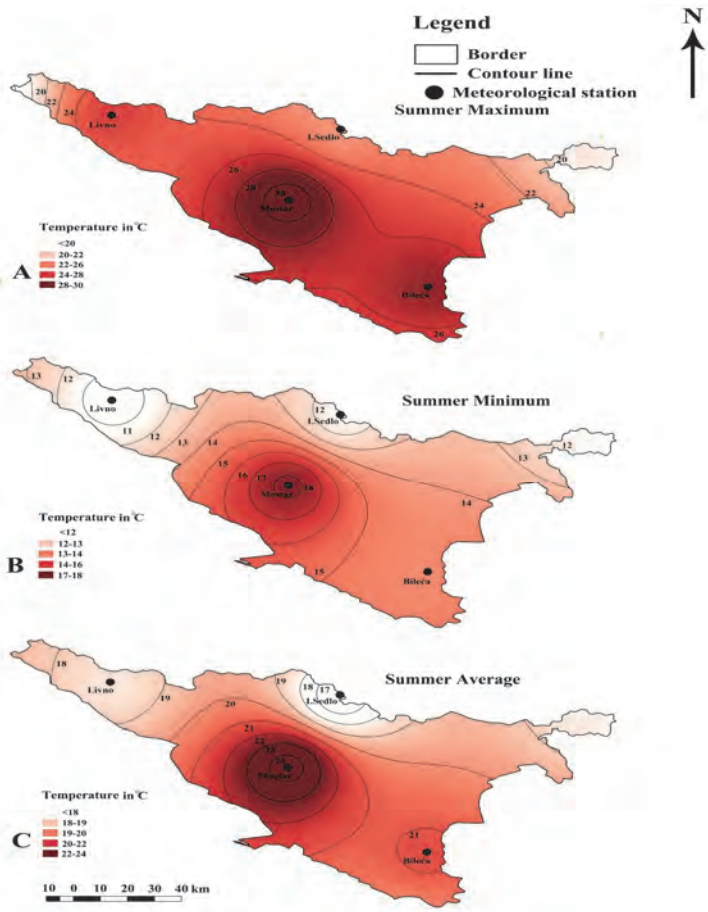

Fig. 5. Average summer, mean maximal, and mean minimal surface air temperatures during the summer from 1961 to 2017 in southern and southeastern Bosnia and Herzegovina.

Fig. 5 shows that the average summer surface air temperatures go from 17 °C to 24 °C. The mean minimal temperatures go from 11 °C to 18 °C, while the mean maximal temperatures go from 20 °C to 30 °C.

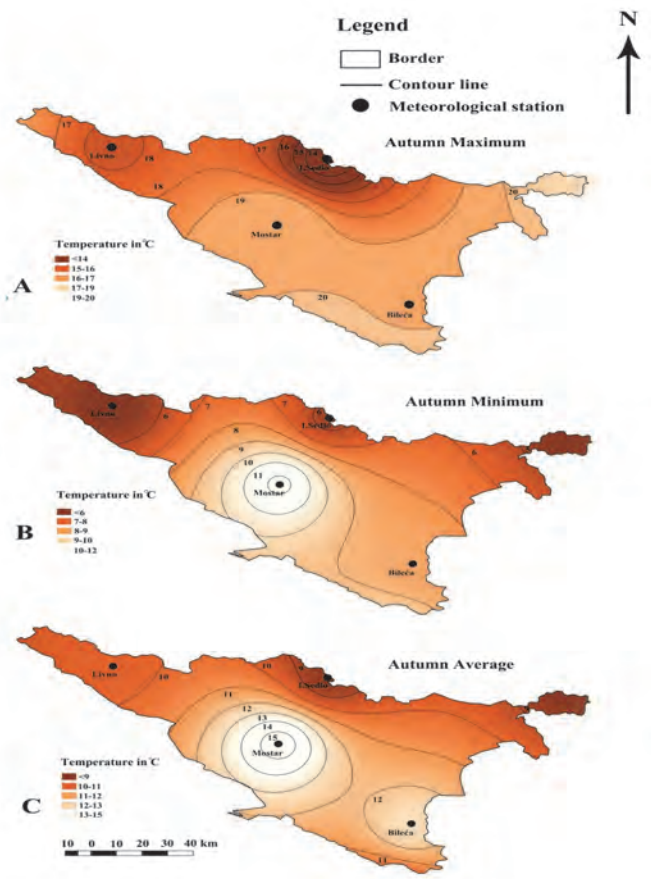

Fig. 6. Average autumn, mean maximal, and mean minimal surface air temperatures during the autumn from 1961 to 2017 in southern and southeastern Bosnia and Herzegovina.

Fig. 6 shows that the average autumn surface air temperatures go from 9 °C to 15 °C. The mean minimal temperatures go form 5 °C to 11 °C, while the mean maximal temperatures go from 14 °C to 20 °C.

5. Discussion

The presented results show that the temperature is increasing in 36 cases, from the 48 cases in total. The summer temperature has the highest growing trend when considering the summer maximal surface air temperatures. This includes the following time series: *L-Su-YTx* (4.2 °C) and *IS-Su-Ytx* (4.1 °C).

The smallest changes are present in the minimal autumn surface air temperatures, for example, *B-A-Ytn* (0.2 °C) and maximal autumn surface air temperature *B-A-Ytx* (0.1 °C) in Bileća. The mean autumn surface air temperatures in Bileća, *B-A-YT* (-0.1 °C), and maximal autumn surface air temperatures in Mostar, *M-A-Ytx* (-0.3 °C) have the decrease of temperature values.

Spring temperatures have the greatest changes when analyzing the maximum surface air temperatures *L-Sp-Ytx* (2.6 °C) and *IS-Sp-Ytx* (1.9 °C). The smallest increase of temperature values during the spring is present in average spring temperatures *B-Sp-YT* (0.9 °C), and in mean minimal surface air temperatures *B-Sp-Ytn* (0.6 °C).

The average increase in temperature is more expressed over the winter in comparison to autumn and spring. The greatest rise in temperature belongs to the winter maximum surface air temperature *IS-W-Ytx* (3.0 °C) and average winter surface air temperature in Ivan Sedlo *IS-W-YT* (1.8 °C). The smallest temperature change has occurred in winter minimal surface air temperature *B-W-Ytn* (0.6 °C), and average winter surface air temperature *B-W-YT* (0.4 °C) in Bileća.

The results from this study are in good agreement to those in previous studies. Even though this region is experiencing such temperature changes, not all the regions on Earth are equally affected (*IPCC*, 2007, 2014, 2018). *Toreti et al*. (2010) found that seasonal temperatures have a positive trend in Italy, even though there are regional differences. Winter temperature trends do not exist, except for the stations at the north. On the other side, there is a positive spring temperature trend (for 1.1 °C). During the summer, there are even negative trends from 1961 to 1981, but positive trends from 1981 to 2006. This resulted in the increase of the mean summer temperatures over Italy for 1.5 °C. The trend in the mean autumn temperatures starts to show up from 1970, until when the temperature raised by 1. 6 °C in Italy. *Espírito Santo et al.* (2014) analyzed seasonal temperatures change in two periods: from 1945 to 1975, and from 1976 to 2006. In the first period, maximal and minimal surface air temperatures decrease in all of the seasons, except in winter. On the other side, only the temperature trend in spring is statistically significant. In the second period, all of the seasons have the increasing of selected parameters, which is statistically significant during the spring and summer, and also in minimal autumn and maximal winter surface air temperatures. *Bilbao et al*. (2019) found positive temperature trend in mean seasonal, mean maximal, and mean minimal temperatures. Mean maximal temperatures intensify during the summer and spring. Mean minimal temperatures are rising more in winter and spring than in autumn. Similar results in rising the mean surface air temperatures are recorded in Vojvodina, Northern Serbia (*Gavrilov et al.*, 2015, 2016), in Central and Western Serbia (*Vukoičić et al.,* 2018), and Slovenia (*Milošević et al.,* 2013, 2017). Spotted temperature changes in the southern and southeastern parts of Bosnia and Herzegovina show similarity to the global temperature change from the 1980's (*Hardy*, 2006). This study shows that there is a comparable process in temperature during the same seasons in the wider region. There are technical, technological, financial, and educational constraints that must

be considered (*Trbić et al.,* 2018). Opportunities for the adaptation of the economic sector to climate change in this country aim to reduce the sensitivity of this sector to the emerging climate trends by a) reducing the negative effects of climate change; b) increasing the resilience of society, and c) seizing the opportunity for development caused by climate change (*Radusin et al*., 2013; *Trbić et al*., 2018; *Popov et al.,* 2019a).

6. Conclusion

In this study, annual and seasonal trends of mean, mean maximal, and mean minimal surface air temperatures over the southern and southeastern parts of Bosnia and Herzegovina were analyzed from 1961 to 2017. Methods can be separated into three parts: a) linear trend equation, b) the magnitude of trend, and c) Mann-Kendall test. There is a statistically significant trend in 36 time series. This increase goes in the interval from 0.1 °C to 4.2 °C. The highest growing trend is discovered in the summer mean maximal surface air temperatures in Livno and Ivan Sedlo stations. There is also a negative trend, which is between -0.1 °C and -0.3 °C, in maximal autumn surface air temperatures in Mostar. Generally, in this study it is found, that the average increase in temperature is more expressed over the winter in comparison to autumn and spring. Our trends fit the wider region and our results confirm the IPCC scenario. These changes have an impact not only on ecosystems but also on the economy. Bosnia and Herzegovina lack the studies about adaptation to the temperature change. The analysis of temperature behavior of the past few decades, like in this study, needs to be the basis of policy, planning, and regional development. The guidelines defined in this way must be fulfilled, having in mind that climate events have the tendency to be more extreme and more frequent in the future.

Acknowledgments: This paper is a result of the projects III43007 and III044006 funded by the Serbian Ministry of Education, Science and Technological Development.

References

Alcamo, J., Moreno, J.M., Nováky, B., Bindi, M., Corobov, R., Devoy, R.J.N., Giannakopoulos, C., Martin, E., Olesen, J.E. and *Shvidenko, A.,* 2007: Europe. In: Parry, *M.L., Canziani, O.F., Palutikof, J.P., van der Linden, P.J.,* and *Hanson, C.E.* (eds.) Climate change 2007: Impacts, adaptation and vulnerability. Contribution of Working Group II to the Fourth Assessment Report of the Intergovernmental Panel on Climate Change. Cambridge University Press, Cambridge, 541–580.

Bačević, R.N., Vukoičić, Z.D., Nikolić, M., Janc, N., Milentijević, N., and *Gavrilov, B.M.,* 2017: Aridity in Kosovo and Metohija, Serbia. *Carpathian J. Earth Environ. Sci. 12*, 563–570.

Bačević, R.N., Pavlović, M., and *Rašljanin, I.,* 2018: Trend Assessing Using Mann-Kendall's Test for Priština Meteorological Station Temperature and Precipitation Data, Kosovo and Metohija, Serbia. *Univ. Thought – Publ. Nat. Sci. (8)2,* 39–43. https://doi.org/10.5937/univtho8-19513

Bačević, N.R., Valjarević, A., Milentijević, N., Kićović, D., Ivanović, M., and *Mujević, M.,* 2020: Analysis of air temperature trens: City of Podgorica (Montenegro). *Univ. Thought – Publ. Nat. Sci. 10(1),* 31–36. https://doi.org/10.5937/univtho10-24790

Bajat, B., Blagojević, D., Kilibarda, M., Luković, J., and *Tošić, I.,* 2015: Spatial Analysis of the Temperature Trends in Serbia during the Period 1961–2010. *Theor. Appl. Climatol. 121,* 289–301. https://doi.org/10.1007/s00704-014-1243-7

Bilbao, J., Román, R., and *De Miguel, A.,* 2019: Temporal and spatial variability in surface air temperature and diurnal temperature range in Spain over the period 1950–2011. *Climate 7*, 16. https://doi.org/10.3390/cli7010016

Blunden, J. and *Arndt, D.S.*, 2015: State of the Climate in 2014. *Bull. Amer. Meteorol Soc. 96(7)*: ES1–32. https://doi.org/10.1175/2015BAMSStateoftheClimate.1

Draper, N.R. and *Smith, H.,* 1966: Applied regression analysis. John Wiley & Sons, New York

Ducić, V. and *Radovanović, M.,* 2005: Climate of Serbia. Institute of Textbooks and Teaching Aids, Belgrade.

EEA, 2018: National Climate Change Vulnerability and risk asssessments in Europe. *European Environment Agency Report No.1/2018.* https://www.eea.europa.eu/publications/national-climate-change-vulnerability-2018. Accessed 06 August 2019

Espírito Santo, F., de Lima, M.I., Ramos, A.M., and *Trigo, R.M.,* 2014: Trends in seasonal surface air temperature in mainland Portugal, since 1941. *Int. J. Climatol. 34*, 1814–1837. https://doi.org/10.1002/joc.3803

Gavrilov, M.B., Marković, S.B., Jarad, A., and *Korać, V.M.,* 2015: The analysis of temperature trends in Vojvodina (Serbia) from 1949 to 2006. *Thermal Sci. 19*, 339–350. https://doi.org/10.2298/TSCI150207062G

Gavrilov, M.B., Tošić, I., Marković, S.B., Unkašević, M., and *Petrović, P.*, 2016: The analysis of annual and seasonal temperature trends using the Mann-Kendall test in Vojvodina, Serbia. *Időjárás 120(2)*, 183-198.

Gavrilov, M.B., Marković, S.B., Janc, N., Nikolić, M., Valjarević, A., Komac, B., Zorn, M., Punišić, M., and *Bačević, N.*, 2018: Assessing average annual air temperature trends using the Mann– Kendall test in Kosovo. *Acta Geographica Slovenica 58*, 8–25. https://doi.org/10.3986/AGS.1309

Ghebrezgabher, M.G., Yang, T., and *Yang, X.,* 2016: Long-term trend of climate change and drought assessment in the Horn of Africa. *Adv. Meteorol. 2016,* ID 8057641. https://doi.org/10.1155/2016/8057641

Gilbert, R.O., 1987: Statistical methods for environmental pollution monitoring. Van Nostrand Reinhold, New York.

Giorgi, F. and *Lionello, P.,* 2008: Climate change projections for the Mediterranean region. *Glob. Planet. Change 63,* 90–104. https://doi.org/10.1016/j.gloplacha.2007.09.005

Hardy, J.T., 2006: Climate change – causes, effects and solutions. Wiley, Chichester.

Heim, R.R., 2015: An overview of weather and climate extremes – Products and trends. *Weather Climate Extr. 10(B),* 1–9. https://doi.org/10.1016/j.wace.2015.11.001

IPCC, 2007: Climate Change 2007: The Physical Science Basis, Contribution of Working Group I to the Fourth Assessment Report of the Intergovernmental Panel on Climate Change. *(eds.: Solomon, S., Qin, D., Manning, M., Chen, Z., Marquis, M., Averyt, K.B., Tignor, M. and Miller, H.L.).* Cambridge University Press, Cambridge.

IPCC, 2014: Climate Change 2014: Synthesis Report. Contribution of Working Groups I, II and III to the Fifth Assessment Report of the Intergovernmental Panel on Climate Change. *(eds.: Core Writing Team, Pachauri, R.K.,* and *Meyer, L.A.). IPCC*, Geneva.

IPCC, 2018: Summary for Policymakers. In: *(eds.: Masson-Delmotte, V., Zhai, P., Pörtner, H.O., Roberts, D., Skea, J., Shukla, P.R., Pirani, A., Moufouma-Okia, W., Péan, C., Pidcock, R., Connors, S., Matthews, J.B.R., Chen, Y., Zhou, X., Gomis, M.I., Lonnoy, E., Maycock, T., Tignor, M. and Waterfield, T.)* Global warming of 1.5 °C. An IPCC Special Report on the impacts of global warming of 1.5 °C above pre-industrial levels and related global greenhouse gas emission pathways, in the context of strengthening the global response to the threat of climate change, sustainable development, and efforts to eradicate poverty. WMO, Geneva, 3–24.

Jones, P.D. and *Briffa, K.R.,* 1991: Global surface air temperature variations during the twentieth century: Part 1, spatial, temporal and seasonal details. *The Holocene 2,* 165–179. https://doi.org/10.1177/095968369200200208

Jovanović, G., Reljin, I., and *Savić, T.,* 2002: NAO Influence on climate variability in FRY. 18th International conference on Carpathian meteorology. Belgrade.

Karmeshu, N., 2012: Trend detection in annual temperature and precipitation using the Mann Kendall test – a case study to assess climate change on select states in the northeastern United States. Master's thesis, 27, University of Pennsylvania, Philadelphia

Kasam, A.A., Lee, B.D., and *Paredis, C.J.J.,* 2014: Statistical Method for interpolating missing meteorological data for use in building simulation. *Build. Simul. 7*, 455–465. https://doi.org/10.1007/s12273-014-0174-7

Kendall, M., 1938: A new measure of rank correlation. *Biometrika 30*, 81–89. https://doi.org/10.2307/2332226

Kilibarda, M., Tadić Perčec, M., Hengl, T., Luković, J., and *Bajat, B.,* 2015: Global geographic and feature space coverage of temperature data in the context of spatio-temporal interpolation. *Spat. Stat. 14(A)*, 22–38. https://doi.org/10.1016/j.spasta.2015.04.005

Luterbacher, J., Dietrich, D., Xoplaki, E., Grosjean, M., and *Wanner, H.,* 2004: European seasonal and annual temperature variability, trends, and extremes since 1500. *Science 303*, 1499–1503. https://doi.org/10.1126/science.1093877

Mann, H.B., 1945: Non-parametric tests against trend. *Econometrica 13*, 245–259. https://doi.org/10.2307/1907187

Milentijević, N., Dragojlović, J., Ristić, D., Cimbaljević, M., Demirović, D., and *Valjarević, A.*, 2018: The assessment of aridity in Leskovac Basin, Serbia (1981-2010). *J. Geograph. Inst. "Jovan Cvijić" 68*, 249–264. https://doi.org/10.2298/IJGI1802249M

Milentijević, N., Valjarević, A., Bačević, R.N., Ristić, D., Kalkan, K., Cimbaljević, M., Dragojlović, J., Savić, S. and *Pantelić, M.,* 2022: Assessment of observed and projected climate changes in Bačka (Serbia) using trend analysis and climate modelling. *Időjárás 126(1),* 47–68. doi:10.28974/idojaras.2022.1.3

Milošević, D., Savić, S., Stankov, U., Žiberna, I., Pantelić, M., Dolinaj, D., and *Leščešen, I.*, 2017: Maximum temperatures over Slovenia and their relationship with atmospheric circulation patterns. *Geografie 122*, 1–20. https://doi.org/10.37040/geografie2017122010001

Milošević, D., Savić, S., and *Žiberna, I.,* 2013: Analysis of the climate change in Slovenia: fluctuations of meteorological parameters for the period 1961–2011 (Part I). *Bull, Serbian Geograph Soc 93(1)*, 1–14. https://doi.org/10.2298/GSGD1301001M

Mishra, K.A. and *Singh, P.V.*, 2010: A review of drought concepts. *J. Hydrol. 391*, 202216. https://doi.org/10.1016/j.jhydrol.2010.07.012

Mohorji, A.M., Şen, Z., and *Almazroui, M.,* 2017: Trend analyses revision and global monthly temperature innovative multi-duration analysis. *Earth Syst. Environ 1(9)*, 1–13. https://doi.org/10.1007/s41748-017-0014-x

Mudelsee, M., 2014: Climate time series analysis:classical statistical and bootstrap methods, 2nd edn. Springer, New York. https://doi.org/10.1007/978-3-319-04450-7

Oliver, E.J., 2005: Temperature Distribution. In (*Ed. E.J. Oliver*), Encyclopedia of World Climatology. Springer, Dordrecht, The Netherlands, 711–716.

Papić, D., Bačević, R.N., Valjarević, A., Milentijević, N., Gavrilov, B.M., Živković, M., and *Marković, B.S.*, 2020: Assessment of air temperature trends in South and Southeast Bosnia and Herzegovina (B&H) from 1961 to 2017. *Időjárás 124(3)*, 381–399. https://doi.org/10.28974/idojaras.2020.3.5

Popov, T., Gnjato, S., and *Trbić, G.,* 2017: Trends in extreme temperatures indices in Bosnia and Herzegovina: A case study of Mostar. *Herald 21*, 107–132. https://doi.org/10.7251/HER2117107P

Popov, T., Gnjato, S., Trbić, G., and *Ivanišević, M.,* 2018a: Recent trends in extreme temperature indices in Bosnia and Herzegovina. *Carpathian J. Earth Environ. Sci. 13*, 211–224. https://doi.org/10.26471/cjees/2018/013/019

Popov, T., Gnjato, S., and *Trbić, G.,* 2018b: Changes in temperature extremes in Bosnia and Herzegovina: A fixed tresholds-based index analysis. *J. Geograph. Inst.“Jovan Cvijić” SASA 68(1)*, 17–33. https://doi.org/10.2298/IJGI1801017P

Popov, T., Gnjato, S., and *Trbić, G.,* 2019a: Effects of changes in extreme climate events on key sectors in Bosnia and Herzegovina and adaptation options. In: (eds: *Leal Filho, W., Trbic, G.* and *Filipovic, D.,*) Climate Change Adaptation in Eastern Europe. Climate Change Management. Springer, Cham, 213–228. https://doi.org/10.1007/978-3-030-03383-5_15

Popov, T., Gnjato, S., and *Trbić, G.,* 2019b: Changes in extreme temperature indices over the Peripannonian region of Bosnia and Herzegovina. *Geografie 124(1)*, 19–40. https://doi.org/10.37040/geografie2019124010019

Radaković, G.M., Tošić, A.I., Bačević, R.N., Mlađan, D., Marković, S.B., and *Gavrilov, M.B.*, 2017: The analysis of aridity in Central Serbia from 1949-2015. *Theor. Appl. Climatol. 133*, 887–898. https://doi.org/10.1007/s00704-017-2220-8

Radusin, S., Oprašić, S., Cero, M., Abdurahmanović, I., Vukmir, G., Avdić, S., Cupać, R., Tais, M., Drešković, N., Trbić, G., and *Jakšić, B.,* 2013: Second national communication of Bosnia and Herzegovina under the United Nations framework convention on climate change. UNDP, Banja Luka.

Razavi, T., Switzman, H., Arain, A., and *Coulibaly, P.,* 2016: Regional climate change trends and uncertainty analysis using extreme indices: A case study of Hamilton, Canada. *Climate Risk Manage. 13*, 43–63. https://doi.org/10.1016/j.crm.2016.06.002

Spinoni, J., Naumann, G., and *Vogt, V.J.,* 2017: Pan-European seasonal trends and recent changes of drought frequency and severity. *Glob. Planet. Change 148*, 113–130. https://doi.org/10.1016/j.gloplacha.2016.11.013

Toreti, A., Desiato, F., Fioravanti, G., and *Perconti, W.*, 2010: Seasonal temperatures over Italy and their relationship with low-frequency atmospheric circulation patterns. *Climatic Change 99*, 211–227. https://doi.org/10.1007/s10584-009-9640-0

Tošić, I., Zorn, M., Ortar, J., Unkašević, M., Gavrilov, M.B., and *Marković, S.B.,* 2016: Annual and seasonal variability of precipitation and temperatures in Slovenia from 1961 to 2011. *Atmosph. Res. 168*, 220–233. https://doi.org/10.1016/j.atmosres.2015.09.014

Trbić, G., Bajić, D., Djurdjević, V., Ducić, V., Cupac, R., Markez, Đ., Vukmir, G., Dekić, R., and *Popov, T.,* 2018: Limits to adaptation on climate change in Bosnia and Herzegovina:insights and experiences. In: *(eds.: Leal Filho, W. and Nalau, J.)* Limits to climate change adaptation. Climate Change Management. *Springer*, Cham, 245–259. https://doi.org/10.1007/978-3-319-64599-5_14

Trbić, G., Popov, T., and *Gnjato, S.,* 2017: Analysis of air temperature trends in Bosnia and Herzegovina. *Geograph. Pannonica 21*, 68–84. https://doi.org/10.5937/GeoPan1702068T

Trenberth, K.E., Fasullo, J.T., and *Shepherd, T.G.,* 2015: Attribution of climate extreme events. *Nat. Climate Change 5*, 725–730. https://doi.org/10.1038/nclimate2657

Trenberth, K.E., Jones, P.D., Ambenje, P., Bojariu, R., Easterling, D., Klein Tank, A., Parker, D., Rahimzadeh, F., Renwick, J.A., Rusticucci, M., Soden, B., and *Zhai, P.,* 2007: Observations: Surface and atmospheric climate change. In: (eds. *Solomon, S., Qin, D., Manning, M., Chen, Z., Marquis. M., Averyt, K.B., Tignor, M. and Miller, H.L.*) Climate change 2007: the physical science basis. Contribution of Working Group I to the Fourth Assessment Report of the Intergovernmental Panel on Climate Change. Cambridge University Press, Cambridge, 236–336

Unkašević, M. and *Tošić, I.,* 2013: Trends in temperature indices over Serbia: relationships to large-scale circulation patterns. *Int. J. Climatol 33*, 3152–3161. https://doi.org/10.1002/joc.3652

Valjarević, A., Djekić, T., Stevanović, V., Ivanović, R., and *Jandziković, B.,* 2018a: GIS numerical and remote sensing analyses of forest changes in the Toplica region for the period of 1953–2013. *Appl. Geogr. 92*, 131–139. https://doi.org/10.1016/j.apgeog.2018.01.016

Valjarević, A., Valjarević, D., Stanojević-Ristić, Z., Djekić, T., and *Živić, N.,* 2018b: A geographical information systems-based approach to health facilities and urban traffic system in Belgrade, Serbia. *Geospat. Health 13(2)*, 131–139. https://doi.org/10.4081/gh.2018.729

Vukoičić, D., Milosavljević, S., Penjišević, I., Bačević, N., Nikolić, M., Ivanović, R., and *Jandžiković, B.,* 2018: Spatial analysis of air temperature and its impact on the sustainable development of mountain tourism in Central and Western Serbia. *Időjárás 122*, 259–283. https://doi.org/10.28974/idojaras.2018.3.3

Zabel, F., Putzenlechner, B. and *Mauser, W.*, 2014: Global agricultural land resources – A high resolution suitability evaluation and its perspectives until 2100 under climate change conditions. *PLOS ONE 9(9)*:e107522. https://doi.org/10.1371/journal.pone.0107522

DOI:10.28974/idojaras.2022.3.6

IDŐJÁRÁS

Quarterly Journal of the Hungarian Meteorological Service
Vol. 126, No. 3, July – September, 2022, pp. 375–385

Markov chain analysis of the probability of days in a heat wave period

Árpád Fekete

University of Public Service
Faculty of Water Sciences, Department of Hydraulic Engineering
Bajcsy-Zs. utca 12-14, 6500 Baja, Hungary

**Corresponding Author e-mail: fekete.arpad@uni-nke.hu*

(Manuscript received in final form May 5, 2021)

Abstract—The impact of global climate change is also felt in Hungary. An undesirable effect of climate change (associated with rising temperatures) is mainly the increase in the frequency, intensity, and length of summer heat waves. In this respect, the region of the Southern Great Plain and the Danube-Tisza Region are particularly endangered, but the number of heat wave days has increased throughout the country in recent decades.

This study takes the climatic data sets of Baja into account, and on this basis, it gives the probability that a particular day falls into a heat wave period. Based on this information we draw a general conclusion about the long-term change of this climatic characteristic of the Southern Great Plain. The mathematical model used in the research applies the theory of Markov chains, which is relatively new in statistical analysis.

Key-words: heat wave, Markov chain, the matrix of transition probabilities, equilibrium distribution, return time of heat wave periods

1. Introduction

In the last century, the climate has warmed in Hungary, too. Compared to the last 100 years, the temperature in Hungary has increased by 1 °C, and a further 2.6 °C is expected by 2050 (*Láng et al.*, 2007). The increase in temperature is most intense in summer (*Bartholy et al.*, 2007). Rising temperatures are associated with heat waves. Heat waves as a hazard often have a negative effect causing heat stress in the man. Heat and drought events are of great importance in most climate regions. Heat waves also have a very detrimental effect on the development of plants, for example, maize does not tolerate heat stress above 35 °C, its development slows down or even stops (*Somfalvi-Tóth*, 2018). It is worth looking

at the yield of maize for the period 2010–2019 (*KSH*, 2019). Weaker yields in 2012, 2015, 2017 may correlate with the number of 31, 32, 33 heat wave days occurring in these years.

The annual number of heat waves was 0.5 in the period from 1961 to 1990 in Hungary (*Bartholy et al.*, 2013). The study in the previous reference predicts an average of 4-5 heat waves per year for the end of the century, i.e., the period from 2071 to 2100. This work also supports the previous estimate. We calculated an average of 3.3 heat waves per year at Baja in the period from 2010 to 2019. We will also show an increasing trend.

Serbian researchers (*Pecelj et al.*, 2019) have also found, among other things, that in addition to the increase in the frequency of heat waves, a growth trend is also detected in their duration.

In this study we take the climatic data sets of Baja into account, and on this basis, our goal is to give the probability that a particular day falls into a heat wave period. In a previous article we examined the annual precipitation sums of the last 30 years in the Baja region and the precipitation relations for six months belonging to the vegetation period (based on the SPI6 precipitation index) using Markov chains, as well (*Fekete* and *Keve*, 2020).

2. The definition of heat wave

It is difficult to determine the universal definition of a heat wave that could be applied in all climate zones. There have been numerous responses to the definition of a heat wave in recent years. However, there is no consistent, globally accepted definition; neither the World Meteorological Organization (WMO) nor the World Health Organization (WHO) (*Robinson*, 2001) have developed a uniform, globally acceptable definition of heat wave.

The national meteorological services have all dealt with the issue used to their own territory and climate, and accordingly, the meaning of the term heat wave is not consistent in the published studies either. Basically, a heat wave is an "unusually" warm period, but it means different things by continent, country, and even region. Therefore, it is difficult to find a threshold that suits all climates. The threshold can be the air temperature or an index that takes the interaction between the human body and its environment into account (*Robinson*, 2001). One way to create a threshold is to define a fixed value that shows the lower limit of the physiological heat wave. The conditions above the fixed limit established in this way lead to a decrease in comfort and increase in health risk. The disadvantage of this method is that it cannot be extended to a large area.

The second option is to examine the deviation from the local normal (expected value). Normal means daily averages or all observations (data so far). The degree of exceedance is a given value or a fixed standard deviation, or a fixed percentage. The use of this method is already advantageous in a larger area, as it takes the local conditions into account.

In Hungary, the heat wave is defined as a period of at least 3 consecutive days in which the average daily temperature exceeds 25 °C (National Institute of Environmental Health). This definition is based on an analysis of meteorological and mortality data between 1970 and 2000. (The choice of threshold is based on the expected value of the daily mortality data. The average daily temperature above 25 °C causes a 15% increase in mortality.) The definition created in this way is a fixed threshold definition, which is practical and easy to use in a small area (*Páldy* and *Bobvos*, 2008). The Hungarian Meteorological Service (OMSZ) defines the heat wave day similarly, i.e., when the average daily temperature exceeds 25 °C.

3. Theoretical background of Markov chains

We consider a discrete-time, discrete-space stochastic process, which we write as $X(t) = X_t$, for $t = 0,1,\ldots$ .The state space S is discrete, i.e., finite or countable, so we can let it be a set of integers, as in $S = \{1, 2, \ldots, k\}$ or $S = \{1, 2, \ldots\}$.

The process $X(t) = X_0, X_1, X_2, \ldots$ is a discrete-time Markov chain if it satisfies the *Markov property*:

$$P(X_{n+1} = j | X_n = i, X_{n-1} = x_{n-1}, \ldots X_1 = x_1, X_0 = x_0) = P(X_{n+1} = j | X_n = i).$$

Markov property means that the past and future are independent when the present is known. This means that if one knows the current state of the process, then no additional information of its past states is required to make the best possible prediction of its future.

The quantities $P(X_{n+1} = j | X_n = i)$ are called the *transition probabilities*. In general, the transition probabilities are functions of the initial state, end state, and time (*i, j, n)*. It is convenient to write them as

$$P_{ij}^{n,n+1} := P(X_{n+1} = j | X_n = i).$$

The Markov chain $X(t)$ is *time-homogeneous* if $P(X_{n+1} = j | X_n = i) = P(X_1 = j | X_0 = i)$, i.e., the transition probabilities do not depend on time *n* (*Karlin* and *Taylor*, 1985). If this is the case, we write $P_{ij} = P(X_1 = j | X_0 = i)$ for the probability to go from *i* to *j* in one step, and $\mathbf{P}=(P_{ij})$ for the *transition probability matrix*. In detail

$$\mathbf{P} = \begin{bmatrix} P_{00} & P_{01} \ldots & P_{0k} \\ P_{10} & P_{11} \ldots & P_{1k} \\ \vdots & & \vdots \\ P_{k0} & P_{k1} \ldots & P_{kk} \end{bmatrix}.$$

The elements P_{ij} are non-negative numbers, and the sum of the elements on each row yields 1, so **P** is a stochastic matrix.

The *n-step transition probabilities* $P_{ij}^{(n)}$ are defined by

$$P_{ij}^{(n)} = P(X_n = j | X_0 = i).$$

Using the law of total probability and the Markov property, it is obvious that

$$P_{ij}^{(n)} = \mathbf{P}^n.$$

The transition matrix **P** of a chain is called *regular* if some power of **P** has no entry equal to zero. We then call the Markov chain itself *regular*.

We assume that at the start (at time 0) there is some initial distribution, that is, the distribution of X_0 is given. Let us denote it by φ_0. It is important that it is a row vector that gives the probabilities of being in each state. The Markov chain is determined completely by the transition matrix **P** and the initial distribution φ_0. The Kolmogorov equation gives that the distribution of X_n is $\varphi_n = \varphi_0 \cdot \mathbf{P}^n$.

The distribution φ_n approaches a limit as the number of steps approaches infinity, i.e., $\lim_{n\to\infty} \varphi_n = \pi$. This limit π is the *limiting (*or *invariant* or *stationary) distribution* of the Markov chain and it is a row vector: $\pi = (P_0, P_1, \dots, P_k)$, with $P_j > 0$ for all j. It is important that $\sum_{j=0}^{k} P_j = 1$, so that π is a probability distribution. If π is a limiting distribution, then it satisfies that $\lim_{n\to\infty} P_{ij}^{(n)} = P_j$ for all *j*=0,1,…,*k*. In other words

$$\mathbf{P}^* := \lim_{n\to\infty} \mathbf{P}^n = \begin{bmatrix} P_0 & P_1 \dots & P_k \\ P_0 & P_1 \dots & P_k \\ \vdots & & \vdots \\ P_0 & P_1 \dots & P_k \end{bmatrix}$$

is the *limiting matrix*.

There are two methods to get the limiting distribution: **P** is exponentiated until the rows of the matrix are identical or applying the idempotence of $\mathbf{P}^*\mathbf{P} = \mathbf{P}^*$, it leads to a linear equation system:

$$\left.\begin{array}{c} P_j = \sum_{v=0}^{k} P_v \cdot P_{vj} \quad (j = 0, 1, \dots, k) \\ \sum_{j=0}^{k} P_j = 1 \end{array}\right\}.$$

The solution of the equation system gives the limiting distribution.

The Markov model is also applicable to predict the frequency of a heat wave of *n* days in a fixed period, in our case for the summer period. To realize this, we use the following formula (*Freidooni et al*., 2015):

$$H_n = 1 + \frac{(N-n)\cdot P_{10}\cdot P_{01}\cdot P_{11}^{n-1}}{P_{10}+P_{01}}, \qquad (1)$$

where H_n is the frequency of the heat wave of *n* days, *N* is the total number of days in the whole period, *n* is the number of heat wave days, and $\begin{pmatrix} P_{00} & P_{01} \\ P_{10} & P_{11} \end{pmatrix}$ is the transition probability matrix. This equation will be applied in Section 5.

4. Presentation of heat wave periods

From the early 1980s, the OMSZ carried out a kind of categorization of heat waves to illustrate the occurrences of heat wave periods and their strength. The evaluation was made on the basis of national daily average temperatures using data from 1981–2016 (*OMSZ*, 2017). *Fig. 1* shows the following heat wave characteristics:

- duration of periods in which the daily average temperature exceeds 25 °C for at least 3 days;
- the highest daily average temperature during a heat wave;
- intensity (sum of temperatures above 25 °C), illustrated by the size of the circles.

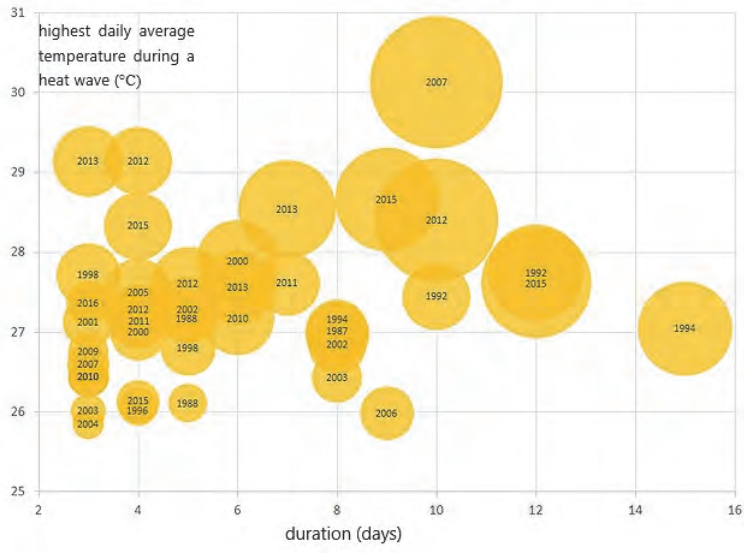

Fig. 1. Heat waves in the period 1981–2016 (*OMSZ*, 2017).

We can see that there was no heat wave until 1986, in the first six years of the observed period 1981-2016. The first heat wave was in 1987. The longest heat wave was in 1994, when the heat lasted for 15 days. However, the intensity of this heat period was not as significant as the heat wave in 2007 (July 15-24), although it lasted only 10 days. The national heat record was also detected: 41.9 ° C was measured in Kiskunhalas on 20 July, 2007. (*OMSZ*, 2017).

In recent years, several researchers have used Markov chains to study heat waves (*Yazdanpanah* and *Alizadeh*, 2000, *Freidooni et al*., 2015). In our research, we examine the average daily temperatures of Baja in summer (June 1–August 31) for the period 2010–2019 and determine the heat wave periods occurring in each year from the data set. This is illustrated in *Table 1* below:

Table 1. The heat wave periods from 2010 to 2019 in Baja

Year	Number of periods	Number of days in the period	Date
2010	3	15	June 10–14, July 12–18, August 13–15
2011	2	13	July 8–15, August 23–27
2012	4	31	June 18–22, June 29–July 11(!), August 2–7, August 20–26
2013	3	17	June 17–22, July 27–29, August 2–9
2014	0	0	
2015	4	32	July 5–8, July 16–25, August 3-16(!), August 28–31
2016	3	10	June 23–26, July 11–13, July 23–25
2017	7	33	June 22–24, July 6–11, July 19-24, July 30–August 7, August 9–11, August 17–19, August 25–27
2018	3	21	July 29–31, August 5–14, August 17–24
2019	4	27	June 10–16, June 25–27, August 10–13, August 19–31(!)

It is worth mentioning, that 199 heat wave days were detected in the period 2010–2019, while 142 such days were numerated in the period 2000–2009.

5. Calculations

With the use of Markov chains we calculate the probability that a particular day falls into a heat wave period for each year (2010–2019) (*Freidooni et al*., 2015). A matrix that shows the frequency at which the system transitions from each state to another state is called a *frequency matrix*. Let state 0 be the non-heat wave day, while let state 1 be the day in the heat wave period. The detailed calculation will be made for the year 2010. Based on this, we expect the probabilities for the other years, as well.

The transition frequency matrix is:

$$\begin{pmatrix} g_{00} & g_{01} \\ g_{10} & g_{11} \end{pmatrix} = \begin{pmatrix} 73 & 3 \\ 3 & 12 \end{pmatrix}.$$

Interpret the g_{01} element. Since there were 3 heat wave periods, it was three times that we switched from a non-heat wave day to a heat wave day and vice versa with respect to the element g_{10}. Interpret the g_{11} element. We have a total of 15 days in the heat wave period, so there are 12 transitions between the days in this state (the transitions start from the first days of the periods, so since there are 3 heat wave periods, there are 12 transitions). Studying the element g_{00}, we realize that there are 77 non-heat wave days in 4 periods (transitions start from the first days of the periods, so since there are 4 non-heat wave periods, there are 73 transitions). Using the transition frequency matrix we get the transition probability matrix:

$$\mathbf{P} = \begin{pmatrix} P_{00} & P_{01} \\ P_{10} & P_{11} \end{pmatrix} = \begin{pmatrix} \dfrac{g_{00}}{g_{00}+g_{01}} & \dfrac{g_{01}}{g_{00}+g_{01}} \\ \dfrac{g_{10}}{g_{10}+g_{11}} & \dfrac{g_{11}}{g_{10}+g_{11}} \end{pmatrix} = \begin{pmatrix} \dfrac{73}{76} & \dfrac{3}{76} \\ \dfrac{3}{15} & \dfrac{12}{15} \end{pmatrix}.$$

We need to calculate the limiting matrix $\mathbf{P}^* = \begin{pmatrix} P_0 & P_1 \\ P_0 & P_1 \end{pmatrix}$. Applying the idempotence of $\mathbf{P}^*\mathbf{P} = \mathbf{P}^*$**,**

$$\begin{pmatrix} P_0 & P_1 \\ P_0 & P_1 \end{pmatrix} \cdot \begin{pmatrix} \dfrac{73}{76} & \dfrac{3}{76} \\ \dfrac{3}{15} & \dfrac{12}{15} \end{pmatrix} = \begin{pmatrix} P_0 & P_1 \\ P_0 & P_1 \end{pmatrix}.$$

This leads to the solution of the following system of equations:

$$\left.\begin{array}{c} \frac{73}{76}P_0 + \frac{3}{15}P_1 = P_0 \\ \frac{3}{76}P_0 + \frac{12}{15}P_1 = P_0 \\ P_0 + P_1 = 1 \end{array}\right\}. \qquad (2)$$

We get that $P_0 = 0.835$ and $P_1 = 0.165$. Based on the data of the year 2010, there is a 16.5% chance of a heat wave day in the summer in the future.

The limiting distribution is calculated in a similar way for the next years (2011–2019). We do not detail the calculations, but the transition probability matrices and the limiting distributions are summarized in *Table 2*.

Table 2. Transition probability matrices and limiting distributions (2010-2019)

Year	P	(P_0, P_1)
2010	$\begin{pmatrix} 0{,}96 & 0{,}04 \\ 0{,}2 & 0{,}8 \end{pmatrix}$	(0,835, 0,165)
2011	$\begin{pmatrix} 0{,}97 & 0{,}03 \\ 0{,}15 & 0{,}85 \end{pmatrix}$	(0,83, 0,17)
2012	$\begin{pmatrix} 0{,}93 & 0{,}07 \\ 0{,}13 & 0{,}87 \end{pmatrix}$	(0,65, 0,35)
2013	$\begin{pmatrix} 0{,}96 & 0{,}04 \\ 0{,}18 & 0{,}82 \end{pmatrix}$	(0,82, 0,18)
2014	there was no heat wave in the summer	(1, 0)
2015	$\begin{pmatrix} 0{,}93 & 0{,}07 \\ 0{,}125 & 0{,}875 \end{pmatrix}$	(0,64, 0,36)
2016	$\begin{pmatrix} 0{,}96 & 0{,}04 \\ 0{,}3 & 0{,}7 \end{pmatrix}$	(0,88, 0,12)
2017	$\begin{pmatrix} 0{,}88 & 0{,}12 \\ 0{,}21 & 0{,}79 \end{pmatrix}$	(0,64, 0,36)
2018	$\begin{pmatrix} 0{,}96 & 0{,}04 \\ 0{,}14 & 0{,}86 \end{pmatrix}$	(0,78, 0,22)
2019	$\begin{pmatrix} 0{,}94 & 0{,}06 \\ 0{,}15 & 0{,}85 \end{pmatrix}$	(0,71, 0,29)

Fig. 2 shows the years with their associated P_1 limiting probabilities.

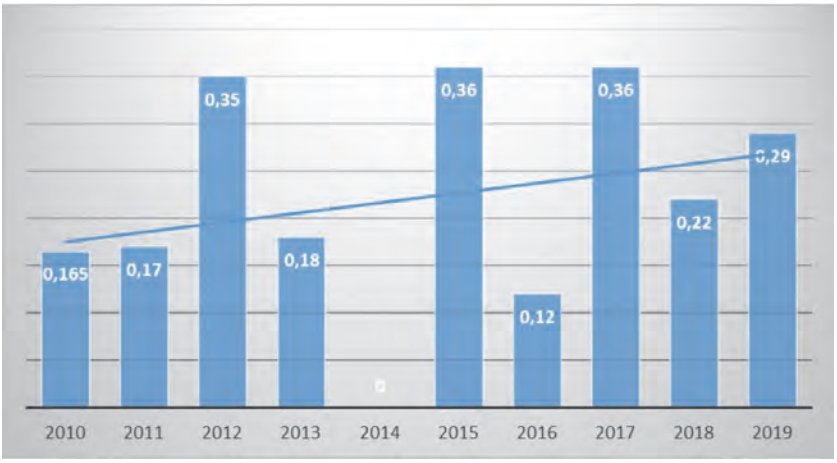

Fig. 2. Limiting probabilities of days in the heat wave period (2010–2019).

The arithmetic mean of the limiting probabilities in *Fig. 2* is 0.2215. It means that a day of the summer period will be a heat wave day with probability 0.2215 in the future. The return time of a heat wave day in summer is therefore 4.51 days (1/0.2215), which is quite worrying for the future.

Eq.(1). is used to calculate the frequency of heat waves of 3, 4,…12 days in future summers. We take the average transition matrix calculated from the 10-year-long data set based on *Table 2*.

$$\mathbf{P} = \begin{pmatrix} P_{00} & P_{01} \\ P_{10} & P_{11} \end{pmatrix} = \begin{pmatrix} 0{,}936 & 0{,}064 \\ 0{,}222 & 0{,}778 \end{pmatrix}.$$

Then we substitute the numbers in Eq.(1). The results of our calculations are included in *Table 3*.

Table 3. Frequencies of heat wave periods of n days in the future during the summer season

n	3	4	5	6	7	8	9	10	11	12
frequency	3,67	3,06	2,58	2,21	1,93	1,71	1,55	1,42	1,32	1,25

The table shows that in summer, a 3-day heat wave can occur 3.67 times, a 7-day heat wave roughly twice, but a 12-day heat wave can occur once on average in the future.

We calculate not only the frequency but also the return time of a heat wave of *n* days with the theory of Markov chains. The following formula is used:

$$R_n = \frac{N}{H_n}, \tag{3}$$

where R_n is the return time of the heat wave of *n* days. *Table 4* shows the calculated return times.

Table 4. Return times of heat wave periods of n days in the future during the summer season

n	3	4	5	6	7	8	9	10	11	12
return time	25,07	30,07	35,65	41,63	47,67	53,8	59,35	64,79	69,7	73,6

Markov chains is also applicable to determine the persistent nature of a process, i.e., whether it is a trend-enhancing process. Persistence is usually measured within the R/S (rescaled range) analysis by the Hurst coefficient (H). It has a value between 0 and 1 and shows that a process is anti-persistent (H<0.5), persistent (H>0.5) or random (H = 0.5), behavior. Persistence in the heat wave study means that if the number of heat wave days increases in one period, the increase is expected to continue in the next period. Alijani (*Alijani*, 2011) used a simple formula to determine persistence related to the theory of Markov chains. If

$$r = P_{11} - P_{01}$$

is positive, then the process is persistent. If it is negative, then the process shows a lack of persistence. Calculating the value of *r* based on the transition probability matrices (*Table 2*), we get that *r*>0, so our process is persistent. The strength of persistence is not examined here now.

6. Conclusions

In summary, examining the data set of the last 10 years in Baja, the number of heat waves increased by 40% compared to the previous period 2000–2009. Based on the data of the last ten years, we calculated the arithmetic mean of the limit probabilities of the days in the heat wave period and the frequency and return time of the heat waves of *n* days (*n* = 1, 2,…, 12).

Based on the analysis of the data series for the period 1971-2019, the number of hot days, tropical nights, and heat wave days increased the most intensively. The length of the heat waves also increased. This also confirms the result of the Prudence project under the 5th Framework Program of the European Union. It states that the temperature in the Carpathian Basin clearly shows a warming trend (*Bartholy et al.*, 2007). The increasing frequency of extreme weather events needs to be given very important attention, because not only the elderly, the chronically ill, and the infants are at risk, but it can also cause a sensitive and then vulnerable condition in anyone.

In our study, we considered data sets from the last 10 years to examine heat waves. Obviously, we will get more accurate results if we work with a longer data set, but our calculations still supported (the increasing trend and the persistence process are proven) the claims of other climate researchers (*Bartholy et al.*, 2013) as we referred to it in the introduction.

Using our calculation method, it is worthwhile to calculate the limit probability of the days in the heat wave period for the future in other areas. Based on this, we could edit a heat wave forecast map.

Aknowledgement: The author gratefully thank to the Referee for the constructive comments and recommendations.

References

Alijani, B., 2011: Evaluation of the Structure of Continuance of the Two Situations of Raining in South Iran by Means of Markov Hidden Status Model. *Geogr. Develop. J. 25*, 1–20.

Bartholy, J., Pongrácz, R., and *Gelybó, Gy.*, 2007: Expected regional climate change in Hungary at the end of the 21st century. *Appl. Ecology Env. Res. 5.*, 1–17. https://doi.org/10.15666/aeer/0501_001017

Pongrácz, R. and *Bartholy, J.* (Eds.), 2013: Alkalmazott és városklimatológia. ELTE TTK, Budapest. (In Hungarian)

Fekete, Á. and *Keve, G.*, 2020: csapadékösszegek és az aszályos időszakok vizsgálata Markov-láncokkal. *Hidrológiai Közlöny 100* (4), 60–70. (in Hungarian)

Freidooni F., Ataei, H., and *Shahriars, F.*, 2015: Estimating the Occurence Probability of Heat Wave Periods Using the Markov Chain Model. *J. Sustain. Develop. 8* (2), 26–45. https://doi.org/10.5539/jsd.v8n2p26

KSH, 2019: Statistical Mirror. Budapest. http://www.ksh.hu/docs/hun/xftp/stattukor/fobbnoveny/2019/index.html

Karlin S. and *Taylor H.M.*, 1985: Sztochasztikus folyamatok. Gondolat Kiadó, Budapest, Hungary. (In Hungarian)

Láng, I., Csete, L., and *Jolánkai, M.*, 2007: A globális klímaváltozás: hazai hatások és válaszok. *Agrokémia és Talajtan. 57.* 199–202.

OMSZ, 2017: Heat waves. https://www.met.hu/ismeret-tar/erdekessegek_tanulmanyok/index.php?id=1969&hir=Hohullamok:_ami_ma_szelsoseges,_az_a_jovoben_valoszinuleg_atlagos_lesz (In Hungarian)

Páldy, A. and *Bobvos, J.*, 2008: A 2007. évi magyarországi hőhullámok egészségi hatásainak elemzése – előzmények és tapasztalatok. *„KLÍMA-21", 52*, 3-15. (In Hungarian)

Robinson, J.P., 2001: On the Definition of a Heat Wave. *J. Appl. Meteorol. 40*, 762–775. https://doi.org/10.1175/1520-0450(2001)040<0762:OTDOAH>2.0.CO;2

Somfalvi-Tóth, K., 2017: Kukorica az éghajlatváltozás tükrében. *Agrofórum Extra* 72, pp. 8-10. https://agroforum.hu/ szakcikkek/novenytermesztes-szakcikkek/a-kukorica-az-eghajlatvaltozas-tukreben/ (In Hungarian)

Pecelj, M., Lukić, Z., Filipović, J., and *Protić, M.,* 2019: Summer variation of the UTCI index and Heat Waves in Serbia. *Nat. Hazard. Earth Syst. Sci. 270*, 1–19. https://doi.org/10.5194/nhess-2019-270

Yazdanpanah, H. and *Alizadeh, T.*, 2000: Estimate the probability of occurrence of heat waves and periods of continuity in the province with the help of Markov chains, *J. Geograph. Res.26(*3), 51–72.

DOI:10.28974/idojaras.2022.3.7

IDŐJÁRÁS

Quarterly Journal of the Hungarian Meteorological Service
Vol. 126, No. 3, July – September, 2022, pp. 387–402

Trend analysis of water flow on Neka and Tajan rivers using parametric and non-parametric tests

Mohammad Salarian [1], **Shamim Larijani** [1], **Hossein Banejad** [1], **Mohammad Heydari** [2], and **Hamed Benisi Ghadim*** [3]

[1]*Department of Water Engineering*
College of Agriculture
Ferdowsi University of Mashhad, Iran

[2]*Department of Civil Engineering*
Faculty of Engineering
University of Malaya, Malaysia

Department of Water Resources and Harbor Engineering
Faculty of Civil Engineering
Fuzhou University, Fuzhou-Minhou, China

*Corresponding author E-mail: benisi.hamed@fzu.edu.cn

(Manuscript received in final form April 26, 2021)

Abstract— River flow is an essential parameter in hydrology and water resources studies with mutual interaction with climate elements. So, studying the discharge change trend in the rivers is crucial for management programs and the design of irrigation and drainage systems. In the present study, river flow data measured at six hydrological stations at Neka (Ablu, Golverd, SefidChah) and Tajan (KordKhil, Rigcheshmeh, Soleimantangeh) rivers in Mazandaran Province have been studied by using Mann-Kendall test, age test, and regression analysis during the statistical period of 1976–2006. The MAKESENS 1.0 software was used to reveal annual and seasonal discharge change trends. Results of the present study showed that only two stations – Soleimantangeh and Rigcheshmeh – had decreasing trend at 5% significance level in yearly terms.

In contrast, the regression analysis showed just significant trends at Soleimantangeh station. No crucial trends have been observed in the seasonal scale; in spring and autumn, most of the stations had a non-significant negative trend. By considering the methods used to evaluate trends in this study (Mann-Kendall test, age test, and regression analysis), it was observed that all the rivers had had decreasing and negative trends. The performance of parametric and non-parametric tests was similar in most cases.

Key-words: Mann-Kendall test, MAKESENS, regression, Mazandaran station, catchment, discharge.

1. Introduction

Today, the global warming caused by increasing greenhouse gases and their impact on climate change is a scientific fact that many researchers have admitted to (*Kweku et al.*, 2017). Scientists believe that human intervention in the atmosphere and greenhouse gas concentrations resulting from fossil fuel consumption led to an increased mean air temperature worldwide. Rising temperatures can lead to changes in the process of some components of the hydrological cycle, including precipitation and stream in different parts of the world (*Lelieveld et al*., 2019; *Shindell* and *Smith*, 2019). It is necessary to study the trends and regular changes in hydroclimatic variables in each area to prepare against the undesirable effects of climate change and reduce the resulting losses. It is required to ensure that appropriate policies and programs for the development and management of water resources must be taken (*Faridah* et al., 2014). Due to this reason, recently, many studies about the process of trend changes in different meteorological and hydrological variables have been conducted (*Fathian et al.*, 2016; *Noori et al.,* 2013; *Salarian et al.,* 2015; *Tosunoglu* and *Kisi*, 2017).

The most common method for hydrology, meteorology, and time series analysis is to assess the presence or absence of trends in them using statistical tests (*Asfawet al*., 2018). So far, several methods for time series trend analysis have been provided, which are divided into two categories: parametric and non-parametric methods (*Kocsis et al*., 2017). Parametric tests are more accurate to determine the trend than non-parametric tests, and while using them, the data should be random (independent) and should have normal distribution. On the other hand, non-parametric tests can have only random data that are not sensitive to the data's normality (*Chen t al*., 2007).

In this regard, we can refer to the research on the trend of changes in meteorological parameters and climate change, such as rainfall *(Jakuschné Kocsis* and *Anda*, 2018; *Malik* and *Kumar*, 2020), drought (*Salarian et al.,* 2016; *Zarei et al.,* 2016), temperature (*Mohorji et al.,* 2017), evapotranspiration *(Khanmohammadi et al*., 2018).

Korhonen and *Kuusisto* (2010) presented the characteristics of long-term changes in the discharge regime in Finland. The Mann–Kendall trend test was applied to assess changes in annual, monthly, and seasonal mean discharges, maximum and minimum flows, and, besides, the date of the annual peak flow. Trend analysis showed a change in the seasonal flow distribution and no overall change in the average annual flow. *Villarini, Smith, Serinaldi,* and *Ntelekos* (2011), used maximum annual and seasonal daily discharge time series for 55 stations in Germany, Switzerland, the Czech Republic, and Slovakia to measure flood frequency from a regional perspective. Analysis of records of maximum daily, seasonal, and annual discharges showed the existence of uniform patterns using Spearman and Man-Kendall tests. *Čanjevac* and *Orešić* (2015) discussed recent changes in the average annual and seasonal river discharges in Croatia. For

assessment purposes, the Kendall-Theil (Sen) non-parametric trend test was carried out for the yearly and seasonal mean discharge values. The results show an increase in evacuation in autumn and winter and a decrease in evacuation in summer. *Chen, Guan, Shao,* and *Zhang* (2016), examined streamflow and precipitation trends in the Huangfuchuan Basin using wavelet analysis and the Mann-Kendall test. The comparative analysis with five MK test methods showed that the modified MK tests with complete serial correlation structure performed better when significant autocorrelations exhibited for more than one lag. *Fathian et al*. (2016) evaluated the trend of hydrological and climatic variables under the influence of four changes in the Mann-Kendall approach in the Urmia Lake Basin in Iran. The correlations between streamflow and climatic variables showed that the Urmia Lake basin's streamflow is more sensitive to temperature changes than precipitation. *Déry, Stadnyk, MacDonald,* and *Gauli-Sharma* (2016) conducted a recent study of recent trends and changes in river discharges in northern Canada for the years 1964–2013. Based on the Mann–Kendall test, no significant annual discharge trend is observed in the Bering Sea, western Arctic Ocean, Western Hudson, James Bay, and Labrador Sea. *Oluoch, Nyabundi*, and *Boiwa* (2017) analyzed meteorological data trends to determine the trend and size of tea production using the Man-Kendall and Sen's Slope estimate tests. The results showed that the weather parameters were still within limits required for optimum tea production despite the changes.

According to studies conducted in Iran, which are focused more on hot and dry areas, no assessments have been done about discharge trend changes in Iran's northern part. Therefore, this article attempts to assess the annual and seasonal trends of northern rivers in Iran. In the present study, the seasonal and annual trends of Neka and Tajan rivers located in northern Iran have been investigated using non-parametric tests. A parametric regression analysis test was also used to determine the trend and to compare it with a non-parametric test.

2. Research methodology

2.1. The case study

The area under study covers about 1906.72 km^2 in Mazandaran Province, and a small part of it is located in the western part of Golestan Province. The Tajan river basin covers an area of 4015.88 km^2 and is located in the range from 52° 50’ to 54° 50’ east longitudes and 35° 35’ to 36 '50° north latitudes. The Neka river basin also flows in the geographical area53° 17’ to 54° 44’ east longitudes and 36° 28’ to 36° 42’ north latitudes (*Fig. 1*).

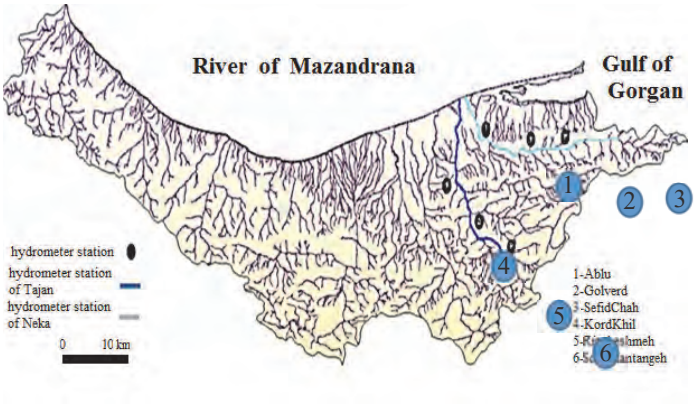

Fig. 1: The studied area of Tajan and Neka rivers.

2.2. *The used data*

Water discharge data have been used in both annual and seasonal scales to study the water flow in Neka and Tajan rivers. Discharge data were taken from the Regional Water Organization of Mazandaran Province relating to six hydrological stations of Neka (Ablu, Golverd, SefidChah) and Tajna (KordKhil, Rig Cheshmeh, Soleimanzadeh) rivers with a statistical length of 31 years from 1976–2006. The characteristics of these stations are summarized in *Table 1*. In this study, MAKESENS 1.0 (Mann-Kendall and Sea's slope estimates) Freeware is used to calculate the statistics related to the Mann-Kendall test and the age slope estimator. MAKESENS was developed at the Finnish Meteorological Institute in 2002 for detecting and estimating trends in time series of annual values. Determining the regression equations has also been performed by SPSS 16 software.

Table 1. Specification of the studied stations and some statistics about annual flow series in the statistical period (1976–2006).

station	Geographical coordinates	Min	Max	Mean	SD	Cs
Ablu	36º 31′ 38″ North 53º 19′ 26″ East	0.63	5.07	2.67	1.244	0.25
SefidChah	36º 36′ 9″ North 53º 11′ 53″ East	0.97	2.7	1.68	0.425	0.4
Golverd	36º 43′ 23″ North 53º 10′ 6″ East	1.03	3.64	2.05	0.749	0.464
KordKhil	36º 30′ 43″ North 53º 29′ 6″ East	0.77	5.08	2.79	1.141	0.305
Soleimantangeh	36º 25′ 9″ North 53º 23′ 17″ East	0.63	5.16	2.48	1.091	0.547
Rig Cheshmeh	36º 21′ 31″ North 53º 26′ 10″ East	0.91	4.96	2.56	0.990	0.269

(Source: Regional Water Organization of Mazandaran Province, 2016)
Mean: average annual flow (m^3/s), SD: standard deviation of annual flow (m^3/s), and Cs: coefficient of skewness (m^3/s)

2.3. Theoretical foundations

2.3.1. Mann-Kendall test

The Mann-Kendall test (*Kendall*, 1948) is one of the most common types of non-parametric tests to determine trends in hydrological data, when normal distributed data is not necessary for using (*Tabari* and *Talaee*, 2011). According to this test, the null hypothesis implies randomness and lack of trend in the data series. Accepting the alternative hypothesis (rejecting the null hypothesis) is evidence of trends in the data series. Statistic *S* can be obtained as follows:

$$S=\sum_{k=1}^{n-1}\sum_{j=k+1}^{n}\operatorname{sgn}\left(x_j-x_k\right), \tag{1}$$

$$\operatorname{sgn}\left(x_j-x_k\right)=\begin{cases}+1 & x_j-x_k>0\\ 0 & x_j-x_k=0\\ -1 & x_j-x_k<0\end{cases}, \tag{2}$$

where S is statistics related to Mann-Kendall, x_j and x_k are the observed values related to jth and ith, respectively, the number of data, and $\operatorname{sgn}(x_j-x_k)$ is the sign function m.

$$\operatorname{Var}(S)=\frac{[n(n-1)(2n+5)-\sum_{i=1}^{m}t_i(t_i-1)(2t_i+5)]}{18}. \tag{3}$$

The number of identical groups (same set of sample data with the same values) and t_i are the same number of data in the ith category. In cases where the sample size is $n>10$, the standard statistics Z is obtained as follows:

$$Z=\begin{cases}\frac{S-1}{\sqrt{\operatorname{Var}(S)}} & \text{if} \quad S>0\\ 0 & \text{if} \quad S=0\\ \frac{S+1}{\sqrt{\operatorname{Var}(S)}} & \text{if} \quad S<0\end{cases}, \tag{4}$$

where positive Z values represent an increasing trend, while negative values indicate a decreasing trend. If the calculated Z is greater than 1.645, the data trend is significant at a confidence level 0.1, and otherwise, it is assumed to be insignificant. Similarly, if the calculated Z is greater than 1.96 and 2.58, the data trend is considered significant at the 0.50 and 0.01levels. Otherwise, the null hypothesis that there is a trend in the data in the considerable level of interest will be rejected (*Tabari* and *Talaee*, 2011).

2.3.2. Estimator method of slope (Sen)

If there is a linear trend in a time series, then the right slope (changes with time) can be estimated by using a simple non-parametric method which was proposed by *Sen* (1968). The slope value of the trend is calculated by using the following equation:

$$Q=\text{Median}\left(\frac{x_j-x_k}{j-k}\right)\forall\, k<j \quad , \tag{5}$$

where x_j and x_k, the data values are over time j and k ($j>k$), respectively. Also, the meaning of Median (u) is the median values of u. If u is even, the data median is the arithmetic mean of two current numbers in the middle sets of data relating to u in ascending or descending order. If the number of u is odd, the data median is the present number in the middle of the ascending or descending order. In this method, the unit slope of the trend line equals with the variable unit studied in the year (in the research cubic meters per second). In the age slope technique, positive and negative values of Q indicate increasing and decreasing data trends. This method is one of the most common scenarios in hydrological studies that are widely used as well.

2.3.3. Linear regression method

Linear regression analysis is also used to study trends in the time series like the Mann-Kendall test and age slope estimator method. The main statistical parameter of this method is the regression line's slope, which shows the desired variable changes. Positive values of this slope indicate an increasing trend, while negative values show a decreasing trend. In the current study, a linear regression model was fitted on the discharge time series data, and the significance of the slope was evaluated at the confidence level of 95% and 99% by using the Pearson correlation:

$$Y=a+bX\,, \tag{6}$$

where the Y is the variable understudying (in this study, discharge), "X" is the time, "a" is a constant number, and "b" is the slope of the regression line.

3. Research findings

3.1. The Annual discharge trend

Table 2 shows the results from the annual discharge trend study (m^3/s) using Mann-Kendall test, age slope estimator method, and linear regression. According

to the table, the obtained results of the different statistics for annual discharge in all stations have a decreasing trend. The linear regression process's annual accepted trend is almost the same as the Mann-Kendall test's obtained trend. The annual trend of most stations was not significant at the 1% and 5% levels. Still, the two stations, Soleimantangeh and Rigcheshmeh, both locate at the Tajan river, have a decreasing trend at the 5% level (indicated with an asterisk).

Table 2. Results of Mann-Kendall test, age slope estimator, and linear regression for the annual discharge

Station	Z	Q	b (m^3/s)	P-value
Ablu	-0.48	-0.018	-0.149	0.423
SefidChah	-0.92	-0.010	-0.155	0.404
Golverd	-1.05	-0.019	-0.228	0.218
KordKhil	-0.24	-0.006	-0.053	0.778
Soleimantangeh	-2.52*	-0.043	-0.423	0.018*
Rig Cheshmeh	-2.18*	-0.051	-0.314	0.085

The only significant observed trend has been obtained by regression analysis in the annual discharge data of Soleimantangeh station. Based on the regression line slope presented in (*Table 2*), it can be concluded that annual discharge has been decreased in Soleimantangeh, Rigcheshmeh, Galuverd, Sefidchah, Ablu, and Kordkhil stations 4.2, 3.1, 2.2, 1.55, 1.49, and 0.5 m^3 in the three decades understudying, respectively. It can be stated that these results are consistent with the results of Mir Abbasi Najaf Abadi and Din Pazhuh (2010). The annual significant decreasing discharge trend of Soleimantanghe and Rigcheshmeh stations is shown in *Fig. 2*.

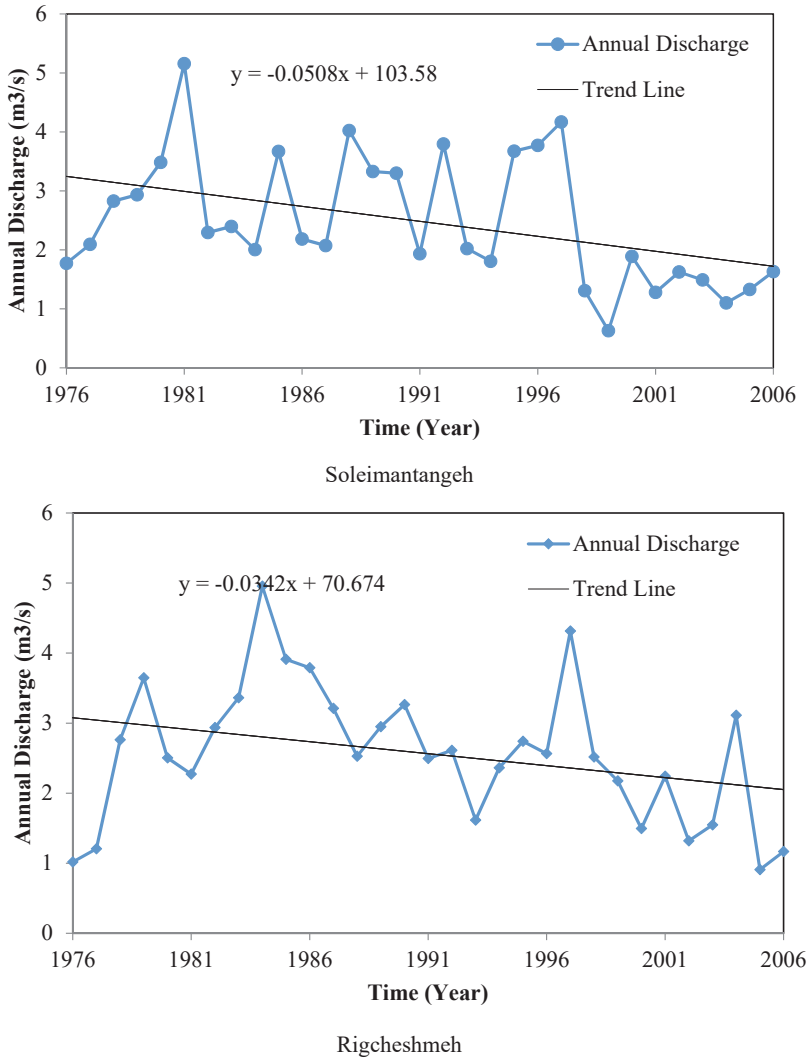

Fig. 2. The annual discharge changing trend of Soleimantangeh and Rigcheshmeh stations in the statistical period 1976–2006.

3.2. Seasonal trend

Spring: According to *Table 3*, based on the values of the Mann-Kendall test, most stations have an insignificant decreasing trend in spring, and only the Kordkheil station had a minor increasing trend. These results are in good agreement with the results of the regression analysis for spring. Based on the regression line slope

given in *Table 3*, it can be concluded that the amounts of seasonal discharge in Soleimantangeh, Rigcheshme, Galuverd, Sefidchah, Ablu, and Kordkhil stations decreased to 2.88, 2.62, 1.04, 0.95, and 0.82 m^3 per decade, respectively. Just Kordkhil station increased to 1.06 m^3 per decade.

Table 3. Mann-Kendall test, age slope estimator and linear regression for spring and summer seasons

Station	Summer				Spring			
	Z	Q	b	P-value	Z	Q	b	P-value
Ablu	-0.39	-0.006	-0.115	0.538	-0.75	-0.019	-0.095	0.611
SefidChah	-2.20*	-0.026	-0.358	0.048*	-0.84	-0.007	-0.082	0.659
Golverd	0.31	-0.004	-0.057	0.761	-0.48	-0.010	-0.104	0.577
KordKhil	0.87	-0.015	-0.096	0.606	-0.76	-0.019	0.106	0.569
Soleimantangeh	-2.66**	-0.049	-0.354	0.051	-0.90	-0.023	-0.288	0.116
Rig Cheshmeh	-2.91**	-0.094	-0.531	0.002**	-1.12	-0.031	-0.226	0.222

Summer: According to *Table 3*, no station has had any significant increasing trend in the summer, and the decreasing trend has been observed for every six stations. In the meantime, SefidChah station at 5% level (marked with *) and Rigcheshmeh and Soleimantangeh stations at 1% level (marked with **) have a significant decreasing trend. Its extreme value *Z*= -2.91is for Rigcheshmeh station. According to the regression analysis results presented in *Table 3*, it can be deduced that the discharge values at Rigcheshme, SefidChah, Soleimantangeh, Ablu, Kordkhil, and Galuverd stations have been decreased to 31.5, 58.3, 54.3, 15.1, 96.0, and 57.0 m^3, respectively.

Autumn: According to *Table 4*, most stations had decreasing trend but insignificant in the autumn and spring. Rigcheshmeh station had a slightly increasing trend. According to the regression analysis results presented in *Table 4*, discharge amounts of SefidChah, Kordkhil, Ablu, Galuverd, and Soleimantangeh stations have been decreased to 7.06, 5.69, 3.28, 2.05, and 0.75 m^3 drop per decade, respectively. Discharge of Rigcheshmeh station has been increased to 1.7 m^3.

Table 4. Results of Mann-Kendall test, age slope estimator and linear regression for autumn and winter seasons

Station	Winter				Autumn			
	Z	Q	b	P-value	Z	Q	b	P-value
Ablu	-0.59	-0.025	-0.126	0.501	-0.85	-0.023	-0.182	0.328
SefidChah	0.07	0	-0.005	0.98	-0.78	-0.006	-0.07	0.706
Golverd	-1.14	-0.027	-0.225	0.223	-1.07	-0.019	-0.234	0.205
KordKhil	-0.82	-0.027	-0.098	0.599	-0.48	-0.010	-0.106	0.569
Soleimantangeh	-1.97*	-0.043	-0.316	0.084	-1.73	-0.042	-0.324	0.075
Rig Cheshmeh	-1.05	-0.016	-0.156	0.401	0.22	0.004	0.069	0.711

Winter: According to *Table 4*, all stations have a decreasing trend in the winter, and just Soleimantangeh station has a significant negative trend at 95% level with *Z*=-1.97 statistical value. Also, SefidChah station had an insignificant increasing trend. According to the results obtained from the regression analysis, the discharge of Kordkhil, Ablu, Rigcheshmeh, Galuverd, and Soleimantangeh stations has been decreased to 5.99, 5.01, 4.01, 2.23, and 0.84 m^3 per decade, respectively, and discharge of SefidChah station has been increased to 9.8 m^3.

Factors such as rising temperatures, decreasing rainfall, harvesting from the river for different uses, and climate change are among the reasons for reducing the slope in annual discharge changes at Sulaymaniyah and Rigcheshmeh stations.

Fig. 3 shows the seasonal changing discharge of the stations having a significant decreasing trend. According to these decreasing trends it is evident, that it would affect the region's agricultural production.

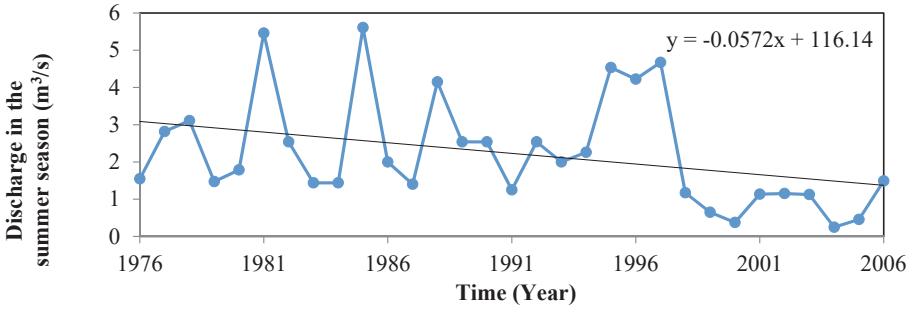

Soleimantangeh station

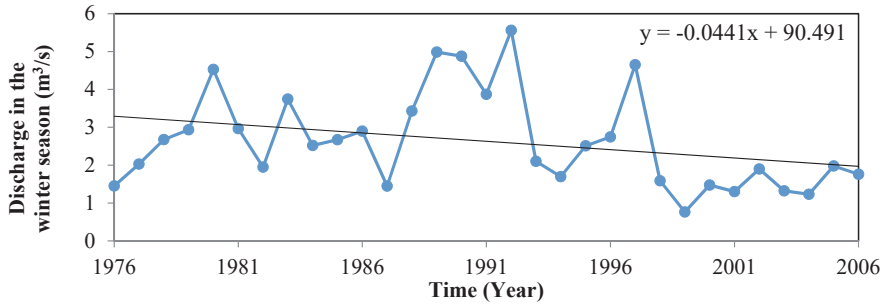

Soleimantangeh station

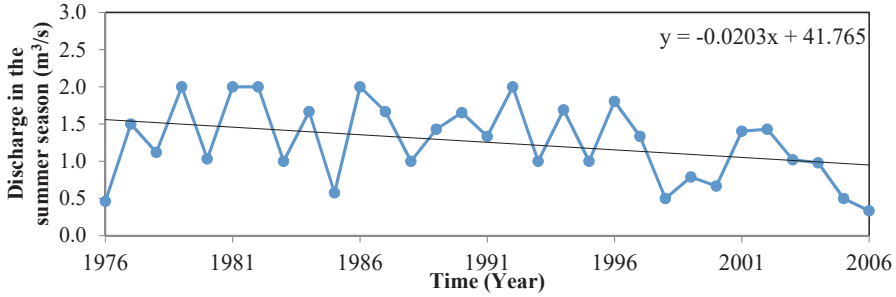

SefidChah station

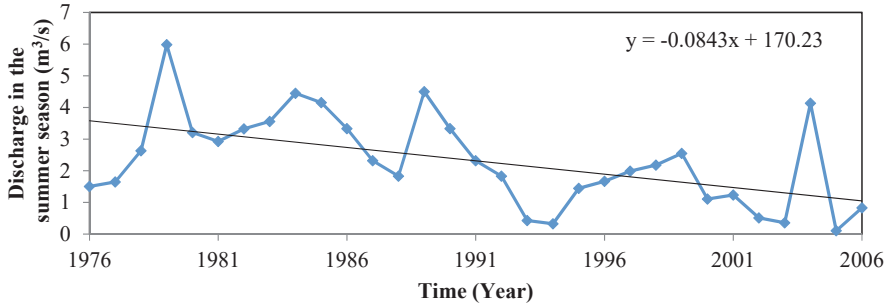

Rigcheshmeh Station

Fig. 3. The seasonal changing discharge of the stations in the statistical period 1976–2006.

Although the present study shows a decreasing discharge in the Neka and Tajan rivers on annual and seasonal scales, many researchers worldwide have studied variable discharge flows (*Kahya* and *Kalaycı*, 2004). It can be noted, that they reported decreasing trend of water flow in the rivers of West Turkey by using the Mann-Kendall test, which is consistent with the results of this study. However, in some areas of the world, an increasing trend has also been reported for discharge flow rate. For example, *Lettenmaier, Wood*, and *Wallis* (1994) reported a rising trend for the river runoff in the United States of America, which does not match the obtained results of this study.

3.3. Results of trend line slope for the discharge data of the studied area

In this study, the trend line slope of quarterly and annual discharge data of six stations in Naka and Tajan rivers were calculated using the age slope estimator method. The obtained results have been demonstrated in annual and quarterly scales (*Tables 2, 3*, and *4*). Inferred from the trend line slope values presented in the tables, the frequency of negative slopes is far higher than that of positive slopes. On an annual scale, the steepest negative slope of the trend line belongs to Rigcheshmeh station with a -0.051 m^3/s per year, consistently with the results of the Mann-Kendall test. This indicates that the Tajan river discharge has been decreased somewhat in the last three decades.

On a seasonal scale, the trend line slope also had negative values for most stations. Only Kordkhil station in spring and Rigcheshmeh station in autumn had a positive trend line slope with the values of 0.019 and 0.004 m^3/s per year. These results are acceptably consistent with the results of the Mann-Kendall test and regression analysis. The steepest negative slope of the trend line on a seasonal scale (summer) belongs to Rigcheshmeh station, it is equal to -0.094 m^3/s per year. This indicates that the average discharged rate of Tajan river in Rigcheshemh station decreased every year in the summer season by about 94 liters per second which most likely due to increased harvesting and use of river water. The most important effect of reducing the amount of river flow is failing to provide sufficient water for agricultural, drinking, and industry use.

Fig. 4 shows the whisker plot of different discharge trends at Neka and Tajan rivers in the past three decades on a seasonal scale. In the box plot, each box shows median values, quartiles, and limit within a class. Lines at the bottom of the box (bottom and top of the rectangle) represent the slope values between the 25 and 75 percentiles, respectively, and the line in the box represents the middle value (mid-slopes). Top and bottom vertical lines represent the highest and lowest observed trend line slope values among the stations. As can be concluded from these figures, the mid-slopes of trend lines are negative for all seasons. Also, it can be concluded that the upper part of boxes is below the horizontal line of zero slopes; thus, the slope of the trend line in these seasons is negative for all stations

in the study area. This indicates that the discharge of Neka and Tajan rivers has been decreased in the last three decades.

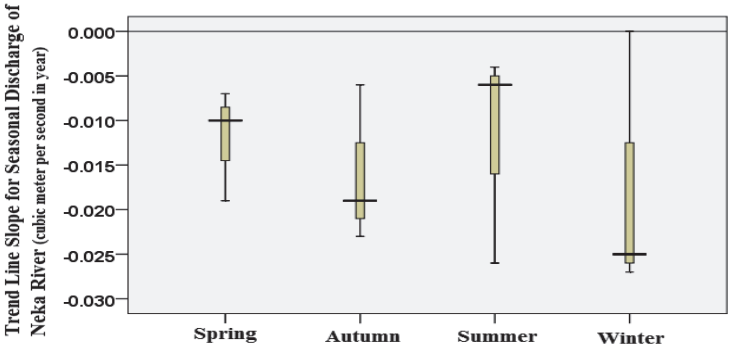

A- Neka River

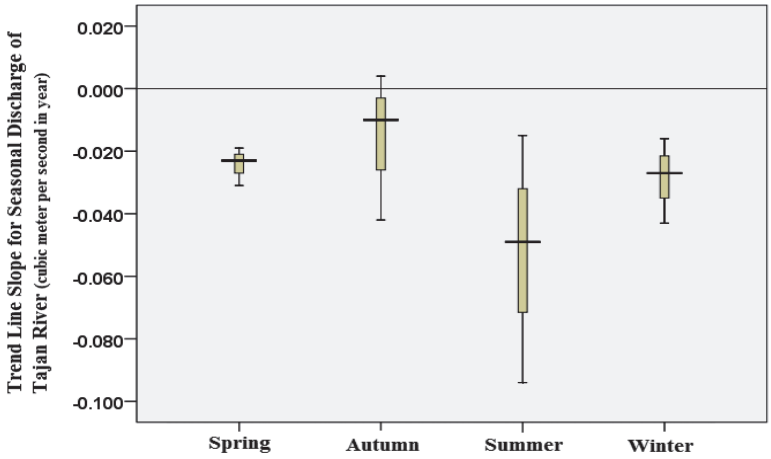

B- Tajan River

Fig. 4. The whisker plot of seasonal discharge trend boxes for Neka and Tajan rivers in Mazandaran Province in the statistical period 1976–2006.

For Tajan river in the summer season and Neka river in the winter season, space between the lower and upper quartiles is higher than that of the other seasons. This approach suggests changes in the discharge trend slope in the summer season in Ablu, Golverd, and SefidChah stations located in the Tajan river and changes in the discharge trend slope in the winter season in Kordkhil, Rigcheshmeh, and Soleimantanghe stations, which are are far more than in other

seasons. Mid-slope in winter season for Neka River and in summer season for Tajan River is the lowest and close to the 25% slope. This represents a decreasing trend of irrigation of most rivers in the area. In summary, based on the slope of the trend lines, it can be concluded that the discharge of Neka and Tajan rivers has been decreased over the three decades studied.

In general, it can be concluded that the efficacy of two non-parametric tests, the Mann-Kendall test and age the slope estimator, are similar in most cases regarding the quarterly and annual discharges and the difference between the parametric test (regression analysis) and non-parametric tests (Mann-Kendall and age slope estimator). The main reason for this difference may be related to the normal distribution degree, which corresponds with the result of *Huth* and *Pokorna* (2004).

4. Conclusions and recommendations

In this study, the seasonal and annual changes in Neka and Tajan rivers in Mazandaran Province, Iran were studied. For this reason, Mann-Kendall and age slope estimator tests and parametric tests of regression analysis were used. The data from 6 hydrological stations in Neka and Tajan rivers (*Table 1*) were used for 31 years from 1976 to 2006. The results of the present study showed that on an annual scale, only two stations, Solaeimantangeh and Rigcheshmeh, at 5% level (with 95% confidence), had a decreasing trend. The only significant observed trend by regression analysis is obtained in the annual discharge data of the Soleimantangeh station. On the seasonal scale, no significant trend has been observed in spring and autumn, and most of the stations in these seasons had insignificant negative trends. Only Rigcheshme station had a minor positive trend in autumn. In summer, both stations, Soleimaniyeh1 and Rigcheshmeh were at 1 percent level with a significant negative trend. In this season, Regression analysis results in Rigcheshmeh station are consistent with the results of the Mann-Kendall test. Also, in winter, just Soleimaniye station had a significant negative trend at the 5% level. The age slope estimator calculated the slope of the trend line. This test's obtained results showed that most of the stations had a negative trend that corresponds with the Mann-Kendall test and regression analysis results. Changes of discharge trend slope of the summer season are much higher than in the other seasons. Compared with the different seasons, the mid-slope in winter is the lowest and close to the 25% slope, indicating a decreasing trend of irrigation rivers in the region. Soleimaniye station located in the Tajan river has had a more significant decreasing trend than other stations.

This study's results can change the direction of the planning schemes of irrigation and water resources management in the future. Still, in the end, it is recommended that the decreasing water flow of rivers in this region and their downtrend will be carefully examined. The reported trends in this study are compared to the trends derived from other tests.

Acknowledgment: The authors are most grateful and would like to thank the reviewers for their valuable suggestions that have led to substantial improvements to the article. We would like to thank the Regional Water Organization of Mazandaran and Distinguished young talent for Fujian province, Fuzhou University, for their technical and financial support.

References

Asfaw, A., Simane, B., Hassen, A., and *Bantider, A.*, 2018: Variability and time series trend analysis of rainfall and temperature in northcentral Ethiopia: A case study in Woleka sub-basin. *Weather Climate Extr. 19*, 29–41. https://doi.org/10.1016/j.wace.2017.12.002

Čanjevac, I., and *Orešić, D.*, 2015: Contemporary changes of mean annual and seasonal river discharges in Croatia. *Hrvatski Geografski Glasnik, 77*, 7–27. https://doi.org/10.21861/HGG.2015.77.01.01

Chen, H., Guo, S., Xu, C.-y., and *Singh, V.P.*, 2007: Historical temporal trends of hydro-climatic variables and runoff response to climate variability and their relevance in water resource management in the Hanjiang basin. *J. Hydrology 344*(3–4), 171–184. https://doi.org/10.1016/j.jhydrol.2007.06.034

Chen, Y., Guan, Y., Shao, G., and *Zhang, D.*, 2016: Investigating trends in streamflow and precipitation in Huangfuchuan Basin with wavelet analysis and the Mann-Kendall test. *Water 8*(3), 77. https://doi.org/10.3390/w8030077

Déry, S.J., Stadnyk, T.A., MacDonald, M.K., and *Gauli-Sharma, B.*, 2016: Recent trends and variability in river discharge across northern Canada. *Hydrol. Earth Syst. Sci. 20*, 4801–4818. https://doi.org/10.5194/hess-20-4801-2016

Faridah, O., Mohammad, H., Mohammad, S. S., Mahmoud, R., and *Mahdi, S.P.*, 2014: The necessity of systematic and integrated approach in water resources problems and evaluation methods, a review. *Adv. Environ. Biol. 8*(19), 307–315.

Fathian, F., Dehghan, Z., Bazrkar, M.H., and *Eslamian, S.*, 2016: Trends in hydrological and climatic variables affected by four variations of the Mann-Kendall approach in Urmia Lake basin, Iran. *Hydrol. Sci.s J. 61*, 892–904. https://doi.org/10.1080/02626667.2014.932911

Huth, R. and *Pokorna, L.*, 2004: Parametric versus non-parametric estimates of climatic trends. *Theor. Appl. Climatol. 77*, 107–112. https://doi.org/10.1007/s00704-003-0026-3

J*akuschné Kocsis, T.* and *Anda, A.* 2018: Parametric or non-parametric: analysis of rainfall time series at a Hungarian meteorological station. *Időjárás 122*, 203–216. https://doi.org/10.28974/idojaras.2018.2.6

Kahya, E. and *Kalaycı, S.*, 2004: Trend analysis of streamflow in Turkey. *J.f Hydrol. 289*(1), 128-144. https://doi.org/10.1016/j.jhydrol.2003.11.006

Kendall, M.G. 1948: Rank correlation methods. 4th edition, Griffin, London.

Khanmohammadi, N., Rezaie, H., Montaseri, M., and *Behmanesh, J.*, 2018: The application of multiple linear regression method in reference evapotranspiration trend calculation. *Stoch. Environ. Res. Risk Assess. 32*, 661–673. https://doi.org/10.1007/s00477-017-1378-z

Kocsis, T., Kovács-Székely, I., and *Anda, A.*, 2017: Comparison of parametric and non-parametric time-series analysis methods on a long-term meteorological data set. *Centr. Eur. Geol. 60*, 316–332. https://doi.org/10.1556/24.60.2017.011

Korhonen, J. and *Kuusisto, E.*, 2010: Long-term changes in the discharge regime in Finland. *Hydrology Res. 41*, 253–268. https://doi.org/10.2166/nh.2010.112

Kweku, D.W., Bismark, O., Maxwell, A., Desmond, K.A., Danso, K.B., Oti-Mensah, E.A., . . . Adormaa, B.B., 2017: Greenhouse effect: greenhouse gases and their impact on global warming. *J.Sci. Res. Rep. 17*(6), 1–9. https://doi.org/10.9734/JSRR/2017/39630

Lelieveld, J., Klingmüller, K., Pozzer, A., Burnett, R., Haines, A., and *Ramanathan, V.*, 2019: Effects of fossil fuel and total anthropogenic emission removal on public health and climate. *Proc. Nat. Acad. Sci. 116*, 7192–7197. https://doi.org/10.1073/pnas.1819989116

Lettenmaier, D.P., Wood, E.F., and *Wallis, J.R.*, 1994: Hydro-climatological trends in the continental United States, 1948-88. *J. Climate, 7*, 586–607. https://doi.org/10.1175/1520-0442(1994)007<0586:HCTITC>2.0.CO;2

Malik, A. and *Kumar, A.* 2020: Spatio-temporal trend analysis of rainfall using parametric and non-parametric tests: case study in Uttarakhand, India. *Theor. App. Climatol.140*, 1–25. https://doi.org/10.1007/s00704-019-03080-8

Mohorji, A.M., Şen, Z., and *Almazroui, M.*, 2017: Trend analyses revision and global monthly temperature innovative multi-duration analysis. *Earth Syst. Environ. 1*, 1–13. https://doi.org/10.1007/s41748-017-0014-x

Noori, M., Sharifi, M. B., Zarghami, M., and *Heydari, M.*, 2013: Utilization of LARS-WG Model for Modelling of Meteorological Parameters in Golestan Province of Iran. *J. River Engin. 1*(1), 5. https://doi.org/10.5281/zenodo.18265..

Oluoch, W., Nyabundi, K., and *Boiwa, M.,* 2017: Makesens trend analysis of agro-meteorological data from Kericho, Kenya. *Tea 38*(1), 9–14.

Salarian, M., Larijani, S., Heydari, M., and *ShahiriParsa,* 2016: Evaluation of drought changes of isfahan city based on the best Fitted probability distribution function. *Int. J. Engineer. Sci. Res. Technol. 5*, 623-631.https://doi.org/10.5281/zenodo.49807

Salarian, M., Najafi, M., Hosseini, S.V., and *Heydari, M.*, 2015: Classification of Zayandehrud river basin water quality regarding agriculture, drinking, and industrial usage. *Amer. Res. J. Civil Struct. Engin. 1*(1). 9, https://doi.org/10.5281/zenodo.18255

Sen, P.K., 1968: Estimates of the regression coefficient based on Kendall's tau. *J. Amer. Stat. Assoc. 63*(324), 1379–1389. https://doi.org/10.1080/01621459.1968.10480934

Shindell, D., and *Smith, C.J.* 2019: Climate and air-quality benefits of a realistic phase-out of fossil fuels. *Nature, 573*(7774), 408–411. https://doi.org/10.1038/s41586-019-1554-z

Tabari, H. and *Talaee, P.H.*, 2011: Temporal variability of precipitation over Iran: 1966–2005. *J. hydrology, 396*, 313–320. https://doi.org/10.1016/j.jhydrol.2010.11.034

Tosunoglu, F. and *Kisi, O.*, 2017: Trend analysis of maximum hydrologic drought variables using Mann–Kendall and Şen's innovative trend method. *River Res. Appl. 33*, 597–610. https://doi.org/10.1002/rra.3106

Villarini, G., Smith, J.A., Serinaldi, F., and *Ntelekos, A.A.*, 2011: Analyses of seasonal and annual maximum daily discharge records for central Europe. *J.hydrology 399*, 299–312. https://doi.org/10.1016/j.jhydrol.2011.01.007

Zarei, A.R., Moghimi, M.M., and *Mahmoudi, M.R.,* 2016: Parametric and non-parametric trend of drought in arid and semi-arid regions using RDI index. *Water Res. Manage. 30*, 5479–5500. https://doi.org/10.1007/s11269-016-1501-9

DOI:10.28974/idojaras.2022.3.8

IDŐJÁRÁS

Quarterly Journal of the Hungarian Meteorological Service
Vol. 126, No. 3, July – September, 2022, pp. 403–423

Observed climate changes in the Toplica river valley - Trend analysis of temperature, precipitation and river discharge

Nataša M. Martić Bursać[1,*], **Milan M. Radovanović**[2], **Aleksandar R. Radivojević**[1], **Radomir D. Ivanović**[3], **Ljiljana S. Stričević**[1], **Milena J. Gocić**[1], **Ninoslav M. Golubović**[1], and **Branislav L. Bursać**[4]

[1] *University of Niš, Faculty of Sciences and Mathematics*
Department of Geography, Višegradska 33,18000 Niš, Republic of Serbia

[2]*Serbian Academy of Sciences and Arts*
Geographical Institute "Jovan Cvijić"
Djure Jakšića 9, 11000 Belgrade, Republic of Serbia

[3]*University of Priština, Faculty of Natural Science*
temporarily seated in Kosovska Mitrovica, Department of Geography,
Ive Lole Ribara 29, 38220 Kosovska Mitrovica, Republic of Serbia

[4]*University of Niš, Faculty of Electronic Engineering*
Aleksandra Medvedeva 14, 18000 Niš, Republic of Serbia

**Corresponding Author e-mail: natasamarticbursac@gmail.com*

(Manuscript received in final form April 12, 2021)

Abstract— Changes in air temperature, precipitation, and the Toplica river discharge were investigated. Annual and seasonal climatic data were collected at weather stations Kursumlija and Prokuplje, and discharge data on hydrological gauges Pepeljevac and Doljevac. The data covered a period of 62 years (1957–2018). Mann-Kendall and Pettitt's tests have been applied for the periods 1957–2018, 1957–1987, 1988–2018, and 1975–1994, which we find as very important period when atmospheric circulation was altered. Mean annual temperature and precipitation were greater in the second half-period, while the discharge was smaller, even all the signals had growth trend. Mean seasonal temperature increased for all seasons, as well as precipitation, except for summer (JJA). The discharge is lower in the second half-period for almost all seasons, with signs of recovery for all seasons except summer.

Key-words: climate change, the Toplica river, temperature, precipitation, discharge, linear trend, change point

1. Introduction

Climate change is accepted to be one of the prevalent difficulties for humankind in this century. Large number of various fields are impacted by climate change. Rising temperatures increase extinction risk for numerous animal and plant species, droughts lead to decline of agriculture production and to problem with drinking water, severe floods cause destruction and loss of lives.

The idea for this research came during the study of the village of Plocnik, located in the middle of the Toplica basin (*Martić Bursać,* 2017). Local people said that the level of the Toplica river was significantly higher during their youth (mostly early 70s of the 20th century), and the winters were colder and longer, with more snow. Guided by these stories, we wanted to determine what has happened with the climate and the river flow over the time. According to latest advances in climate science, we assumed that global climate change, especially global warming, is the primary cause of these changes. We have examined changes in temperature, precipitation in the Toplica river valley and discharge of the Toplica river in the period from 1957 to 2018.

The climate system is very complex, and so is the climate. Complex systems can respond unexpectedly and abruptly to changes within the system, and these changes can be highly nonlinear. Nonlinear interactions among atmosphere, hydrosphere, and biosphere cause climate variables to exhibit highly nonlinear characteristics. The complexity of rainfall and temperature dynamics has been widely used to indicate the extent of the complexity of climate systems (*Kyoung et al.,* 2011). A variety of sophisticated techniques have been developed in order to quantify system complexity (*Di et al.,* 2018). The major factor of climate change is the increasing temperature. Mean air surface temperature increased globally by 0.85 °C over the 1880–2012 period (*IPCC,* 2013). Another important factor is the variability of precipitation. One of the reasons for the change in hydrological cycle is the increased energy for evapotranspiration, whereas increased temperature changes water holding capacity of the atmosphere (*Trenberth,* 2011). Exact impacts of climate change on water cycle are hard to predict. There is a general consensus among scientists that it will result in more frequent and more severe hydrologic extremes (*IPCC,* 2013). Precipitation is the primary input of water in a river basin, and while it plays dominant role in year-to-year streamflow variability, the effect of temperature on total annual discharge may become more important during multiyear droughts. In both wet and dry years, when the flow is substantially different than expected, given precipitation, air temperature, and soil moisture can modulate the dominant precipitation influence on streamflow (*Woodhouse et al.,* 2016). Different initial soil conditions are primary cause of runoff nonlinear response to rainfall. In general, the wetter the catchment prior to an input of rainfall is, the greater the volume of runoff that will be generated, and faster response will be, and vice versa. This general role drops after high intensity, low frequency storms. In that case, hydrological

response is independent of the initial soil water content (*Castillo et al.,* 2003). In semiarid areas, as the Toplica valley, medium and low intensity precipitation is most frequent, and the antecedent soil water content is an important factor controlling runoff. Various infiltration models are specifically derived to eliminate the errors caused by the complex initial soil conditions in rainfall-runoff models (*Wang et al.,* 2017). Temperature can modulate the streamflow in various ways. Increase of temperature during winter changes the rate of accumulation, duration, density, and melting of snow cover. During the warmer part of the year, increased temperature changes soil conditions through evaporation, and reduces the amount of precipitation available for streamflow and groundwater recharge. It is not a one way relation, soil moisture-temperature coupling could be strong, especially during heatwaves (*Castillo et al.,* 2003).

Numerous studies of climate change in Serbia were conducted, focused on mean temperature change (*Vukovic et al.*, 2018; *JCERNI*, 2014; *Gavrilov et al.,* 2015), extreme temperature and precipitation indices (*Ruml et al.,* 2017; *Djordjevic S.,* 2008; *Unkasevic* and *Tosic,* 2013), increase in frequency and intensity of heat waves (*Unkaševic* and *Tošic,* 2015), accelerated temperature increase (*Unkasevic* and *Tosic,* 2013), prediction of intensification and acceleration of floods, forest fires, disturbance in agriculture, and health of ecosystem (*Vukovic, et al.,* 2018; *JCERNI*, 2017).

Projections of regional climate models predict that by the end of this century, the annual average temperatures will increase from 2.4 °C to 2.8 °C according to an optimistic scenario (A1B1), respectively from 3.4 °C to 3.8 °C according to a pessimistic scenario (A2). Situation with rainfall is more complex, under the A1B1, a reduction of precipitation is expected throughout Serbia, while according to the A2 scenario, the precipitation will increase in Vojvodina, while it will remain the same or decrease in the other parts of Serbia, with an increased number of floods and droughts (*Sekulić et al.*, 2012)

The impact of climate change on river discharge has been observed by many researchers: globally - change in stream flow extremes (*Asadieh* and *Krakauer*, 2017); in Europe - frequency of river floods (*Alfieri et al.,* 2015) modifying river flow regimes (*Schneider et al.*, 2013); in the region - impact on rivers discharge in Eastern Romania (*Croitoru* and *Minea*, 2015), impact on the Vrbas river discharge (Bosnia and Herzegovina) (*Gnjato et al.*, 2019), etc.

2. Data and methodology

2.1. Study Area

The basin of the Toplica river is located in southern Serbia, in the central part of the Balkan Peninsula (*Fig. 1*). Relief of the basin was formed in Oligo-Miocene, and is one of the oldest landmasses of the Balkan Peninsula. During the Neogene, the basin was filled with water of the Pannonian Sea, reaching 760 meters above

sea level. After withdrawal of the lake, the Toplica river with the network of its tributaries was formed in a shallow and wide valley. The valley is elongated in the direction east-west, with the longer axis of about 30 km and shorter axis of about 10 km. The relief is hilly and gradually decreases from north to south (*Martić Bursać,* 2017; *Martić Bursać et al*., 2016b). The height of the basin is 633 m above sea level on average, the maximum height being 2016 m, and the minimum 187 m.

Climate of the Toplica basin is highly determined by its geographical position and relief. To the east, the basin is open to the South Morava river valley, where the continental air mass freely penetrates. From the north it is enclosed by the ranges of the mountains Veliki and Mali Jastrebac, from the south by the mountains of Radan, Sokolovica, Vidojevica, and Pasjaca, while the west is fenced by the massif of the mountain of Kopaonik. With their height and direction, these mountains represent barriers for the entry of somewhat milder air from the southwest, as well as colder continental air from the north and northeast (*Martić Bursać et al*., 2016a; *Rudić*, 1978). The basin of the Toplica has a moderate continental climate with a strong continental character. In addition to the very dominant continental influences, there are also influences of the Aegean and the steppe climate, which occur locally (*Ducić* and *Radovanović,* 2005; *Martic Bursac* and *Stricevic,* 2018). According to the Köppen climate classification, most of the basin belongs to group C, with an exception of the mountainous area, which belongs to group D (*Dukić,* 1999).

The river Toplica was formed by merging the rivers Djerekarusa and Lukovska near the village of Mercez, on the eastern slopes of the mountain of Kopaonik. The source of the river Djerekusa is a main source (1650 m above sea), with the total length of 130 km and the catchment area of 2180 km². The Toplica river is the largest left tributary of the South Morava, considering both the surface of the basin and water quantity. In the total area of the South Morava basin, the Toplica basin share is 14.9%, whereas in the total discharge its share is 10.9% (*Gavrilović,* 2011; *Martic Bursac et al*., 2016a).

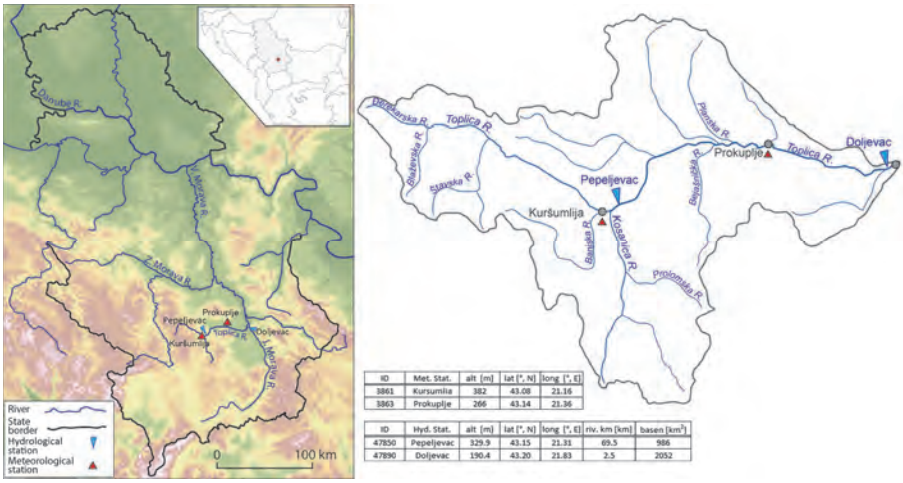

ID	Met. Stat.	alt [m]	lat [°, N]	long [°, E]
3861	Kursumlia	382	43.08	21.16
3863	Prokuplje	266	43.14	21.36

ID	Hyd. Stat.	alt [m]	lat [°, N]	long [°, E]	riv. km [km]	basen [km^2]
47850	Pepeljevac	329.9	43.15	21.31	69.5	986
47890	Doljevac	190.4	43.20	21.83	2.5	2052

Fig. 1. Geographical position of Toplica Valley.

The Toplica basin is symmetrical, right and left tributaries are approximately equally long. The Toplica river has a very unstable river regime. The highest flow rate is in March and April, when the discharge is more than doubled due to the melting snow from the surrounding mountains, while the lowest flow rate is in August and September, when the discharge often drops below 1 m^3/s, and some of the tributaries dry up (*Rudić,* 1978).

In order to regulate the river regime and provide additional water supply to the towns of Kursumlija, Prokuplje, and Nis, an accumulation was built on the Toplica river. Dam construction in the village of Selova lasted from 1986 to 2006. Due to large erosion in the upper course, it was necessary to apply anti-erosion measures, which are still in progress. At the moment, the accumulation is not functional and does not affect the flow of the river (*Kostadinov*, 2008; *Martić Bursać*, 2016a).

2.2. Data

Seasonal and annual climate data were examined, temperatures and precipitation in the towns of Kursumlija and Prokuplje, as well as discharge data from the two gauges on the Toplica river, in the villages of Pepeljevac and Doljevac. Monthly and annual temperature and discharge means, as well as monthly and annual sums of precipitation for all the stations in the period of 62 years (1957–2018), were provided by the Republic Hydrometeorological Service of Serbia (RHMZ).

Seasons are defined as three-month temperature and discharge averages, and three month total sums for precipitation. Winter season (DJF) corresponds to December of the previous year, and January-February of the calendar year, while all the other seasons, spring (MAM), summer (JJA), autumn (SON) correspond to the calendar year.

The time series of the observed signals is 62 years long, between 1957 and 2018, and that period will be referred to as "the entire period". We divided it into two equal 31-year-long half-periods, in order to find out if there are changes in signals, if the series is homogenous, if it is a trend, and what the possible cause of the changes is. The term "the first period" will hereinafter be used for the period between 1957 and 1987, "the second period" will be used for the period between 1988 and 2018. We also define the third, 20-year-long period between 1975 and 1994, where we found some important changes in the observed signals.

2.3. Method used

2.3.1. Pettitt's homogeneity test

We used Pettitt's test for homogeneity of series and change points (*Pettitt,* 1979). The change point detection is an important aspect to assess the period from which significant change occurred in a time series. The Pettitt's test for change detection is a nonparametric test useful for evaluating the occurrence of abrupt changes in climatic records. According to Pettitt's test, if there is a change point in a series of n observed data, then the distribution function of the first t samples F_1 would be different from the distribution function of the second part of the series F_2. The null hypothesis H_0 implies that the data are homogeneous throughout the period of observation, and the alternative hypothesis H_1 implies the presence of a non-accidental component among data causing a shift of the location parameter at a particular moment. The test statistic $U_{t,n}$, K_t, and the associated confidence level ρ for the sample length n for this test are given in the following equations:

$$U_{t,n} = \sum_{i=1}^{t} \sum_{j=i+1}^{n} sgn(x_i - x_j), \tag{1}$$

$$; \quad K_t = \max_{1 \le t < n} |U_{t,n}|, \tag{2}$$

$$\rho = e^{-K/(n^2+n^3)}. \tag{3}$$

When ρ is smaller than the specified confidence level, the null hypothesis is rejected. The approximate significance probability p for a change-point is defined as $p = 1 - \rho$.

Quality control of datasets was made by RHMZ, and we assumed that any detected step changes are due to climate variability.

2.3.2. Mann – Kendall trend test

The Mann-Kendall (MK) trend test is a nonparametric approach, and it was used in this study to detect trends in temperature, precipitation, and discharge. The magnitudes of the trend in a time series have been estimated by the Sen's estimator

method (*Kendall,* 1948). The test analyzes the difference in signs between earlier and later data points. The idea is that if a trend is present, the sign values will tend to either increase or decrease constantly. The hypothesis H_0- is that there is no trend in the series; alternatively, in hypothesis H_1, monotonic trend is present. First we calculated sign difference *S*, after that variance *VAR(S),* and in the end MK test statistic Z_{MK}.

$$S = \sum_{i=1}^{n-1} \sum_{j=i+1}^{n} sgn(x_i - x_j) \tag{4}$$

where

$$sgn(x) = \begin{cases} 1 & if\ x > x_i \\ 0 & if\ x = x_i \\ -1 & if\ x < x_i \end{cases} . \tag{5}$$

$$VAR(S) = \frac{1}{18}\left[n(n-1)(2n+5) - \sum_{p-1}^{g} t_p(t_p - 1)(2t_p + 5)\right] \quad . \tag{6}$$

$$Z_{MK} = \begin{cases} \frac{S-1}{\sqrt{VAR(S)}} & if\ S > 0 \\ 0 & if\ S = 0 \\ \frac{S+1}{\sqrt{VAR(S)}} & if\ S < 0 \end{cases} , \tag{7}$$

where x_i and x_j are sequential values in the series, n is the sample size, g is the number of tied groups, and t_p is the number of observations in the pth group.

A positive (negative) value of Z_{MK} indicates that the data tend to increase (decrease) with time. If α is the Type I error rate, where $0 < \alpha < 0.5$, and $Z_{1-\alpha}$ is the 100(1-α)th percentile of the standard normal distribution (provided in statistics books or statistical software packages), then H_0 will be rejected, and replaced with the alternative H_1 if $Z_{MK} \geq Z_{1-\alpha}$ for the upward, or $Z_{MK} \leq -Z_{1-\alpha}$ for the downward trend.

2.3.3. Polynomial approximation

We have used higher order polynomial functions for the least square approximation of signals in order to gain a better insight of their tendencies. Using MatLab Curve Fitting tool, all approximate polynomials of degree 2 to 10 have been examined. We have found that all the polynomials of degree 6 and greater have the same shape of the curve in general, so we have chosen polynomial to be

of minimal 6th order to avoid polynomial wiggle as much as possible. Due to this effect, the shape of the curve at the ends of the time series should be taken with caution (*Cheney* and *Light.,* 2000). These polynomials are conditioned very badly, and cannot be used for quantitative calculations, but they can give us a good qualitative insight of changing signal in time. They are given as purple lines in *Figs. 2, 3,* and *4*.

3. Results and discussion

3.1. Temperature

Average temperature for the period 1957–2018 is 10.4 °C and 11 °C in Kursumlija and Prokuplje (*Table 1*), respectively. Average temperatures increased by 0.5 °C in Kursumlija and 0.6 °C in Prokuplje in the second period. In 1998, a change point in mean annual temperatures was detected at both stations during the entire period. In the first period, the change point was found in Prokuplje in 1968, and in the second period, it was found at both stations in 2006. Linear trend of average annual temperatures increased in the entire period at both stations; in Kursumlija increasing is statistically significant. At both stations, there is a statistically significant decreasing temperature trend in the first period, and increasing in the second period. Besides the opposite trend in the first and the second half of the period, our attention is drawn to the fact that there is a significant discontinuity of mean temperature, precipitation, and discharge in the Toplica river between the periods. This discontinuity shows us that there is probably a period in between these two half-periods when something happened with climate signals. For this reason, the curves of polynomial approximations were used, and we clearly identified period 1975–1994 as a period where some dramatic changes happened. The curves of polynomial approximations (*Fig. 1*) at the beginning show temperature decrease at both stations, where the minimum is in the early eighties in Kursumlija, and a little earlier, in the late seventies, in Prokuplje. After that, the temperature increases, and the increase is more emphasized in Kursumlija than in Prokuplje. The trend of mean annual temperatures in the period 1975–1994 at both stations is increasing, but not statistically significant. In this case, nothing dramatic happened with temperature, but that is not the case with some other parameters.

The mean winter (DJF) temperature in Kuršumlija and Prokuplje increased by 0.5 °C in the second period (*Table 1*). The Pettitt test detects data inhomogeneity in Kuršumlija in the second period with a change point in 2006, while the significance probability *p* in Prokuplje is above the threshold. The trend of DJF temperature (*Fig. 2*) is decreasing in the first period and in the period 1975–1994, and increasing throughout the second, but in all cases, it is statistically insignificant.

Table 1. Parameters of seasonal and annual temperatures in Kursumlija and Prokuplje

	Period	Kursumlija						Prokuplje					
		Mean [°C]	σ	p	C.p.	m1/m2 [°C]	L.t. [°C/dec]	Mean [°C]	σ	p	C.p.	m1/m2 [°C]	L.t. [°C/dec]
	57-18	1.0	1.29	0.09	2006		0.16	1.2	1.49	0.37	2006		0.14
DJF	57-87	0.7	1.23	0.52	1960		-0.12	0.9	1.44	0.47	1961		-0.19
Winter	88-18	1.2	1.32	0.03	2006	0.8/1.9	0.43	1.4	1.53	0.25	2006		0.38
	75-94						-0.34						-0.23
	57-18	10.3	1.04	0.00	1998	10/11.1	0.23 **	11.1	1.02	0.02	1998	10.9/11.7	0.15 **
MAM	57-87	10.0	0.95	0.95	1963		0.07	10.9	0.94	0.93	1972		-0.04
Spring	88-18	10.6	1.05	0.01	1998	9.8/11.1	0.58 *	11.3	1.07	0.08	1998		0.43 *
	75-94						0.02						0.14
	57-18	19.4	1.21	0.00	1991	18.8/20.1	0.32 ***	20.4	1.15	0.00	1991	19.8/21.1	0.27 ***
JJA	57-87	18.8	1.07	0.02	1972	19.2/18.3	-0.38 *	19.8	0.82	0.00	1968	20.3/19.4	-0.38 *
Summer	88-18	19.9	1.08	0.00	2006	19.4/20.7	0.69 ***	20.9	1.16	0.55	1991		0.32 ***
	75-94						0.96 *						1.36 *
	57-18	10.7	1.15	0.25	1969		0.07	11.4	1.22	0.16	1968		0.05
SON	57-87	10.7	1.21	0.03	1968	11.3/10.2	-0.27	11.2	1.25	0.00	1968	12.1/10.6	-0.55
Autumn	88-18	10.8	1.1	0.08	2007		0.52 *	11.5	1.18	0.39	2011		0.28 *
	75-94						0.47 *						1.08 *
	57-18	10.4	0.68	0.00	1998	10.1/11	0.17 **	11.0	0.67	0.00	1998	10.8/11.5	0.15
	57-87	10.1	0.53	0.63	1968		-0.31 *	10.7	0.53	0.02	1968	11.1/10.5	-0.3 *
Annual	88-18	10.6	0.7	0.00	2006	10.2/11.3	0.56 ***	11.3	0.68	0.00	2006	11/11.8	0.35 ***
	75-94						0.26						0.26

Note: Mean [°C] – mean temperature for period; σ – standard deviation; p – significance probability (Pettitt);C.p.– changing point (Pettitt) [year]; m1/m2 [°C] – mean value before and after change point, for p<α=0.05 (Pettitt); L.t.[°C/dec] – slope of linear trend (no star – no statistical significance,
* – α=0.05, ** – α=0.01, *** – α=0.001, Mann-Kendall)

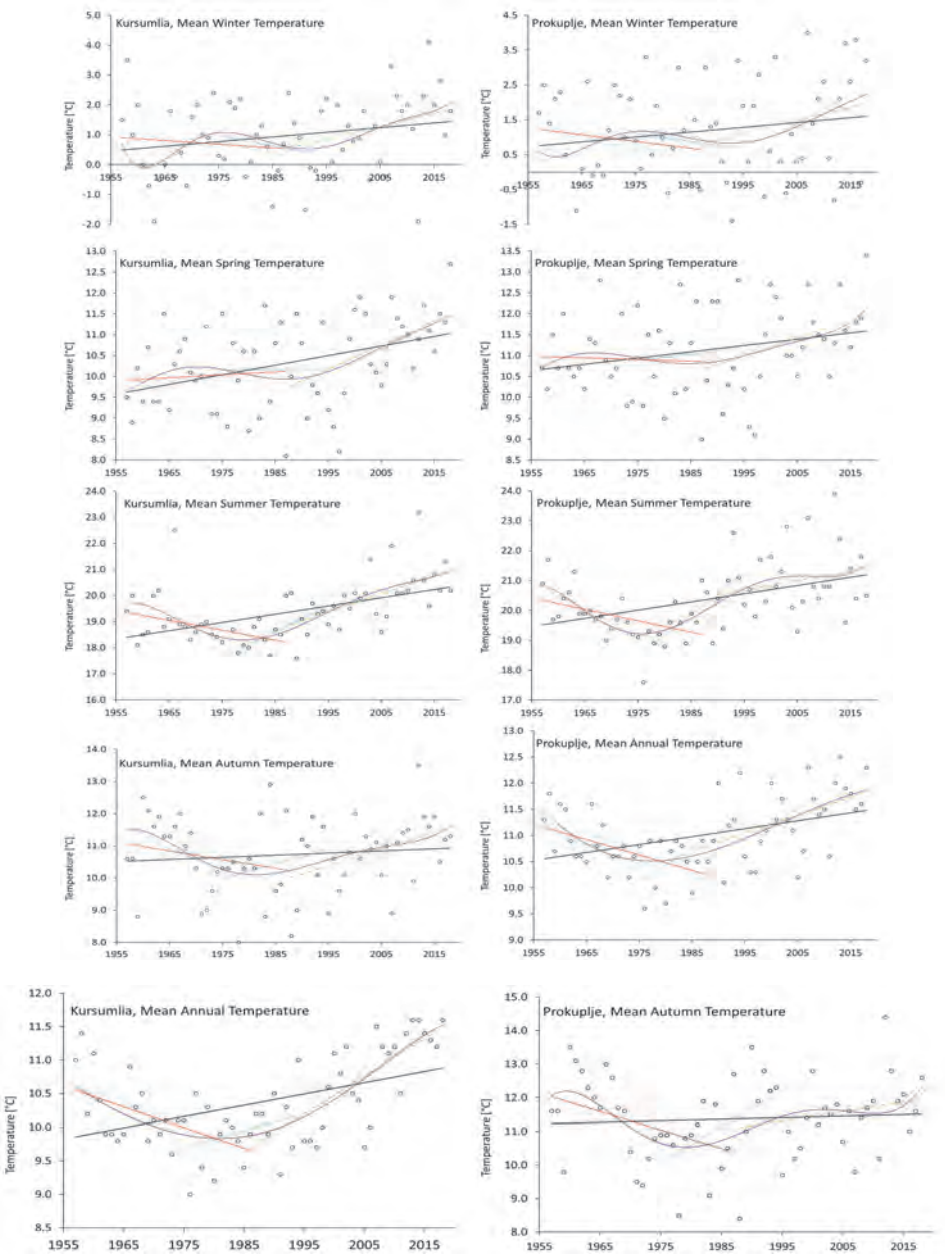

Note: black dots – mean temperatures; lines – temperature trends for different periods: black (1957–2018); red (1957-1987); green (1988-2018); blue (1974-1995); purple –polinomial approximation

Fig. 2. Annual and seasonal temperature in Kursumlija and Prokuplje.

The mean spring (MAM) temperature is higher in the second period by 0.6 °C in Kuršumlija, and 0.4 °C in Prokuplje. A change point in the data was detected in 1998 in the entire and the second period at both stations, but in the second period the probability significance in Prokuplje was above the set value ($p = 0.05$), so the initial hypothesis of data homogeneity could not be discarded. The temperature trend (*Fig. 2*) in the MAM season generally increased at both stations. In the first period we do not detect any trend, while in the second period there is a significant increasing temperature trend at both stations.

The mean summer (JJA) temperature is 1.1 °C higher in the second than in the first period at both stations, which is the largest absolute increase in temperature compared to other seasons. In 1991, a change point was detected at both stations during the entire period. In the first period, change points were also detected at both stations, in Kursumlija in 1972, and in Prokuplje in 1968, while in the second period, change points were detected only in Kursumlija in 2006. A statistically significant trend of temperature exists in all the examined periods. In the first period, there is a negative trend of air temperature at both stations, while in the second period it is increasing. In the period 1975–1994, at both stations we recorded an extremely high temperature growth trend of 0.96 °C/dec in Kursumlija and 1.36 °C/dec in Prokuplje.

In the autumn season (SON), the smallest increase in temperature was recorded between the two periods, 0.1 °C in Kursumlija and 0.3 °C in Prokuplje. A change point was detected at both stations in the first period in 1968. A trend of statistically significant increase in air temperature exists at both stations in the second period, where we have almost twice as much growth in Kursumlija than in Prokuplje. There is a significant growth trend in the period 1975–94 at both stations, in Prokuplje it is extreme, 1.08 °C/dec, while in Kursumlija it is twice smaller, but still very large.

3.2. Precipitation

Unlike in temperatures, where the situation is quite clear and we have a more or less pronounced increase in all cases, the situation with precipitation is more complicated. This situation is ultimately predicted by climate models (*Sekulić*, 2012).

Average precipitation for the entire period is 651.9 mm in Kursumlija and 563.8 mm in Prokuplje (*Table 2*). A change point in 1994 was detected in Prokuplje. The increase in the average precipitation in the second period is 2.5% in Kursumlija and 8.6% in Prokuplje.

The Mann-Kendal test reveals that the linear trend of total annual precipitation in the entire period is increasing and statistically significant at both stations, with a rate of 15.5 mm/dec in Kursumlija and 19.2 mm/dec in Prokuplje. In the first period, change point was not detected at the stations, and the precipitation trend has a different sign. In Kursumlija the trend is increasing, while

in Prokuplje it is decreasing, in both cases without statistical significance. In the second period, a change point was detected at both stations in 2003, and in both cases there is an abrupt jump of mean value of over 100 mm. The linear trend of precipitation in the second period is positive and statistically significant at both stations. The situation in the period 1975–1994 is especially interesting, where at both stations precipitation trend is highly decreasing by about 90 mm/dec.

Table 2. Parameters of seasonal and annual precipitations in Kuršumlija and Prokuplje

		Kursumlia						Prokuplje					
	Period	Mean [mm]	Cv	p	C.p.	m1/m2	L.t. [mm/dec]	Mean [mm]	Cv	α	C.p.	m1/m2	L.t. [mm/dec]
DJF Winter	57-18	143.8	0.36	0.38	1993		3.11	124.9	0.39	0.02	1993	109/149	8.75 *
	57-87	144.8	0.3	0.36	1977		5.85	112.4	0.32	0.62	1976		4.04
	88-18	142.9	0.42	0.15	1993		22.83	137.3	0.42	0.30	2002		21.24
	75-94						-8.96						-1.6
MAM Spring	57-18	175.4	0.3	0.09	2005		4.92	152.7	0.36	0.02	2000	138/189	7.72
	57-87	169.6	0.27	0.13	1962		-15.15	141.9	0.31	0.38	1964		-13.88
	88-18	181.1	0.32	0.02	2005	156/215	32.36 *	163.4	0.38	0.01	2004	134/199	36.57 **
	75-94						-12.18						-16.65
JJA Summer	57-18	169.1	0.46	0.25	1971		3.68	149.7	0.44	0.00	1983		-2.9
	57-87	170.2	0.46	0.01	1971	133/205	25.65	159.3	0.41	0.35	1971		7.79
	88-18	168.1	0.47	0.93	2013		7.8	140.1	0.46	0.96	2010		4.73
	75-94						-29.35 *						-56.19 *
SON Autumn	57-18	162.5	0.41	0.62	1995		4.73	137.8	0.43	0.49	1991		5.4
	57-87	156.6	0.44	0.37	1969		4.01	126.8	0.41	0.91	1964		5.3
	88-18	168.3		0.62	1995		11.27	148.8	0.43	0.93	2013		6.45
	75-94						-36.24 *						-14.61
Annual	57-18	651.9	0.19	0.07	2000		15.54 *	563.8	0.2	0.00	1994	528/621	19.18 *
	57-87	643.8	0.16	0.12	1971		19.72	540.6	0.16	0.63	1971		-5.47
	88-18	660.0	0.21	0.00	2003	598/726	73.31 **	587.0	0.23	0.00	2003	535/636	69.19 *
	75-94						-91.55 *						-89.49 *

Note: Mean [mm] – mean precipitation for period; Cv – coefficient of variation; p – significance probability (Pettitt) ; C.p. – changing point (Pettitt) [year]; m1/m2 [mm] – mean value before and after change point, for p<α=0.05 (Pettitt); L.t.[mm/dec] – slope of linear trend (no star – no statistical significance, * – α=0.05, ** – α=0.01, *** – α=0.001, Mann-Kendall)

The winter season (DJF) in Kursumlija is quite stable, and there are no significant differences between the periods. The average is slightly lower in the second period, in all the cases without change points and a significant linear trend. In Prokuplje, the situation is different, there is a change point detected in 1993, in the entire period, linear trend is positive and statistically significant. There is also a significant increase in the average value of 22% in the second period. In the period 1975–1994, there is a slight negative trend at both stations, somewhat higher in Kursumlija, in both cases without statistical significance.

In the spring season (MAM) both stations recorded increasing trend in the entire period, with a change point in Prokuplje in 1993. In *Fig. 3* it is clear, that there is a declining trend in the entire first period, not only in the period 1975–1994, although without statistical significance. In the second period, the change point was found in 2004 in Prokuplje, and in 2005 in Kursumlija. In both cases there is a sudden jump in the mean value. At both stations in the second period, a statistically significant growing precipitation trend was found, with the rate of over 30 mm/dec.

In the summer season (JJA) there is a decrease in the mean value between the first and second period at both stations, despite the fact that in both half-periods there are positive precipitation trends. The positive trend in the first period is much more pronounced in Kursumlija, with a change point in 1971 (*Fig. 3*). The cause of lower mean precipitation in the second period, and the negative trend in the whole period in Prokuplje, despite the positive precipitation trend in both half-periods is in a very pronounced decline in 1975–1994. At both stations in this period there is a statistically significant decrease in precipitation and a simultaneous increase in temperature. In *Figs. 2* and *3*, for JJA we see that the polynomial approximation of precipitation almost mirrors the temperature polynomial. The decrease in precipitation in this season is more pronounced in Prokuplje than in Kursumlija.

In the autumn season (SON), similarly to summer, we found a significant decrease in the precipitation amount in the period 1975–1994, but in this case the decrease is higher in Kursumlija than in Prokuplje. However, the precipitation increase in the second period of the SON season is greater than the increase in the JJA season, so this decrease is compensated for. Therefore, there is an increase in mean precipitation in the second period at both stations. There are no change points in any period, while the trend is slightly positive without statistical significance.

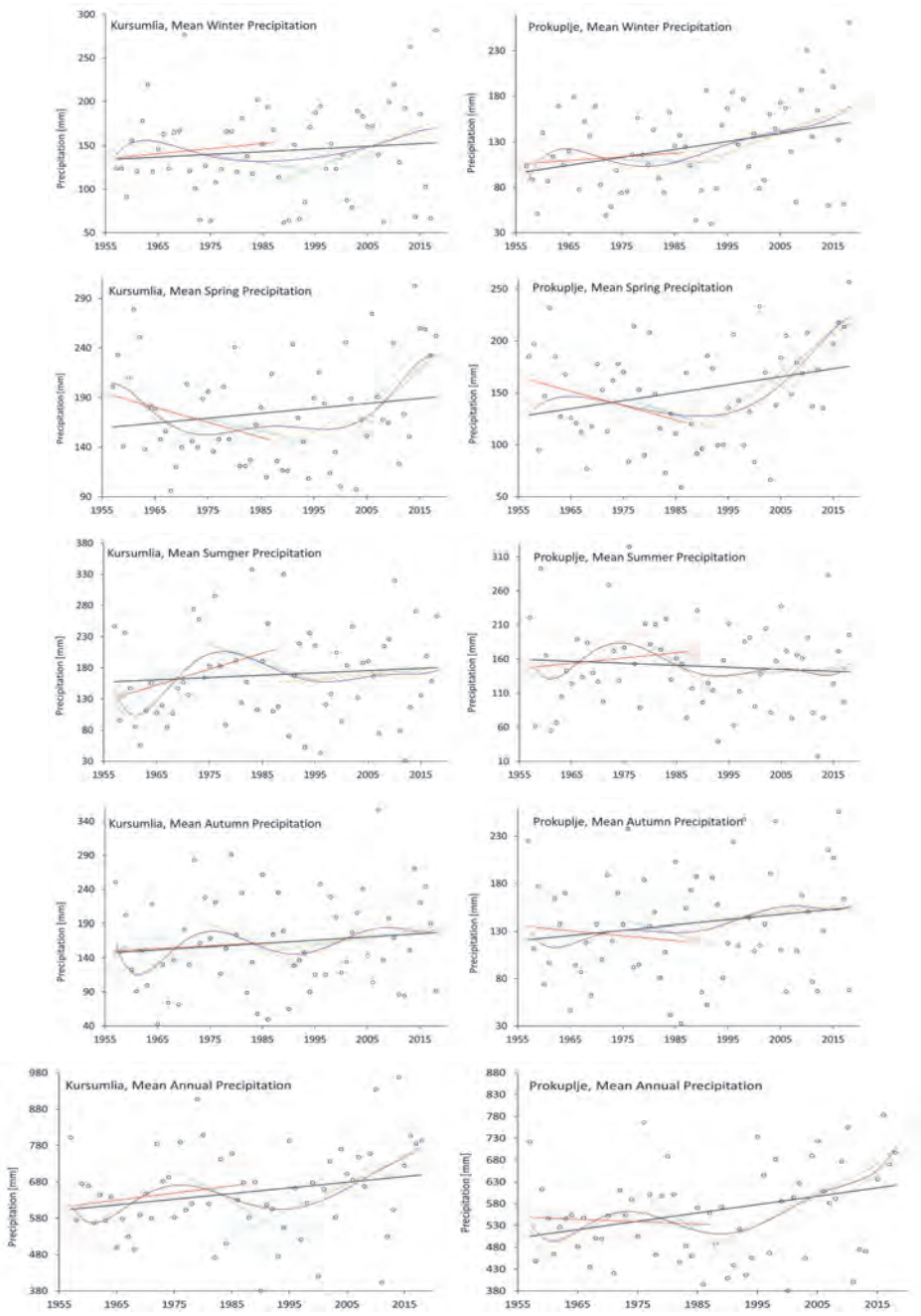

Note: black dots – precipitation; lines – precipitation trends for the periods: black (1957–2018); red (1957–1987); green (1988-2018); blue (1974–1995); purple –polinomial approximation.

Fig. 3. Annual and seasonal precipitation in Kuršumlija and Prokuplje.

3.3. Discharge

The average discharge of the Toplica in the entire period in Pepeljevac is 7 m^3/s with a slight positive trend; in Doljevac it is 9.9 m^3/s with a slight negative trend (*Table 3*). There is a change point in Doljevac in 1982, where the mean value of the discharge dropped. The mean value of the discharge is higher in the first period at both stations, although in both half-periods there is a slight trend of increasing discharge. In the period 1975–1994, there is a very pronounced, statistically significant decreasing trend in discharge at both stations (*Fig. 4*). This is certainly to be expected, considering that there is a significant drop in precipitation in that period. However, total precipitation at both stations increases significantly in the entire period, so decrease is not to be expected in the discharge in Doljevac in the same period. Therefore, the cause of this decline and the appearance of the change point cannot be fully explained by the changes of precipitation in 1975–1994. Apparently, a significant increase in temperature, especially during the summer period, led to an increase in evaporation in the basin, and therefore, there was an additional decrease in discharge. Additional decrease in summer discharge is probably of anthropogenic nature, since intensive agricultural production of the remaining rural households has led to increased use of water, both from the river stream and groundwater near the river.

In the DJF season, there was a decrease in the mean annual discharge at both stations in the second period. In Doljevac, the average discharge was 21.1% lower in the second period, while precipitation was higher by 22.2%. The answer to this anomaly could again be found in the period 1975–1994. In this period, there was a decrease in precipitation at both measuring stations, but this decrease is the lowest of all the seasons, so it could not cause such a reduction in discharge. At the same time, in this period, the temperature dropped at both stations, which apparently significantly slowed down the melting of snow from the mountains, primarily from Kopaonik as the largest massif in the basin, which practically led to such a reduction in discharge.

In the MAM season, there is a trend of increasing discharges in the entire period in the upper course of the river and a declining trend in the lower, without statistical significance. In Pepeljevac, the average discharge increased by 12.1% in the second period, while at the same time, the increase in precipitation in Kursumlija was 6.8%. As there is also a positive trend of average temperature in Kursumlija, the most probable cause of additional discharge during this season comes from the melting of snow accumulated during the DJF season, primarily on Kopaonik. During the entire second period, there is a positive, statistically significant trend of increase in precipitation and temperature in Prokuplje, which lead to a positive trend in the mean discharge in Doljevac. Even so, meane discharge in Doljevac dropped 9% in the second period.

Table 3. Parameters of seasonal and annual discharges on Toplica river in Pepeljevac and Doljevac

	Period	Pepeljevac						Doljevac					
		Mean [m^3/s]	Cv	p	C.p.	m1/m2	L.t. [$m^3/s/dec$]	Mean [m^3/s]	Cv	p	C.p.	m1/m2	L.t. [$m^3/s/dec$]
	57-18	7.9	0.51	0.69	1995		0.13	11.0	0.53	0.17	1982		-0.37
DJF	57-87	8.1	0.48	0.16	1976		0.9	12.3	0.5	0.91	1976		0.29
Winter	88-18	7.6	0.56	0.08	1995		1.21	9.7	0.55	0.08	1995		1.84
	75-94						-4.15 **						-6.67 *
	57-18	13.2	0.49	0.45	2004		0.73	19.1	0.49	0.70	1965		-0.21
MAM	57-87	12.4	0.44	0.79	1979		0.08	20.0	0.5	0.56	1965		-2.2
Spring	88-18	13.9	0.52	0.23	2004		2.94	18.2	0.48	0.26	2004		4.05
	75-94						-2.01						-3.19
	57-18	3.6	0.58	0.00	1989		-0.21	5.1	0.55	0.09	1989		-0.3
JJA	57-87	4.0	0.59	0.05	1974	3.2/5.1	0.36	5.7	0.54	0.84	1980		-0.25
Summer	88-18	3.2	0.53	0.77	1992		-0.35	4.5	0.55	0.60	2004		0.04
	75-94						-2.25 *						-2.81 *
	57-18	3.2	0.75	0.46	1981		-0.17	4.4	0.83	0.41	1981		-0.42
SON	57-87	3.6	0.83	0.05	1971	2.8/4.4	0.03	5.2	0.9	0.46	1971		-0.82
Autumn	88-18	2.8	0.58	0.79	1994		0.13	3.6	0.54	0.56	1994		0.55
	75-94						-2.44 **						-3.34 **
	57-18	7.0	0.33	0.00	2013		0.11	9.9	0.34	0.03	1982	11.2/9	-0.33
	57-87	7.1	0.29	0.07	1974		0.33	10.8	0.29	0.41	1963		-0.75
Annual	88-18	6.9	0.37	0.00	1994		0.96	9.0	0.38	0.22	1994		1.62
	75-94						-2.76 **						-4.01 ***

Note: Mean [m^3/s] – mean discharge for period; Cv – coefficient of variation; p – significance probability (Pettitt) ; C.p. – changing point (Pettitt) [year]; m1/m2 [m^3/s] – mean value before and after change point, for $p<\alpha=0.05$ (Pettitt); L.t.[$m^3/s/dec$] – slope of linear trend (no star – no statistical significance,

* – $\alpha=0.05$, ** – $\alpha=0.01$, *** – $\alpha=0.001$, Mann-Kendall)

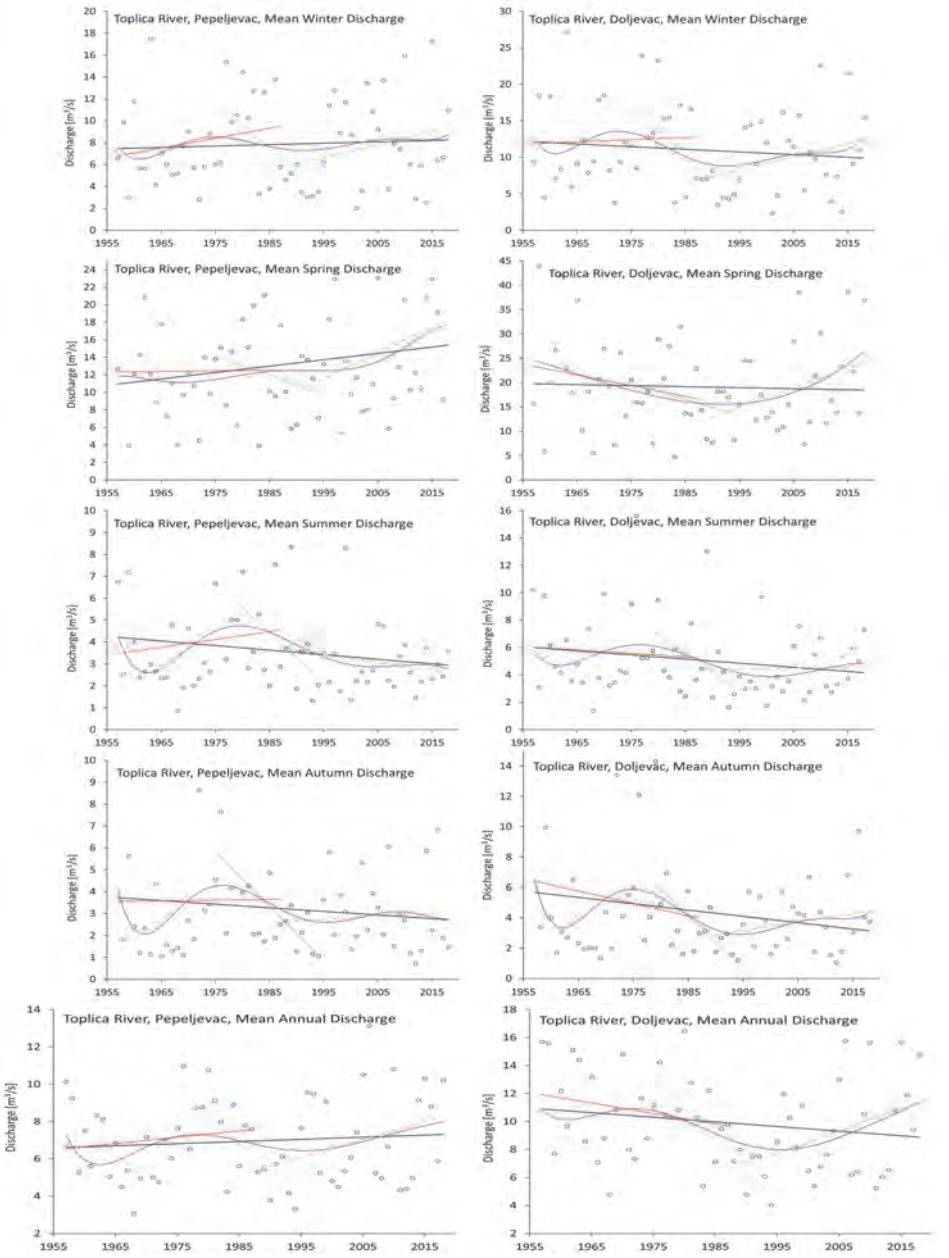

Note: black dots – discharge; lines – discharge trends for different periods: black (1957–2018); red (1957–1987); green (1988–2018); blue (1974–1995); purple –polynomial approximation

Fig. 4. Seasonal and annual discharge on Toplica river in Pepeljevac and Doljevac.

The discharge trend throughout the summer season declined at both stations. The mean discharge in the second period is lower by 20% in Pepeljevac and 14% in Doljevac. This decline was mostly affected by a strong negative trend in the period 1975-1994, which is statistically significant at both stations. In Pepeljevac, the discharge trend in the second period is negative, despite the positive precipitation trend in Kursumlija. The answer is probably in the very pronounced positive trend of temperature in Kursumlija and the increased evaporation in the upper course of the Toplica river. In Doljevac, the trend in the second period is neutral, despite the positive precipitation trend in the second period in Prokuplje.

In the summer and autumn seasons, the trend of decreasing discharge is most strongly expressed at both stations in the period 1975–1994. with great statistical reliability. The decline in the mean discharge between the two observed periods is most pronounced in the SON season. In Pepeljevac, the discharge was 22% lower in the second period, while in Doljevac it was lower by 34.6%. At the same time, we found that the average precipitation is higher by 7.5% in Kursumlija and 17.4% in Prokuplje compared to the first period. This imbalance is again a consequence of a strong drop in precipitation and discharge during 1975–1994, and of a simultaneous increase in temperature.

4. Summary

The paper studies annual and seasonal changes in temperature and precipitation at two meteorological stations in the Toplica valley, Kursumlija and Prokuplje, and the discharge of the Toplica river at two hydrological stations, Pepeljevac and Doljevac.

The trend of the parameters was examined by the Mann-Kendall test, and the homogeneity of data by the Pettitt's test, in the period of 62 years, from 1957–2018. This period was divided into two equal half-periods of 31 years: 1957–1987 and 1988–2018, in order to examine the changes between the two periods. The period 1975–1994 was identified as the period in which the change in atmospheric circulation most likely occurred, which strongly influenced all the observed parameters. The changes in this period are easily noticeable on the graphs of the polynomial approximation.

In the entire period, the mean temperature and precipitation increased at both examined stations. In the first period, temperature trends decreased with statistical significance at both stations, the precipitation trend in Kursumlija increased, whereas in Prokuplje it decreased, without statistical significance in both cases. In the second period at both stations, temperature and precipitation trends strongly increased, with statistical significance. The period 1975–1994 is characterized by an increase in temperature, without statistical significance and, at the same time, an extremely strong drop in precipitation of about 90 mm/dec at both stations. This period had a large impact on the river Toplica discharge.

Average values of temperature and precipitation in the second period at both stations are higher than in the first, while the discharge is reversed, in the second period the mean value is lower than in the first. This is certainly a consequence of a strong drop in precipitation, and thus in discharge in the period 1975–1994. During this period, the flow decreased so much (about 2.8 m^3/s /dec in Pepeljevac and 4 m^3/s /dec in Doljevac) that the mean value of the discharge did not recover, despite the strong increasing precipitation trend in the second period.

Mean seasonal values of discharge at both stations are in all cases lower in the second period, except in the MAM season in Pepeljevac. In the DJF season, at both meteorological stations there is an increase in the mean precipitation and temperature in the second season, and a simultaneous decrease in discharge. In this season, in the period 1975–1994, both precipitation and temperature dropped, which additionally slowed down the melting of the accumulated snow and thus negatively affected the discharge. In Pepeljevac, in MAM season, there is an increase in the average discharge, which is expected considering that in the second period there was an increase in precipitation and temperature at both stations, so that the melting of snow from the mountains left behind in the DJF season increased the mean. The anomalous situation is found at the station in Doljevac, where an even larger increase in the average discharge is expected than in Pepeljevac, but the discharge has decreased. In the period 1975–1994, there were no drastic changes in either temperature or precipitation, and the research conducted in this study is not sufficient to explain this change. In the summer season, the mean discharge of the Toplica river declined at both stations. At the Pepeljevac station, we also recorded a drop in the discharge in the second period, while in Doljevac it stagnated. At both stations, the average is 20% lower in the second period. Increased evaporation due to the increase in temperature is probably to blame for this decline. The situation is similar in the autumn season, but there is a positive trend in the second period at both stations.

In conclusion, we can say that the changes in temperatures in the Toplica valley due to climate change are quite expected and in line with all the previous research (*Vukovic et al.* 2018; *Gavrilov,* 2015; *Ruml et al.,* 2017; *Unkasevic, Tosic,* 2013). Precipitation changes are more complicated, which is also known, and for now they do not fit into the predictions of either the A1B1 or A2 models (*Sekulić*, 2012), but are likely to rise in all seasons.

Changes in discharge vary considerably from river to river, and thus, need to be investigated at a local scale, for each individual basin. For example, negative discharge trends were detected in the Vrbas river (Bosnia and Herzegovina) during all seasons, and the observed changes in river discharges were strongly related to the large-scale atmospheric circulation patterns over the Northern Hemisphere (*Gnjato,* 2019). On the other hand, upward trends for annual, summer, and autumn discharges were detected in East Romania (*Croitoru*, 2015).

The strongest increase is in the MAM season, which has led to large floods in the last decade, in the middle and lower course of the Toplica river, as the

catastrophic flood in 2014. The discharge of the Toplica river dropped dramatically in the period 1975–1994, and since that it has been recovering. However, it seems that the already poor discharge distribution is getting worse over time, floods are becoming more frequent in spring,0 and the water level is getting lower in summer. The increase in temperature in the Toplica basin has hit the summer season discharge the hardest, when the water is most needed, both directly through increased evaporation and indirectly through anthropogenic factors, increased consumption of water for agriculture and irrigation.

Reference

Alfieri, L., Burek, P., Feyen, L., Forzieri, G., 2015: Global warming increases the frequency of river floods in Europe. *Hydrol. Earth. Syst. Sci. 19*, 2247–2260. https://doi.org/10.5194/hess-19-2247-2015

Asadieh, B. and *Krakauer, N.,* 2017: Global change in streamflow extremes under climate change over the 21st century. Hydrol. *Earth Syst. Sci. 21*, 5863–5874. https://doi.org/10.5194/hess-21-5863-2017

*Castillo,V., Gómez-Plaza,A., Martínez-Mena,M.,*2003: The Role of Antecedent Soil Water Content in the Runoff Response of Semiarid Catchments: A Simulation Approach. *J. Hydrol. 284*. 114–130. https://doi.org/10.1016/S0022-1694(03)00264-6

Cheney, W. and *Light, W.*, 2000: A Course in Approximation Theory. Amer. Meteor Soc., 2000

Croitoru, A.E. and *Minea, I.,* 2015: The impact of climate changes on rivers discharge in Eastern Romania. *Theor. Appl. Climatol. 120*, 563–573. https://doi.org/10.1007/s00704-014-1194-z

Di, C., Wang, T., Yan,g X., and *Li, S.,* 2018: Technical note: An improved Grassberger–Procaccia algorithm for analysis of climate system complexity, *Hydrol. Earth Syst. Sci. 22*, 5069–5079. https://doi.org/10.5194/hess-22-5069-2018

Djordjevic, S., 2008: Temperature and precipitation trends in Belgrade and indicators of changing extremes for Serbia. *Geographica Pannonica 12*, 62–68. https://doi.org/10.5937/GeoPan0802062D

Ducić, V. and *Radovanović, M.* 2005: Klima Srbije, Zavod za udžbenike I nastavna sredstva, Beograd,. (in Serbian).

Dukić, D. 1999: Klimatologija, Geografski fakultet., Univerzitet u Beogradu, Beograd,.(in Serbian)

Gavrilov, M., Marković S., Jarad A., Korać V., 2015: The Analysis of Temperature Trends in Vojvodina (Serbia) from 1949 to 2006, *Thermal Sci.. 19*, Suppl. 2, S339–S350. https://doi.org/10.2298/TSCI150207062G

Gavrilović, Lj. 2011. Reke Srbije, Zavod za udžbenike. i nastavna sredstva, Beograd, (in Serbian)

Gnjato, S., Popov, T., Trbić, G., and *Ivanišević, M.*, 2019: Climate Change Impact on river Discharges in Bosnia and Herzegovina: A Case Study of the Lower Vrbas river Basin. In (eds. *Leal Filho W., Trbic G., Filipovic D.*) Climate Change Adaptation in Eastern Europe. Climate Change Management. Springer, Cham. https://doi.org/10.1007/978-3-030-03383-5_6

IPCC, Climate Change 2013*:* The Physical Science Basis, AR5, 2013: Cambridge University Press, Cambridge, UK and New York, NY, USA. https://doi.org/10.1017/CBO9781107415324

JCERNI, 2014: Report climate and climate change data on national level Republic of Serbia, 2014, Institute for Development of Water Resources "Jaroslav Černi" Belgrade, 2014

JCERNI, 2017: The Second National Communication on Climate Change under the United Nations Framework Convention on Climate Change, 2017, Ministry of Environmental Protection, Belgrade,

Kendall, M.G., 1948 Rank correlation methods. Griffin, London, UK.

Kostadinov S., Dragović N., Todosijević M., 2008: Influence of anti-erosion measures in the Toplica river basin upstream of the "Selova" dam on the intensity of soil erosion (in Serbian); Vodoprivreda 40, 231–233.

Kyoung, M., Kim, H., Sivakumar, B., Singh, V., Ahn, K., 2011: Dynamic characteristics of monthly rainfall in the Korean Peninsula under climate change. *Stoch. Environ. Res. Risk Assess. 25*, 613–625. https://doi.org/10.1007/s00477-010-0425-9

Martić-Bursać, N., Stričević, Lj., Nikolić, M., Ivanović, R., 2016a: Statistical analysis of average, high and low waters of the Toplica river, *Bull. Serbian Geograph. Soc. 96*, 26–45. https://doi.org/10.2298/GSGD1601026M

Martić-Bursać, N., Đokić, M., Gocić, M., 2016b: Fluvio-denudational structures in the valley of the Toplica in the area of the settlement of Pločnik, *Serbian J. Geosci. l2*, 11–23.

Martić Bursać, N., 2017:Pločnik – antropogeografska proučavanja. Univerzitet u Nišu, Prirodno-Matematički fakultet. (in Serbian).

Martic Bursac, N. and *Stricevic, Lj.* 2018: Agro-climatic conditions for agricultural production in Toplica micro region, Proceedings, XXII naučni skup, Regionalni razvoj i demografski tokovi zemalja jugoistočne Evrope, Ekonomski fakultet, Univerzitet u Nišu 23, 253–262. https://doi.org/10.1080/1059924X.2018.1470048

Pettitt, N., 1979: A non-parametric approach to the change-point problem, *Appl. Stat. 28*, 126–135. https://doi.org/10.2307/2346729

Rudić, B.V., 1978: Stanovništvo Toplice, Srpska akademija nauka i umetnosti, Etnografski institut, Posebna izdanja, knjiga 17, Beograd, (in Serbian).

Ruml, M., Gregorić, E., Vujadinović, M., Radovanović, S., Matović, G., Vuković, A., Počuča, V., Stojičić, Đ., 2017: Observed Changes of Temperature Extremes in Serbia over the Period 1961−2010, *Atmosph. Res. 183*, 26–41. https://doi.org/10.1016/j.atmosres.2016.08.013

Sekulić, G., Dimović, D., Kalmar, Z., Jović, K., Nataša, T., 2012, Climate Vulnerability Assessment – Serbia. Environmental Improvement Centre: World Wide Fund for Nature, Belgrade.

Schneider, C., Laizé, C., Acreman, M., Flörke, M., 2013: How will climate change modify river flow regimes in Europe? *Hydrol. Earth Syst. Sci., 17*, 325–339. https://doi.org/10.5194/hess-17-325-2013

Trenberth, K. 2011: Changes in Precipitation with Climate Change. Climate Change Research. *Climate Res. 47*, 123–138. https://doi.org/10.3354/cr00953

Unkasevic, M. and *Tosic, I.,* 2013: Trends in Temperature Indices over Serbia: Relationship to Large Scale Circulation Patterns, *Int. J. Climatol. 33*, 3152–3161. https://doi.org/10.1002/joc.3652

Unkaševic, M., and *Tošic, I.,* 2015: Seasonal Analysis of Cold and Heat Waves in Serbia during the Period 1949-2012, *Theor. Appl. Climatol. 120*, 29–40. https://doi.org/10.1007/s00704-014-1154-7

Vuković, A., Vujadinović, M., Rendulić, S., Đurđević, V., Ruml, M., Babić, V., Popović, D., 2018: Global Warming Impact on Climate Change in Serbia. *Thermal Sci. 22*, 2267–2280. https://doi.org/10.2298/TSCI180411168V

Woodhouse, C., Pederson, G., Morino, K., McAfee, S., McCabe, G., 2016: Increasing influence of air temperature on upper Colorado river streamflow. *Geophys. Res. Lett. 43*. 2174–2181. https://doi.org/10.1002/2015GL067613

Wang, K., Yang, X., Liu, X., Liu, C., 2017: A simple analytical infiltration model for short-duration rainfall, *J. Hydrol. 555* ,141–154. https://doi.org/10.1016/j.jhydrol.2017.09.049

INSTRUCTIONS TO AUTHORS OF *IDŐJÁRÁS*

The purpose of the journal is to publish papers in any field of meteorology and atmosphere related scientific areas. These may be

- research papers on new results of scientific investigations,
- critical review articles summarizing the current state of art of a certain topic,
- short contributions dealing with a particular question.

Some issues contain "News" and "Book review", therefore, such contributions are also welcome. The papers must be in American English and should be checked by a native speaker if necessary.

Authors are requested to send their manuscripts to

Editor-in Chief of IDŐJÁRÁS
P.O. Box 38, H-1525 Budapest, Hungary
E-mail: journal.idojaras@met.hu

including all illustrations. MS Word format is preferred in electronic submission. Papers will then be reviewed normally by two independent referees, who remain unidentified for the author(s). The Editor-in-Chief will inform the author(s) whether or not the paper is acceptable for publication, and what modifications, if any, are necessary.

Please, follow the order given below when typing manuscripts.

Title page should consist of the title, the name(s) of the author(s), their affiliation(s) including full postal and e-mail address(es). In case of more than one author, the corresponding author must be identified.

Abstract: should contain the purpose, the applied data and methods as well as the basic conclusion(s) of the paper.

Key-words: must be included (from 5 to 10) to help to classify the topic.

Text: has to be typed in single spacing on an A4 size paper using 14 pt Times New Roman font if possible. Use of S.I. units are expected, and the use of negative exponent is preferred to fractional sign. Mathematical formulae are expected to be as simple as possible and numbered in parentheses at the right margin.

All publications cited in the text should be presented in the *list of references*, arranged in alphabetical order. For an article: name(s) of author(s) in Italics, year, title of article, name of journal, volume, number (the latter two in Italics) and pages. E.g., *Nathan, K.K.,* 1986: A note on the relationship between photosynthetically active radiation and cloud amount. *Időjárás 90,* 10–13. For a book: name(s) of author(s), year, title of the book (all in Italics except the year), publisher and place of publication. E.g., *Junge, C.E.,* 1963: *Air Chemistry and Radioactivity.* Academic Press, New York and London. Reference in the text should contain the name(s) of the author(s) in Italics and year of publication. E.g., in the case of one author: *Miller* (1989); in the case of two authors: *Gamov* and *Cleveland* (1973); and if there are more than two authors: *Smith et al.* (1990). If the name of the author cannot be fitted into the text: *(Miller,* 1989); etc. When referring papers published in the same year by the same author, letters a, b, c, etc. should follow the year of publication. DOI numbers of references should be provided if applicable.

Tables should be marked by Arabic numbers and printed in separate sheets with their numbers and legends given below them. Avoid too lengthy or complicated tables, or tables duplicating results given in other form in the manuscript (e.g., graphs). *Figures* should also be marked with Arabic numbers and printed in black and white or color (under special arrangement) in separate sheets with their numbers and captions given below them. JPG, TIF, GIF, BMP or PNG formats should be used for electronic artwork submission.

More information for authors is available: journal.idojaras@met.hu

Published by the Hungarian Meteorological Service

Budapest, Hungary

ISSN 0324-6329 (Print)

ISSN 2677-187X (Online)